Improving the land subsidence model Phoenix

Graduation Internship – master Water Science and Management

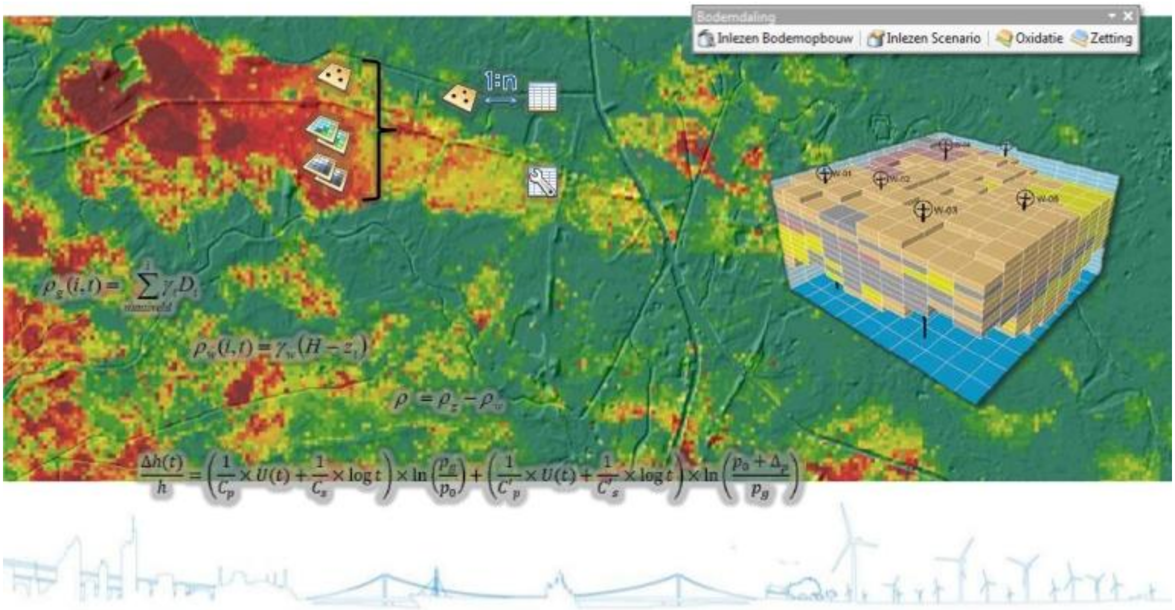

Source: (Bakker, 2012)

Msc. Student:	Len Geisler
Student number:	3407802
Phone:	0031 6 53 43 33 80
Email:	lengeisler@gmail.com
University supervisor:	Dr. Paul Schot
Internship organization:	Hoogheemraadschap De Stichtse Rijnlanden
Internship supervisor:	Henk van Hardeveld
ECTS:	30
Period:	Blocks 3 & 4
Academic year:	2013-2014

Table of Contents

Summary

Land subsidence is a problem in the Dutch peat lands. These lands subside when low groundwater tables are maintained, and result in an increased safety risk, more complex water management and CO_2 production. In order to predict this subsidence Hoogheemraadschap De Stichtse Rijnlanden and the province of Utrecht created the land subsidence model Phoenix. The problem was that this model was not complete. Two improvements that could be made to this model were identified. The first improvement was adding regional differences in land subsidence due to for example differences in water management and soil characteristics. An attempt was made to implement these regional differences by identifying historical land and surface water subsidence, and how they relate. It was found that the average land subsidence in the study area over the past 40 years has been around 7,7 mm/y, with outliers up to 60 mm/y in Zegveld. The surface water levels on average have subsided less rapid resulting in a decrease in freeboard over this same time period. Although regional differences were observed, they cannot be implemented responsibly as they were explained by errors in input data. The second improvement was the implementation of the increase in land subsidence due to temperature changes caused by climate change. The impact of climate change, according to scenario W+ of the KNMI, on land subsidence causes the peat soils to subside up to twice as fast in 2200 compared to 2000, having the same freeboard and soil characteristics. This climate change impact was added to Phoenix and modelled up to 2200. This run was then compared to a base run. The result was that soils with 30 cm clay had the largest additional land subsidence up to 2,4m. The largest percentage difference in land subsidence was observed in soils with 60 cm clay, which may subside up to an additional 270%.

Abbreviations and Terminology:

AHN1	:General Elevation Map of the Netherlands 1
AHN2	:General Elevation map of the Netherlands 2
TOPh	:TOPhoogteMD
AP	:Regional ordnance datum, *Algemeen Peil* in Dutch
NAP	:Dutch ordnance datum, *Nieuw Amsterdams/Algemeen Peil* in Dutch
SW	:Surface water
WIS	:Water Information System 2.0 (of HDSR)
DP	:Data point
AAED	:All available elevation data
DEM	:Digital Elevation Maps
SW	:Surface water
HDSR	:Hoogheemraadschap de Stichtse Rijnlanden.
RD	:Regional differences value [m y^{-1}]
RQ	:Research question.

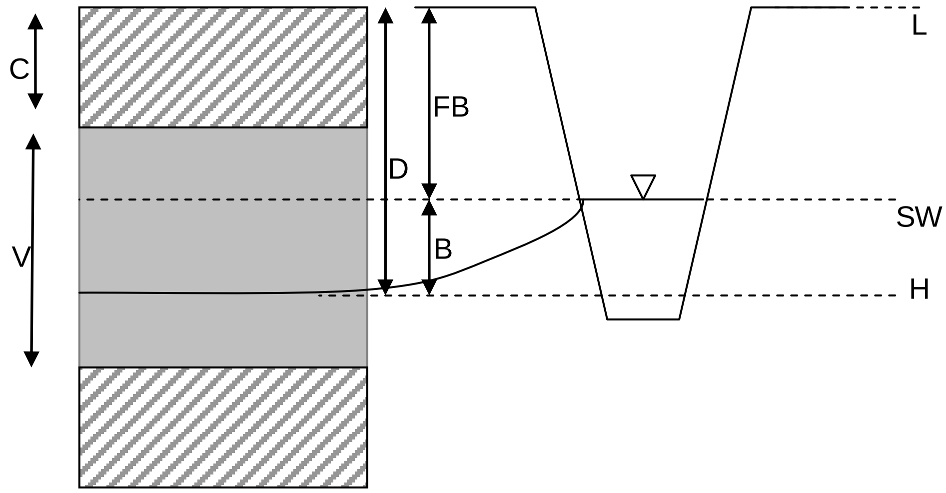

C	: Thickness mineral layer (clay layer) [m]	
V	: Thickness peat layer [m]	
D	: Drainage [m]	
FB	: Freeboard [m]	
B	: Differential head [m]	
L	: Land elevation [m+NAP]	
SW	: Surface water level [m+NAP]	
H	: Groundwater level [m+NAP]	
a	: Land subsidence [1/y]	[-0,023537]
b	: Clay constant [1/y]	[0,01263]
c	: Soil composition constant [1/y]	[0,00688]
d	: Peat growth factor [m/y]	[0,001]
i	: *Peilindexatie* [-]	[0 - 1]

1 Introduction:

1.1 History of land subsidence in Dutch peat areas

The history of land subsidence starts over a thousand years ago. The low moor peat soils in the old polders of the western Netherlands were reclaimed between the 9th and 14th centuries. These previously inundated regions were now above the water table, allowing the soil to subside due to natural processes such as oxidation, loss of buoyancy, shrinkage and consolidation (van den Akker et al., 2007, Stouthamer et al., 2008), but also due to excavation of peat for fuel. At this time the soil surface of these peat lands were equal to or somewhat above the mean sea level (Schothorst, 1977; Querner, Jansen,, van, & Kwakernaak,, 2012). In the beginning dewatering was done using a gravitational system, where water was deposited via sluices during low tide and closed during high tides. Around the 16th century the land had subsided below the low tide level so this method was no longer applicable, henceforth windmills were used to pump out the water artificially. In 1870 these windmills were starting to be replaced by the more effective steam pumps. During this eight to ten centuries period, even though only shallow drainage was applied the soil surface had subsided to about one to two meter below mean sea level (Schothorst, 1977)**.** The past few centuries the Dutch peat lands have been subsiding with several millimetres a year (van den Akker, Beuving, Hendriks, & Wolleswinkel, 2007; Querner, Jansen,, van, & Kwakernaak,, 2012).

Until the end of the fifties the interests in the peat land areas were varied. One farmer desired sufficient water to boat through the ditches whereas another farmer desired sufficient reclamation so that he could drive over his land. Due to this conflict it was hard to mechanize farming in these peat lands and counteract the increasing labour costs, as was possible in other agricultural areas. The absence of the possibility to structurally intensify livestock agriculture caused this sector to come into financial difficulties during the sixties. At this point a shift took place: the water levels were lowered. The lowering of the water tables resulted in land subsidence rate doubling due to the previously mentioned natural processes. The drainage depth in many of the western peat land areas had increased to roughly 60 cm below ground surface level (van den Akker et al, 2007)**.** People feared land subsidence even around this time (Schothorst, 1977).

1.2 Relevance of land subsidence and problem description

The problem of land subsidence hits many aspects of society. The impacts are explained starting at the national scale, followed by the regional scale of the peat lands and finally the local scale of the nature areas and cities within the peat lands.

The Netherlands is a country where already one third of the land is below mean sea level. The coastal zones face a unique safety risk which only increases due to land subsidence (Hoogland, van den Akker, & Brus, 2012). The water safety in the Netherlands is for a large part the responsibility of the regional water authorities (Waterwet, 2014), of which one is Hoogheemraadschap De Stichtse Rijnlanden (HDSR).

The cycle of land subsidence starts with the desire of farmers and governmental organizations to have economically feasible agriculture on peat land areas. Of the 289.000 ha of peat lands present in the Netherlands roughly 77% is in agricultural use (van den Akker et al, 2007). In order to achieve agriculture on these lands, the water level has to be sufficiently below the land surface. Due to uneven land subsidence the variations in elevation within *peilgebieden* (area in which one and the same water level is maintained) increases. In order to maintain an appropriate water level within all polders of said *peilgebied,* more *peilgebieden* have to be created resulting in more expensive and complex water management for which the regional water authorities such as HDSR are responsible. The desire for sufficient freeboard, which is the distance between the land surface and the surface water, and the water level adjustments to support this, causes the system to never stabilize and thus subside further.

The largest contributing process to land subsidence in peat land areas is oxidation (Stouthamer, Berendsen, Peeters, & Boumand, 2008). This oxidation converts biological matter in CO_2. A soil which subsides with 10 mm y^{-1} may emit as much as 22 tones CO_2 during that year (van den Akker, et al., 2007; Hoogland et al, 2012). Peat soil oxidation is responsible for 2,5% of the Dutch anthropogenic national emissions, similar to that of 1.7 million cars (van den Akker, 2007). Land subsidence also elevates the risk of increasing upward seepage of brackish and nutrient rich ground water (Hoogland et al, 2012). On a local scale nature areas drain towards the increasingly deepening agricultural areas and desiccate (Hoogland et al, 2012; Querner et al, 2012).

The problem however is not limited to the rural areas. In urban areas consolidation is the largest contributing process to land subsidence. Here the loading of sand, stones or roads on compression susceptible soils results in entire urban areas subsiding (Wolters et al, 2011; (Roscience Inc., 2001-2009)). Impacts of land subsidence in urban areas are water on the streets and damage to infrastructure, to rainwater storage and to the sewer system (Wolters et al, 2011). This results in high maintenance costs for the subsiding urban areas (van Hardeveld, 2014). Additionally, wooden foundations of buildings may end up above the water table allowing oxygen to reach the wood which makes it susceptible to organic decomposition and destabilize the buildings (van den Akker et al, 2007; (Wolters, Hoekstra, & Boerefij, 2011).

Due to increase in safety risk, in costs and in complexity of water management and damage to urbanized areas, land subsidence is of interest to both HDSR and the province of Utrecht which are responsible for these tasks. Their aim is to prevent as many negative impacts due to land subsidence as possible. In order to do so, it is important to have an estimate of land subsidence as a result of their policies. Therefore they have set up a model named Phoenix (van Bokhoven, Personal contact, 2014; van Hardeveld, personal contact, 2014). This instrument attempts to predict land subsidence for various future scenarios by combining subsoil characteristics and water management. The output of this model is then used in a model named "Waterpas HDSR", which, among other things, portraits the (social) costs of land subsidence. For example, the required investments for water management infrastructure are assessed, as well as the damage to specific houses and their foundations (van Hardeveld et al, 2013). The land subsidence information obtained using Phoenix, allows for support when making policy decisions for specific areas (van Hardeveld, 2014).

During the creation of Phoenix a number of questions have risen on the validity of the simulations (van der Schans & Houhuessen, 2012) produced. Phoenix is based on an empirical relation found by van den Akker et al, 2007 (see Ch 2. Physical theory & Model theory). However variations in for example soil characteristics, permeability and (downward) seepage may result in different subsidence rates for different regions. However the same empirical relation is used for all peat soils and clay settlements (van der Schans & Houhuessen, 2012). This resulted in the question about the robustness of this empirical relation and the possible identification of regional differences in land subsidence which then might be used to adjust the empirical formula per region or soil composition (van der Schans & Houhuessen, 2012). Additionally, the influence of temperature increase due to climate change (CC) on microbial activity is missing. Currently the impact of CC on the groundwater levels and thus the land subsidence are taken into account (van der Schans & Houhuessen, 2011), however the impact of increased temperature on the microbial activity is lacking which results in an underestimation of the severity of the oxidation process in peat soil.

1.3 Research aim

The general aim of this master thesis is to improve the Phoenix model. During the start-up of the internship two possible improvements were identified. One addresses the regional differences in land subsidence, while the other addresses the impact of temperature on microbial activity and thus oxidation rate. Once these two adjustments are made the final step is to determine whether the calculated land subsidence with these adjustments is significantly different compared to the original model. Although there are more improvement possibilities these were deemed too much within the set time frame of this thesis.

1.4 Research questions

The main research question that will be addressed in this thesis is:

> *What are the effects on calculated land subsidence with the Phoenix model when taking into account regional differences in soil types and historical water management, and increased peat oxidation due to future temperature increases following global climate change?*

The research questions will be answered using the following sub questions:

1. *How can the effects of regional differences in soil type and in surface water subsidence on land subsidence be implemented in Phoenix?*
    1. *What has the historical land subsidence been within the Phoenix model area?*
    2. *What has the historical surface water subsidence been within the Phoenix model area?*
    3. *How are 1) and 2) related to each other, as a function of soil characteristics?*
    4. *How can 3) be translated into regional differences and the general empirical land subsidence formula used in Phoenix be adapted to incorporate these differences?*
2. *How can the effect of increase in temperature due to climate change be implemented in Phoenix?*
    1. *What is the predicted temperature increase due to climate change?*
    2. *What is the influence of increase in temperature on microbial activity, oxidation and land subsidence?*
    3. *How can the increase in land subsidence due to temperature changes caused by climate change be implemented in Phoenix?*
3. *How do the regional differences (in soil characteristics and surface water subsidence) and the effects of temperature increases following climate change affect the simulated land subsidence compared to the original Phoenix model?*

2 Theory on land subsidence processes:

2.1 Physical theory on land subsidence processes:

In peat areas there are several processes that result in land subsidence. Figure 1 gives a schematic visualization of these processes.

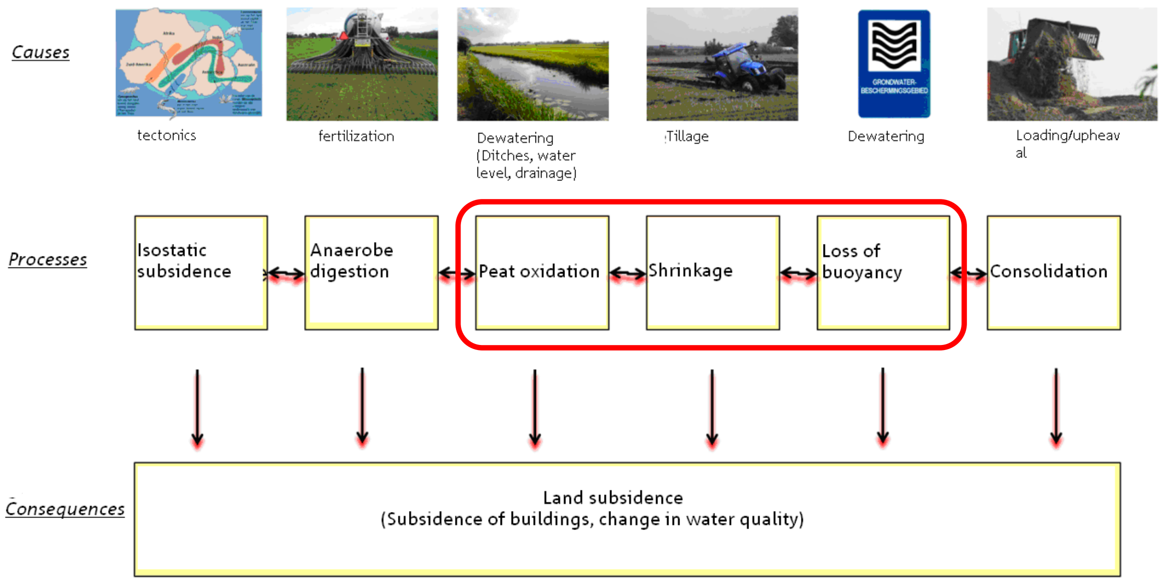

Figure 1: *Overview of causes and consequences of land subsidence, with the three most important ones for rural areas in red (van der Schans & Houhuessen, 2012)*

The lowering of the water table results in peat ending up above the water table and allow the above mentioned processes to occur. For the rural areas the three most important processes are explained (figure 1) (Stouthamer et al, 2008). Consolidation which is important in urban areas is explained as well.

Loss of buoyancy

The soil is carried by the solid particles (the soil itself) and by the hydrostatic pressure. This means that solid soil particles partly “float” within the ground water, as they experience an upward force via this hydrostatic pressure. When the water table is lowered the hydrostatic pressure decreases which results in a loss of this buoyancy. The water in the unsaturated zone is pressed out by the weight of the top soil itself, this results in compaction of the soil. This happens until a new equilibrium is reached. Depending on the thickness and conductivity of the peat this process can take some time (van den Akker et al, 2007).

Shrinkage

Shrinkage is a seasonal process. When peat ends up above the water table, the soil shrinks and largely rebounds when it becomes wet again. However virgin soils, soils that are above the water table for the first time, have a significant permanent shrinkage. Due to repeated drying and wetting this processes becomes more and more reversible (van den Akker et al, 2007). That is until the groundwater table is permanently lowered and new virgin soil comes into play which can permanently shrink again.

Oxidation

Peat above the water table is susceptible to air intrusion making aerobe processes possible. These aerobe processes allow for biological decomposition of the peat which exists out of 23 to 100 percent of organic materials. Soil organisms mineralize the organic matter in several ways: during dissimilation the organic matter is used for respiratory functions and during assimilation the organic matter is used to build organic matter. These two processes are the driving forces behind the decomposition process (van den Akker et al, 2007). During aerobe circumstances the process works with oxygen as an electron receptor (Eq. 1), under anaerobe circumstances (Eq. 2) this electron receptor is nitrate. This process however is less efficient.

$$C_6H_{12}O_6 + 6O_2 \rightarrow 6CO_2 + 6H_2O + 2870\ kJ\ per\ mol\ glucose \quad \text{(Eq. 1)}$$

$$C_6H_{12}O_6 + 6NO_3^- + 6H^+ \rightarrow 6CO_2 + 9H_2O + 3N_2O + 2280\ kJ\ per\ mol\ glucose \quad \text{(Eq. 2)}$$

Since this process burns off biological matter and transforms it into CO_2 and water this process is irreversible and responsible for most of the continuous subsidence of peat areas in the Netherlands. Due to continues lowering of the water table in accordance with the land surface this aerated zone remains. This process continues to burn off peat, especially in the summer when the temperature is higher and the groundwater tables are lower. If a clay layer is present on top of the peat layer oxidation is reduced (van den Akker et al, 2007)**.** This decomposition process is temperature independent, the rate at which this process happens is not. Most of the microorganisms function best around a temperature of 35˚ C. It is possible to approximate their activity using:

$$f_{t,Q_{10}} = Q_{10}^{(\frac{T-Tr}{10})} \quad \text{(Eq. 3)}$$

Where Q_{10} represents the impact 10˚ C temperature change has on the biological activity, f_t is the correction factor for temperature influence, T is the actual temperature and T_r is the reference temperature where $f_t = 1$. The influence of temperature increases with depth, because the microorganisms near the top of the soil have adapted more to seasonal fluctuations in temperature and thus do not respond as severely to these fluctuations (van den Akker et al, 2007). However, infiltration of oxygen becomes increasingly harder in deeper soils becoming a limiting factor for oxidation (van den Akker, 2014). This additional influence of temperature is important to take into account when modelling in the future where climate change plays a significant role (Querner et al, 2012).

Consolidation

Within urban areas the influence of the three aforementioned processes is limited compared to the rural areas. Here soil consolidation plays a large role (Hoekstra et al, 2011). This consolidation occurs under external pressure. The placement of weight on a soil, for example by placing a road or house on the soil, results in the expulsion of the water and causes the soil particles to pack together more tightly, thus increasing the bulk density as the volume decreases and the surface level subsides. This process is divided into three sub processes: the elastic settlement which happens immediately after placement; the primary consolidation which occurs due to expulsion of pore water from the voids of the soil; and the secondary consolidation which is a result of the rearrangement of the soil particles (Dinesh, sine anno; Roscience Inc., 2001-2009).

For the total peat area in the Netherlands the division of the subsidence processes looks as follows (figure 2):

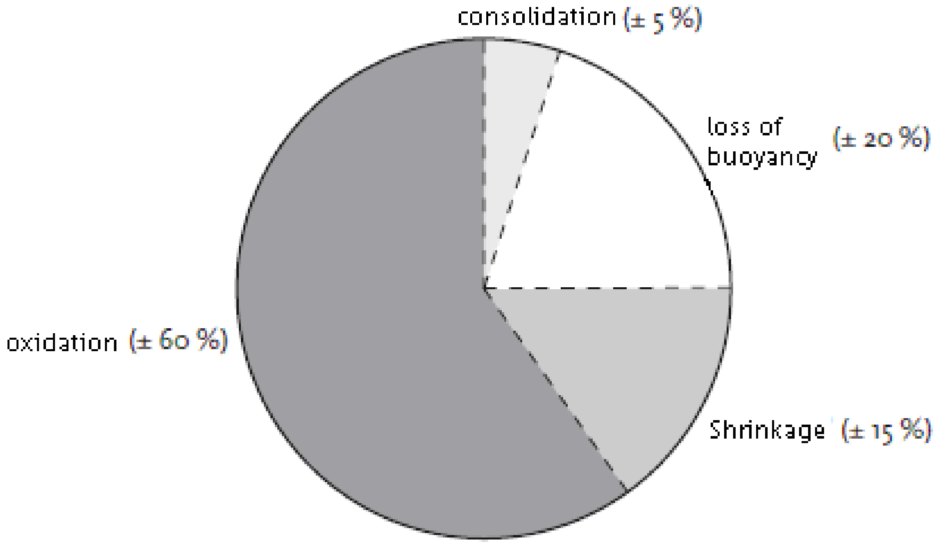

Figure 2: *Process contribution of oxidation (±60%), shrinkage (±15%), loss of buoyancy (±20%) and consolidation (±5%) (Stouthamer et al, 2008).*

This distribution is over the area average. Some processes play a significantly larger role in one area compared to the other. For example the subsidence in Kockengen, a village in the north east of the study area (figure 4), is almost exclusively a result of consolidation and not oxidation which is the case for most of the rural areas (Hoekstra et al, 2011)**.**

2.2 Phoenix model theory

Phoenix works with four major steps in ArcGIS. The first step creates the soil profile, followed by the second step which adds hydrological data and the scenario input for the HDSR jurisdictional area. In the third and fourth steps the calculations for oxidation and consolidation are done.

Step 1: Preparation of the soil profile data

First the area of HDSR is divided into calculation points on a regular grid, which can vary in detail (100x100m or 25x25m etc.), these points have a number and a location. Connected to these points are the elevation data at the ground surface via the AHN2 (Het Waterschapshuis, 2008). Also connected to these points are soil characteristics.

Step 2: Input of hydrological and scenario data

The hydrological circumstances are entered such as the mean high groundwater level (Dutch: GHG) and the mean low groundwater level (Dutch: GLG), modelled in HYDRO-MEDAH, and various calculation constants (more about this in step 3). Also adaptation techniques such as water drains, which influence the difference between the mean high water level (during the winter) and mean low water level (during the summer) can be implemented. The final input is the expected future policy. It is possible to decide the degree to which the water levels are adjusted in accordance with the land subsidence. This future water management parameter is named *peilindexation*.

Step 3: Oxidation calculation

Calculations are done in this step. The three most important physical processes on rural land subsidence are present in the model. However these are implicitly present in the van den Akker formulas (Eq. 4&5). These linear relations were established in several polders among which Zegveld. Zegveld is located in the north of the study area figure 4. This relation was obtained for a soil without clay layer (Eq. 4) and with a thin clay layer (<40 cm) (Eq. 5) respectively (van den Akker et al, 2007):

$$\Delta L = 23{,}537 * GLG - 6{,}68 \qquad \text{(Eq. 4)}$$

$$\Delta L = 23{,}537 * GLG - 10{,}47 \qquad \text{(Eq. 5)}$$

Or in a general form as (Eq. 6):

$$\Delta L = A * GLG + B \qquad \text{(Eq. 6)}$$

Wherein

A	:velocity factor [y^{-1}]
B	:Soil type factor [m y^{-1}]
ΔL	:Land subsidence [m y^{-1}]
GLG	:Lowest 3 measurements every year for 8 years [m –land surface]

These formulas together were conjugated so that one formula can be used for the entire area of HDSR. This formula requires only one set of parameters which includes clay thickness and GLG (van der Schans & Houhuessen, 2011). The suggested formula looks as follows (Eq.7):

$$\Delta L = \underbrace{-0.023537 * D}_{\text{“Velocity term”}} + \underbrace{0.01263 * C}_{\text{“Clay inhibition term”}} + 0.00668 \qquad \text{(Eq.7)}$$

Wherein

ΔL	:Land subsidence [m y^{-1}]
D	:Depth to the groundwater table [m below land surface]
C	:Thickness mineral layer (clay layer) [m]

It is important to note that the land subsidence cannot be positive, so when ΔL>0, this is changed to ΔL=0. In Appendix A the conjugation process, and the confusion revolving around how it was previously done in the Phoenix documentation (van der Schans & Houhuessen, 2011; van der Schans & Houhuessen, 2012) is explained.

When an area is completely inundated, peat formation occurs (Eq.8). The lack of oxidation and an inhibition on the biological activity while underwater causes organic matter from plants such as reeds or grass not to decompose. This process adds organic matter to the peat soil rather than the usual consumption of organic matter by organisms (van der Schans & Houhuessen, 2011). This assumption is based on the manner in which the initial formation of peat soils occurred during the Holocene (van den Akker et al, 2007).

$$\Delta L = d\ (if\ D < 0) \quad \text{(Eq.8)}$$

Wherein
ΔL = Land subsidence [m y^{-1}]
d = Peat growth factor [m y^{-1}]
D = depth to the groundwater table [m below land surface]

This growth factor "d" (Eq.8), which is set at 1 mm y^{-1}, replaces the basic formula (Eq.7) when the groundwater level (D) exceeds the land surface (L) (van der Schans & Houhuessen, 2011). There are more requirements than just inundation for peat to form, so whether or not this assumption is valid, could be argued.

In this step the previously created points, the corresponding soil data (C-variable), the hydrological data (D-variable) and the scenario data (Peilindexation and adaptation strategies) are all used to calculate the land subsidence, which for a large part consists of oxidation.

Step 4: Consolidation calculation

The final important process is the consolidation of the soil. As described in 2.1 (physical theory) the process works with elastic settlement, primary consolidation and secondary consolidation. This process is modelled using the combined Koppejan-Terzaghi-Buisman formula. This formula is widely used to approximate the land subsidence due to loading (Das & Sobhan, 2012; den Haan, 2003; Roscience Inc., 2001-2009). For each soil layer this consolidation is calculated vertically using an iterative approach. As of this point no more attention is paid to this specific process as it falls outside the scope of this research.

3 Methods

In the methods the data used, the way the data is treated, the system boundaries and the way data will be presented in the results are explained. This research is conducted in several steps which corresponds with the research questions. For the first research question a dataset, to which all relevant available data is linked, is created. This dataset is then used to answer the sub questions for determining the regional differences in land subsidence [RQ1]. In the second research question the influence of temperature on land subsidence is calculated. This is then implemented into Phoenix. The new model outputs are compared to the original model outputs without any adjustments.

For each of the sub questions the data used to answer the question (data used), the way in which the data is treated to obtain an answer to the research question (data processed) and finally how the data will be presented in the results (data presented).In figure 3 the flow diagram shows how each sub question contributes to answering the main research question. The content is explained in more detail in the text below.

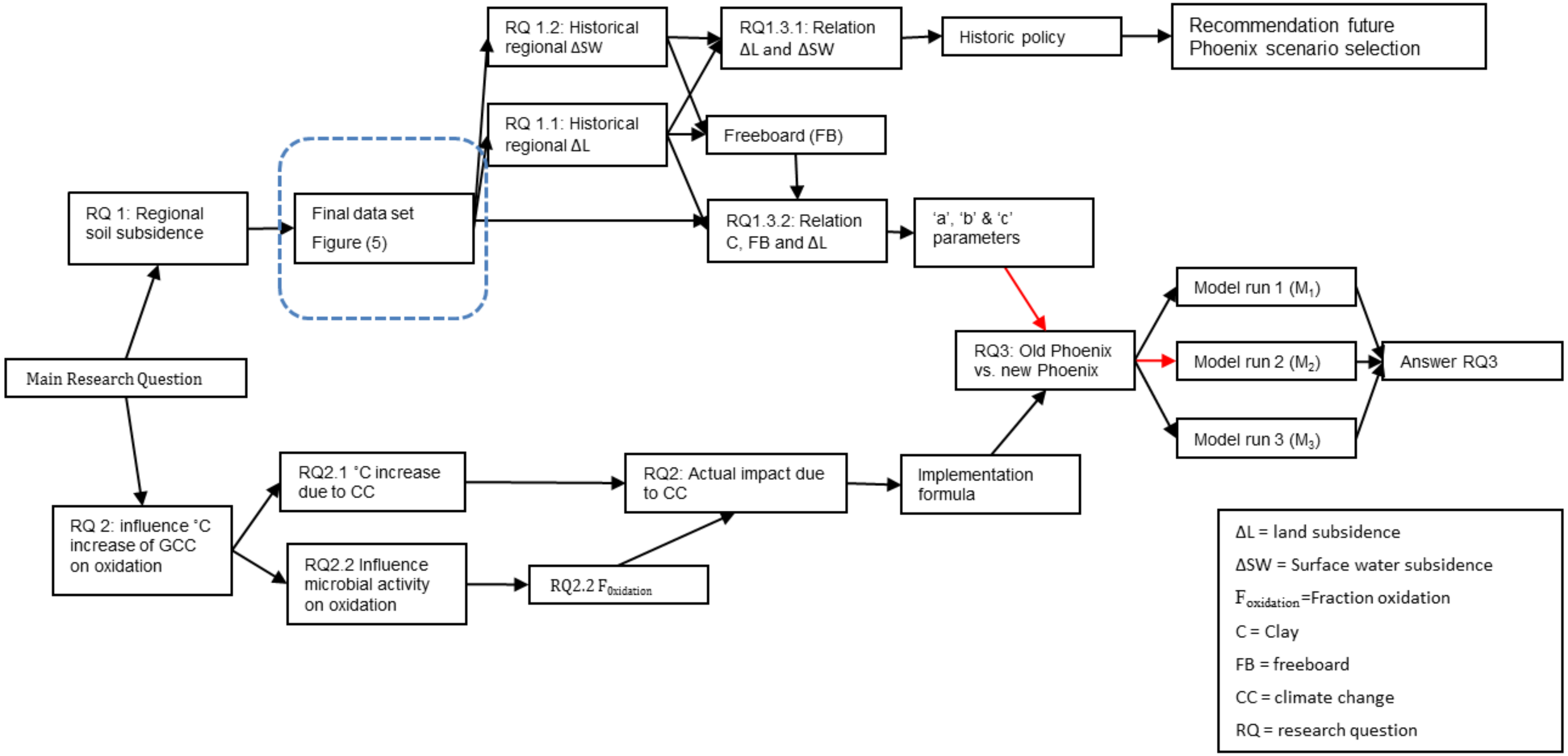

Figure 3: *Flow diagram of the research questions and the way they contribute to answering the main research question of this master thesis, in the dashed box the pre-processing takes place (figure 5). The red arrows represent dead ends.*

3.1 [RQ1]Effects of regional differences in soil characteristics and surface water subsidence on land subsidence

For this research question the geographical system boundaries are as shown in figure 4. This region will henceforth be addressed as "the study area" . This area is located in the western area of the jurisdictional area of HDSR (red outline). In this region mostly peat areas are present with various clay cover thicknesses. The shaded area shows the polders that are taken into account. These specific polders were selected based on their location; the western boundary was set at the boundary of the HDSR jurisdictional area, the north-eastern boundary was selected based on the current use of the polder, the excluded north-eastern polders were classified as "VINEX" (specific type of a Dutch urbanized area) in (Hoogheemraadschap De Stichtse Rijnlanden, sine anno) and finally, the gap between the separate polder in the southern most area and the polders directly above was related to polygon issues of this same internal ArcGIS file (Hoogheemraadschap De Stichtse Rijnlanden, sine anno). The shaded polders are deemed sufficient as they make up the majority of the peat areas in the of the HDSR jurisdictional area.

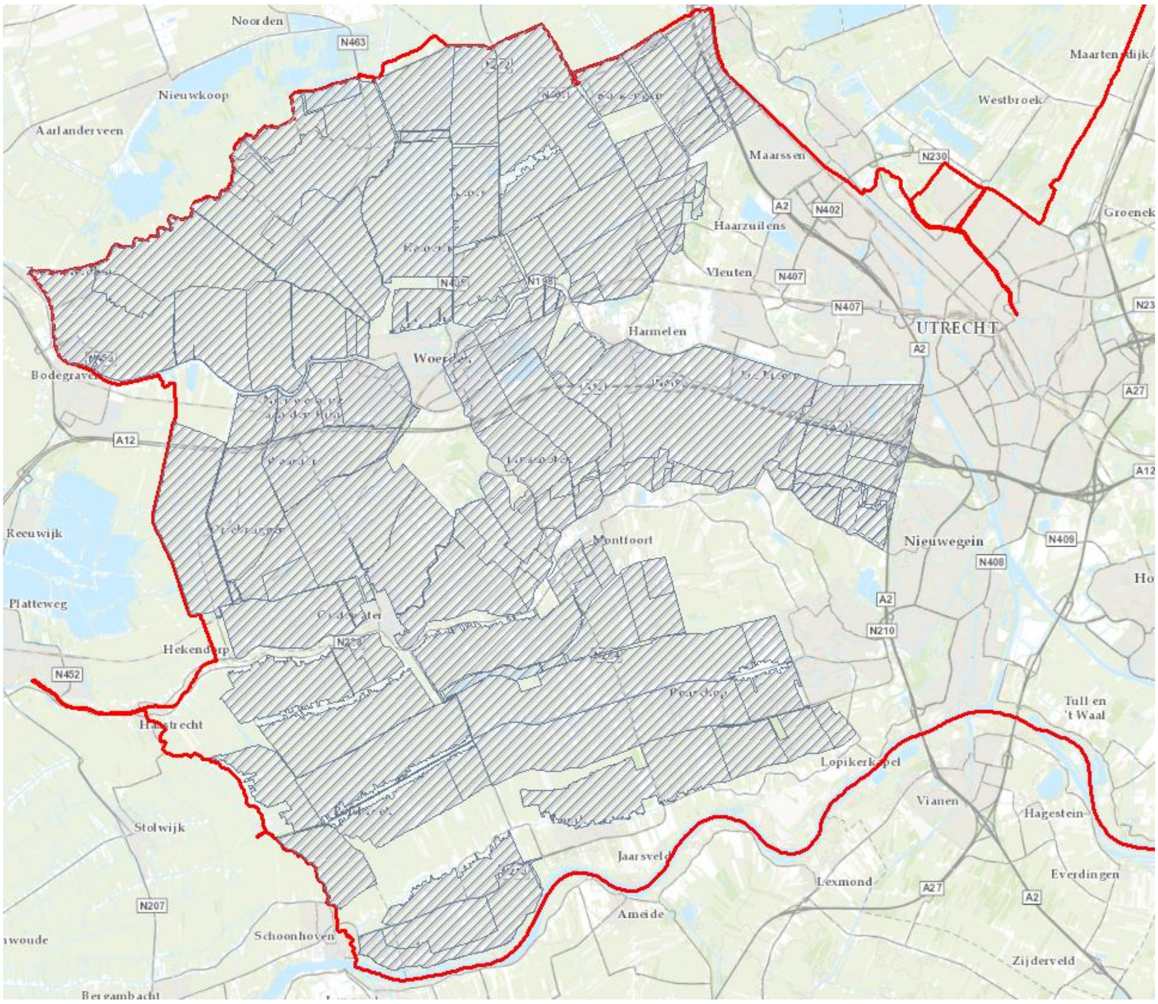

__Figure 4:__ The study area applied in RQ1

3.1.1 Pre-processing of RQ1

In order to properly answer RQ1 a convenient data set is established in which the elevation of the land surface over time is incorporated, the surface water levels over time are present, clay thickness is known and the soil type is specified. First a base data set is selected to which the information is linked, after which analyses are done to adjust or exclude unreliable data. The results and execution of the pre-processing can be found in Appendix B. Each sub question of RQ1 is answered using the data from the final data set (figure 6).

Data used

The data sources used are explained separately in the categories land elevation, surface water elevation and soil characteristics.

The land elevation sources that are used report elevation with respect to NAP:

- *Waterstaatskaarten*[1] report elevation points that represent the surface elevation at that specific location during that time. These points were established between 1950 and 1981.
- *Peilbesluiten*[2] give elevation data for areas within polders which are split up in areas with similar elevations or soil type. Elevation data are reported between 1956 and 2001.
- Digital elevation maps such as:
    - TOPhoogteMD (Meetkundige Dienst van Rijkswaterstaat, 1992) which is a map with 25m by 25m cells with one specific elevation. This map was made by digitizing elevation points from the Meetkundige Dienst van Rijkswaterstaat and interpolating this data (Rijksoverheid, 2014). Depending on the location the data was collected between 1947 and 1982. Where the exact measurement date is not known it is interpolated from the surrounding measurement collection dates.
    - Actueel Hoogtebestand Nederland 1 (AHN1) (Het Waterschapshuis, 1998) for HDSR was collected between 1998-2000 using laser altimetry from a plane or helicopter. With 2-3 measurements per m2 (van der Zon, 2013). The measurements are done during the winter months when the vegetation is low to minimize vegetation impacts on measurements (Actueel Hoogtebestand Nederland, sine anno).
    - Actueel Hoogtebestand Nederland 2 (AHN2) (Het Waterschapshuis, 2008) was collected in the same way as AHN1, albeit with more measurement per m^2, better accuracy and better filtering (van der Zon, 2013). The laser altimetry flights were done between 02-02-2008 and 26-3-2008 (Actueel Hoogtebestand Nederland, sine anno).

---

[1] (Rijkswaterstaat, 1869a) (Rijkswaterstaat, 1869b) (Rijkswaterstaat, 1869c) (Rijkswaterstaat, 1869d) (Rijkswaterstaat, 1870a) (Rijkswaterstaat, 1870b) (Rijkswaterstaat, 1870c) (Rijkswaterstaat, 1870d) (Rijkswaterstaat, 1882a) (Rijkswaterstaat, 1882b) (Rijkswaterstaat, 1919) (Rijkswaterstaat, 1920a) (Rijkswaterstaat, 1920b) (Rijkswaterstaat, 1921) (Rijkswaterstaat, 1940) (Rijkswaterstaat, 1941) (Rijkswaterstaat, 1950a) (Rijkswaterstaat, 1950b) (Rijkswaterstaat, 1959) (Rijkswaterstaat Directie Algemene Dienst, 1960) (Rijkswaterstaat Directie Algemene Dienst, 1967) (Rijkswaterstaat Directie Algemene Dienst, 1969) (Rijkswaterstaat Directie Algemene Dienst, 1972) (Rijkswaterstaat, 1981a) (Waterstaatskartografie, 1981b) (Waterstaatskartografie, 1981c) (Rijkswaterstaat, 1981d)

[2] (Groot-Waterschap van Woerden, 1994a) (Groot-Waterschap van Woerden, 1994b) (Groot-Waterschap van Woerden, 1994c) (Groot-Waterschap van Woerden, 1994d) (Groot-Waterschap van Woerden, 1994e) (Groot-Waterschap van Woerden, 1994f) (Groot-Waterschap van Woerden, 1994g) (Groot-Waterschap van Woerden, 1994h) (Groot-Waterschap van Woerden, 1994i) (Groot-Waterschap van Woerden, 1994j) (Hoogheemraadschap De Stichtse Rijnlanden, 1996) (Hoogheemraadschap De Stichtse Rijnlanden, 1997) (Hoogheemraadschap De Stichtse Rijnlanden, 1997) (Hoogheemraadschap De Stichtse Rijnlanden, 2002) (Brouwer groep, 1994) (Ingenieurs bureau BCC, 2003)

More land elevation sources were explored such as historical topographical maps and elevation measurements from soil drillings in DINOloket. There were two reasons that these sources were not added; Primarily because the gain from adding these sources would be additional points in space, but seldom more points in time. This thus makes the addition less valuable for the overall elevation development over time. Secondly, the translation from a map to useful digital data takes a considerable amount of time. For these reasons it was decided not to introduce these sources.

Surface water (SW) levels are obtained using both historical and digital data. The historical sources give the SW levels (height of the water in the ditches) for a specific moment of the year, usually only the summer. Depending on the date of the source this is with reference to AP or NAP. The sources used are:

- Historical data:
    - Privately financed historical maps such as (van de Kasteele, 1850) and (Hoekwater, 1901).
    - An historical book containing the summer surface water levels, size and drainage of the polders of the water authorities in the Province of Utrecht in 1883 (Provinciale Waterstaat, 1883).
    - A historical map from the hoogheemraadscahp Amstelland (Amstelland, 1898).
    - Five different *Waterstaatskaarten* created by Rijkswaterstaat between 1869 and 1981.
    - A military topographical map created by Ministry of War (Ministerie van Oorlog, 1910a; Ministerie van Oorlog, 1910b). For the study area this map was established in 1910.
- Area averaged surface water levels obtained from the water information system (WIS) (WIS-HDSR, 2013) of HDSR. Depending on the polder this source becomes available starting at 1990. Although data is available for every day of the year only the 1st and the 16th of the months June till August are used.
- An internal ArcGIS map (Hoogheemraadschap De Stichtse Rijnlanden, sine anno) containing the *peilbesluit* water levels of the currently valid *peilbesluit*. This is used only for the polders with missing WIS 2.0 data.

Data on soil characteristics:

- The clay thickness of the layer on top of the peat layer is obtained using the base data of Phoenix. This map has clay values in one cm intervals. In the data there are three major groups of 0, 30 and 60 cm clay. This has to do with the way the data is collected and translated from soil type to clay thickness (van der Schans & Houhuessen, 2012), in reality much more variation is present (van Hardeveld, 2014). The assumption is made that the thickness of the current top clay layer, which does not oxidize, remains the same throughout time.
- The soil types added are from (Stouthamer et al, 2008). Using these soil types a multiple regression relation is established, this relation however is identical to the relation obtained for the clay data set. As the clay data set was directly translated from this soil map. So the three major groups described in the bullet point above (0, 30 and 60 cm clay) are three different soil types coded as hVb, pVb and Rv01C respectively. The soil types are thus included within the data set but henceforth not reported for further analyses.

Data processed

All these sources can be transformed into data points (DP). This single point in space has several land and surface water elevations throughout time. First a base data set is chosen to which all the data is connected, a choice between all available elevation data (AAED) and only the digital elevation maps (DEM) is made. After the base data set is established the land elevation is added and DPs are excluded based on:

- Land use, using LGN6 (Hazue, Schuiling, Dorland, Oldengarm, & Gijsbertse, 2012). All land uses other than agricultural grass are deleted. In this way the land use in the data set is uniform and thus does not impact the land subsidence rate.
- Limited correlation. DPs where the linear land elevation vs. time is $r^2 < 0,75$ are assumed to have measurement errors and are therefore deleted.
- Visual outliers. DPs that have subsidence rates or elevations far exceeding that of their neighbours are manually deleted.

The SW levels are added using polders as a region with one and the same SW level at some point in time. Polders tend to split up over time. This means that polders as they existed in 1890, might currently exist as five smaller polders. For this reason polder shapes in ArcGIS are established reasoning backwards from current (small) polders to historic (large) polders. In case of the above mentioned example this would mean that the polder exists out of five different polygons with all the same summer water level in 1890 and five different summer water levels in 2014. Two adjustments are made to the SW levels after they are connected to the DPs:

- AP to NAP correction. Data sources prior to 1910 use AP (Regional ordnance datum) which is slightly different from the NAP (Dutch ordnance datum) (Stichting Normaal Amsterdams Peil, sine anno). Using an interpolation technique named spherical areal interpolation in ArcGIS., the reported AP-NAP relations for several municipalities in 1888 (Nederlandsche Rijkscommissie voor Graadmetingen Waterpassing, 1888) can be transposed to all existing municipalities as they existed at this time (University Utrecht, sine anno). Using these AP-NAP relations the SW levels of the historical sources prior to are adjusted.
- Locations where the SW level exceeds the land elevation in 2008 are reported to be under water, but in reality are not under water. These points are excluded.

After the addition of the land and SW elevation data, the clay thickness is added. For some DPs there is a lack in data. At least one of the four added variables (land or SW elevation, clay or soil type) is lacking. These DPs are deleted. The end result is a data set suitable for the representation of land subsidence as a consequence of freeboard, water levels, clay thickness and soil type.

The pre-processing is visualized in figure 5.

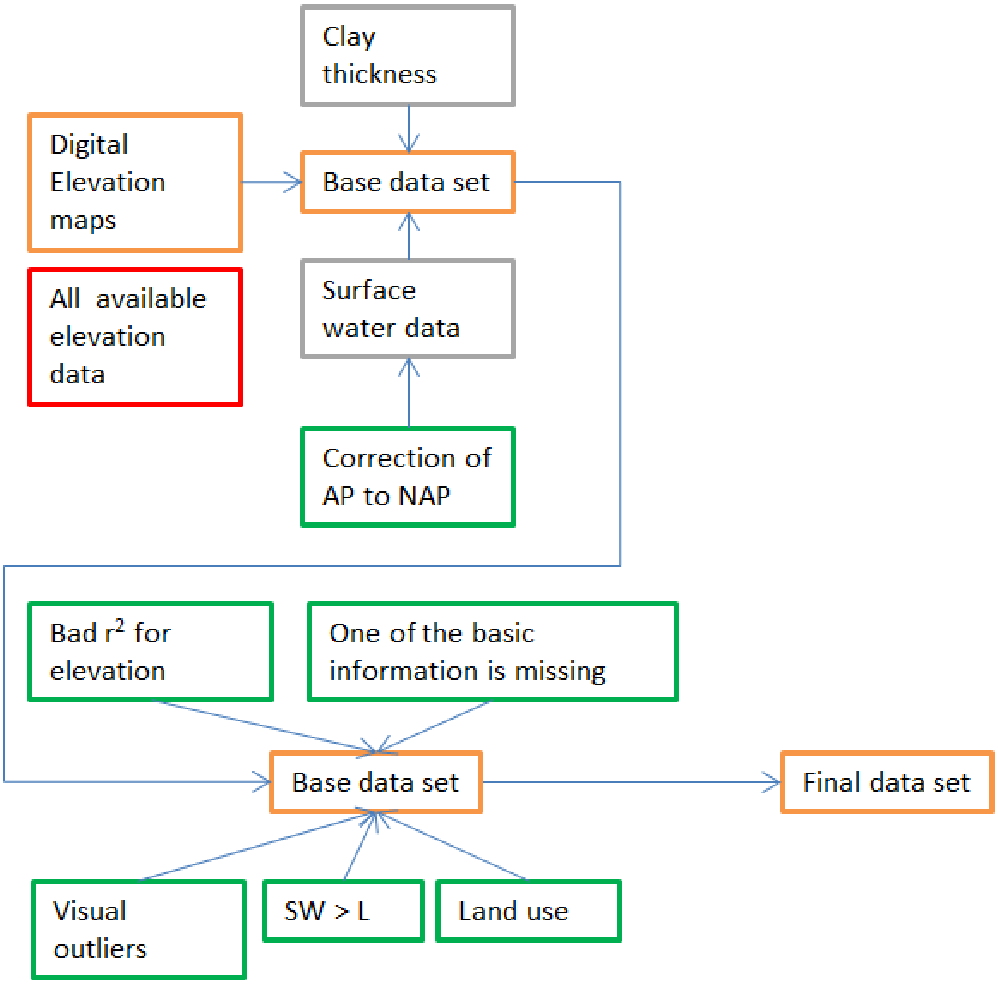

Figure 5: *Flow scheme of preprocessing, unfit data set (red), used data set (orange), added data (grey), adjustment or deletion (green). The location of this pre processing within the entire research can be seen within the dotted box in figure 3.*

Final data set of the pre-processing

The actual pre-processing can be found in Appendix B. The output of this pre-processing is a data set containing DP with surface water elevations, land elevations and clay thickness as shown in figure 6.

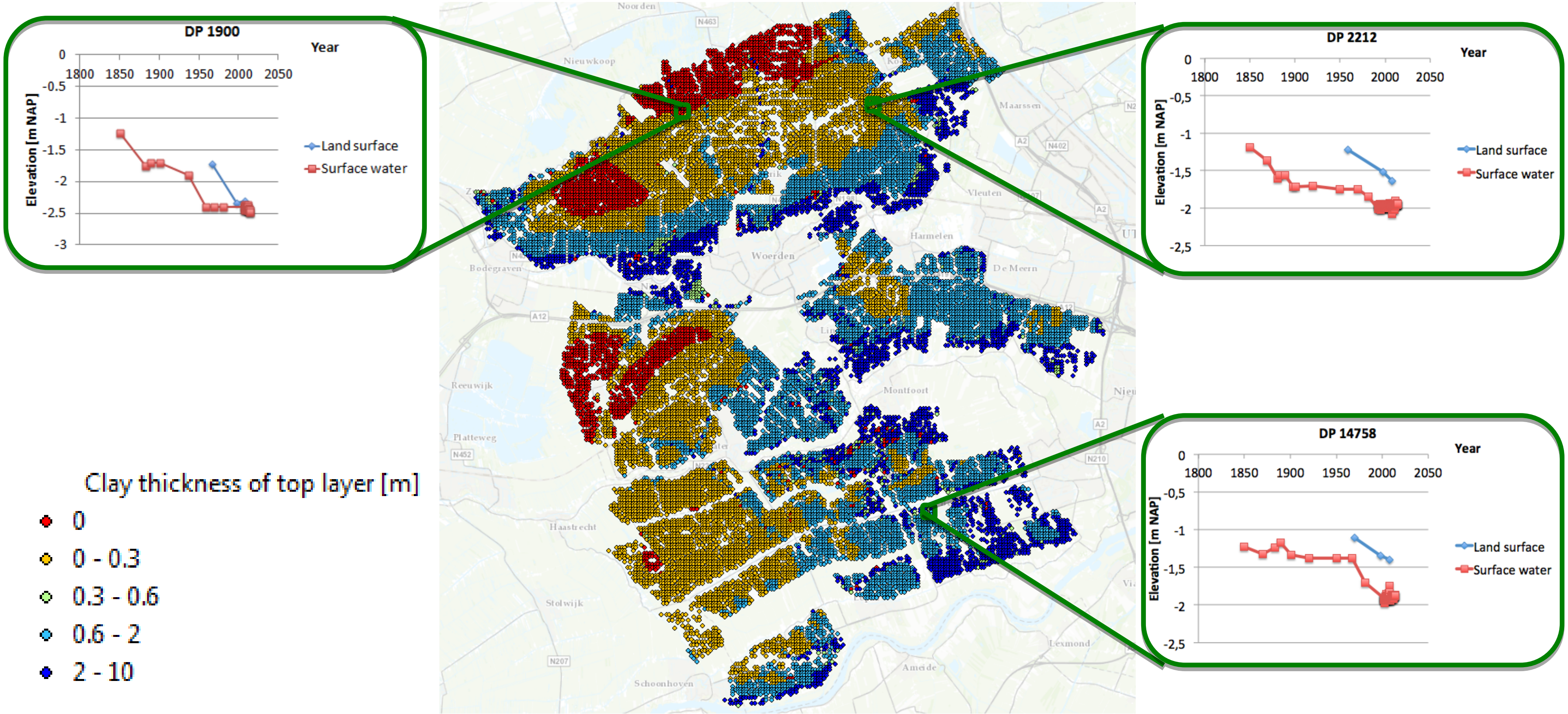

Figure 6: *Final data set including 18174 data points visualized by different colours according to clay thickness of the top layer. The elevation data and surface water data over time were added for three arbitrary points seen in the graphs.*

3.1.2 [RQ1.1] Determination of historical land subsidence

Data processed

Every DP has several land elevation measurements over time. For these land elevations both a linear and second order polynomial function is established, the derivative of these functions represents the land subsidence rate. There are three reasons for establishing the linear land subsidence. Primarily because linear land subsidence can be viewed as the average land subsidence rate between the first measurement and the final measurement, regardless of the variation in subsidence speed over this time[3]. Secondly, if elevation data is irregular or unrealistic the r^2 value can be used to exclude these DPs, as was done in the pre-processing. Finally, if a specific point in time has a measurement error the impact on the overall land subsidence rate is less compared to a second order function.

The higher order polynomial function is required to determine land subsidence rates at different moments in time, not just the average. Considering that land subsidence is dependent on the freeboard this makes sense (van den Akker, 2007; van der Schans & Houhuessen, 2011). If the freeboard does not change the subsidence rate would remain the same over time, hence a linear relation is sufficient (land elevation 1: figure 7). However if the water levels are not adjusted the freeboard would decrease over time and thus the subsidence rate is expected to decrease (land elevation 2: figure 7).

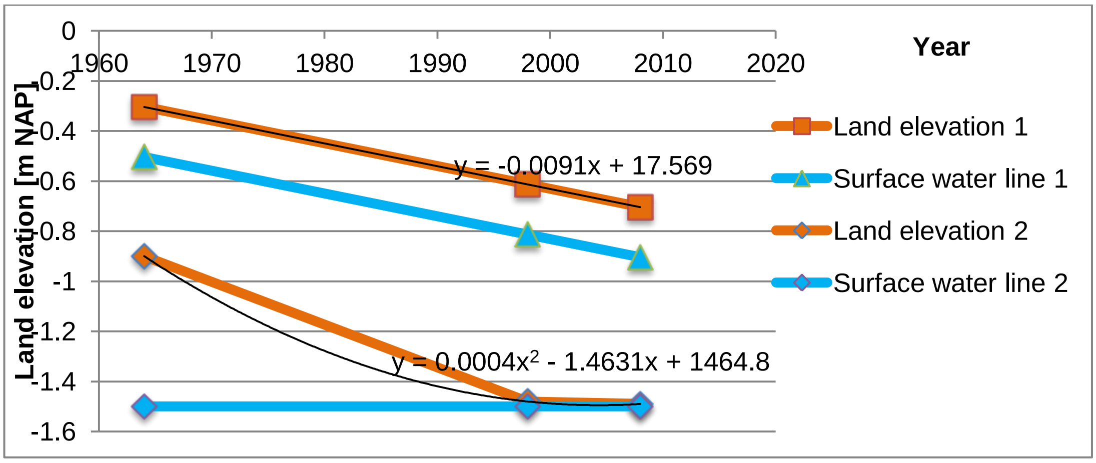

Figure 7: *Reasoning for the requirement of land subsidence as a second order functionby looking at the expected relation between land elevation (orange) and surface water elevation (blue) over time. Land elevation (orange) in the top line (land elevation 1) describes land subsidence as a linear function in a situation where it is viable, the bottom line (land elevation 2) describes land subsidence as a second order function in a situation where it is needed.*

As the subsidence rate is the derivative of the elevation decline over time (the polynomial second order function) and thus dependant on time it is able to have different land subsidence rates in different time periods. As will be shown in 4.1.3, for most polders the land subsides faster than the surface water thus having a decreasing freeboard over time, making

[3] The first elevation measurement varies between 1948 and 1972 the total subsidence ought to be described as for example one meter in 54 years for the 1948 DPs and 78 cm in 42 years for the 1972 DPs, both however can be described as 1,85 cm/y. For this subsidence it does not matter whether or not the soil subsided with 3 cm/y in the first years and far slower in the last years, or vice versa .

the polynomial function necessary. These polders will thus have decreasing subsidence rates over time. The explanation for the second order polynomial function given here is the reasoning as to why a linear function does not suffice when establishing land subsidence relations for various moments in time.

Data presented

To demonstrate the average land subsidence the linear land subsidence rate for the study area will be shown in a geographical map, to illustrate fast and slow subsiding areas. Whether or not a polynomial function results in an observable difference compared to the linear function will be demonstrated by plotting the average land elevation development over time relative to 1970, with elevation observed in 1970 indexed as 0 m. This indexation of 0 m was done because the development of the land subsidence is of interest and not the exact elevation of the data point with respect to NAP which varies greatly in the study area. The land subsidence rate as a derivative of the polynomial function versus time is also given which demonstrates the change in land subsidence rate over time and thus proves whether or not a polynomial function gives a different land subsidence according to the data used. Two maps for the land subsidence rate in 1970 and 2010 are given to show the changes in land subsidence rates according to the data used.

3.1.3 [RQ1.2] Determination of historical surface water subsidence

Data processed

Surface water subsidence rates are established for all DPs. This is done using a linear function even though surface water subsidence rates can vary over time much like land subsidence rates. Because surface water elevations can vary much more (for example 20 cm's in 16 days (observed difference between two reported measurements using (WIS-HDSR, 2013)) this was reasoned to create more inaccurate functions. This was checked visually for three polders. The decision was made to stick with the linear function. For the SW subsidence three data sets are established named SW1850, SW1910 and SW1967:

- **All available historical surface water data (SW1850):** This data set uses all available historical data starting with the oldest source (van de Kasteele, 1850).
- **Post NAP introduction (SW1910):** Previous to 1910 each municipality had its own regional ordnance datum (AP) which was transferred to the Dutch ordnance datum (NAP). Although officially the date of the introduction of the NAP was on 1 January 1891 (Stichting Normaal Amsterdams Peil, 2014; Platformfundering, 2014) only the historical sources used after 1910 use NAP as a reference level, previous to this moment AP was still used.
- **Increase in freeboard (SW1967):** During the end of the sixties and the beginning of the seventies water levels were lowered significantly for agricultural purposes (van den Akker et al, 2007). This means that the corresponding land subsidence after 1967 is expected to be faster than it was prior to 1967 due to this larger freeboard. Currently relatively large freeboards, compared to prior to 1967 are still maintained.

Data presented

The geographical SW subsidence rates for SW1850, SW1910 and SW1967 are given, as well as a bell curve to show the normal distribution of each data set. After this an argument is made about which data set ought to be used for further analyses supported by using a graph for illustrative purposes to demonstrate characteristics of SW1850, SW1910 and SW1967.

Visualization of functions in RQ1.1 and RQ1.2

For additional understanding of the established relations in RQ1.1 and RQ1.2 box 1 is added.

Box 1: Visualization of the established functions

The trend lines established for each individual data point are as follows. The DP used in this example is data point 1900, this is the same DP used in figure 6 top left.

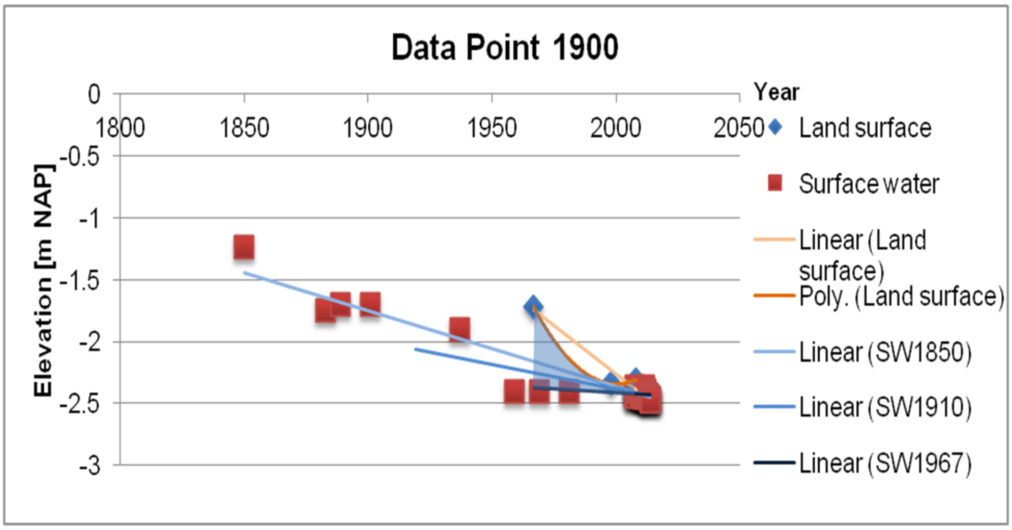

Figure B.1: *surface water and elevation measurements for data point 1900 with the corresponding regression relations established, freeboard (shaded blue)*

As can be seen in figure B.1 a total of 5 different functions are used. For the land subsidence the linear land subsidence as well as the second order polynomial function. For the three surface water groups a linear function is applied and lastly the shaded blue area represents the freeboard (established in RQ1.3). The functions corresponding to the trend lines and their derivatives are used in RQ1.

3.1.4 [RQ1.3]Relation between land subsidence and surface water subsidence (as a function of soil composition)

In this research question two relations can be read. The first is how do land subsidence and surface water subsidence relate to one another. This relation describes the way in which the policy has been adjusted to match the land subsidence. The second relation is the relation between the land subsidence as a function of freeboard and the soil composition: clay thickness of the top layer.

Data processed

Relations between variables can be extracted directly from the DPs. Different variables which can be obtained from the data connected to these DPs do have to be created and are discussed for the respective relation below.

Relation land subsidence vs. surface water subsidence

For the first relation describing the policy development a new variable is introduced, namely *peilindexation*. The SW levels found in the historical sources are based on *peilbesluiten* which are manmade decisions. These decisions can either be made in accordance with land subsidence so that the freeboard remains the same, or it can deviate for example by not changing the SW levels and thus letting the freeboard diminish at the rate of land subsidence. Reasons for this deviation can be changes in policy, changes in land use or redistribution of land (Nederlof, 2014).The variable that describes the degree to which adjustments are made in accordance with the land subsidence is named peilindexation. Calculated as follows:

$$i = \frac{linear\ \Delta SW}{linear\ \Delta L} \qquad \text{(Eq. 9)}$$

Wherein:
i :Peilindexation
ΔSW :linear SW subsidence rate
ΔL :linear land subsidence

Here the linear land subsidence is used as it can be seen as an average subsidence over the time period it is measured[4]. The meaning of the variable Peilindexation is explained in table 1:

Table 1: *Meaning of the variable Peilindexation.*

i	Policy	Meaning
< 0	Inverse policy	Surface water subsidence goes in the opposite direction of land subsidence
0 - 1	Independent policy	Surface water subsidence rate is slower than land subsidence rate
=1	Reactive policy “*Peil volgt functie”.*	Land subsidence dictates surface water subsidence
>1	Exceeding policy	Surface water subsides more rapid than land subsidence

Multiple regression relation land subsidence vs. clay thickness, freeboard

As stated in the theory (Eq. 7) land subsidence is dependent on both thickness of the unsaturated zone and the clay thickness. Because surface water levels are known and not groundwater levels the freeboard (surface water level to earth surface) is used instead of the unsaturated zone (groundwater level to earth surface). Freeboard is defined using the following function:

$$FB_t = L_t - SW_t \qquad \text{(Eq. 10)}$$

Wherein:
L_t : Soil elevation (m+NAP)
SW_t : Surface water level (m+NAP)
FB_t : Freeboard (m)
t : Time (Calendar year)

[4] Because the first elevation measurement varies between 1948 and 1972 the average subsidence ought to be described as for example one meter in 54 years for the 1948 DPs and 78 cm in 42 years for the 1972 DPs, both however can be described as 1,85 cm/y. For this average subsidence it does not matter whether or not the soil subsided with 3 cm/y in the first years and far slower in the last years.

FB_T is established for each specific data point with a 10 year interval adding up to 5 FB_T values since 1970, this start date is chosen because the selected surface water data set starts in 1967 and the start date of the elevation data is 1970. This is done using the polynomial land subsidence rate (Box 1).

In order to properly compare the observed relations with the Phoenix formula a similar form has to be used. It is possible to create a multiple regression relation where one variable is dependent on two others by creating a 3D plot. When using a linear function in the direction of both independent variables the relation looks as (Eq. 12). This is the same form as the original Phoenix formula with the only difference being that it is with respect to surface water and not groundwater. So in order to compare the relations obtained in this master thesis with the relations obtained by van den Akker et al, 2007 the formula needs to have the same independent variables.

In van den Akker et al, 2007 the basic formulas (Eq. 5 and Eq. 6) are given with respect to GLG. In van den Akker et al., 2007 this same relation was also established for ditch water levels, i.e. surface water levels and is conjugated in the same way as the general Phoenix formula in Appendix D. The resulting formula is:

$$\Delta \mathrm{L} = -15.5 * \mathrm{FB} + 20.9 * \mathrm{C} - 2.75 \qquad \text{(Eq.11)}$$

The established multiple regression relations in this thesis using completely separate data is done by applying a linear function in the direction of both independent variables being the clay thickness and freeboard. This results in the following formula which is identical in form to Eq.11.

$$\Delta \mathrm{L} = \mathrm{a} * \mathrm{FB} + \mathrm{b} * \mathrm{C} + \mathrm{c} \qquad \text{(Eq.12)}$$

Wherein:

a	:Land subsidence variable [10^{-3}/y]
b	:Clay constant [10^{-3}/y]
c	:Soil composition constant [mm y^{-1}]
ΔL	:Land subsidence rate [mm y^{-1}]
FB	:Freeboard [m]
C	:Clay thickness of the top mineral layer [m]

The units of the 'abc'-variables correct for the different units on the left and right hand side. The addition of units to the regression constants is quite common (van Beek, 2014). The 'abc' variables are compared to the van den Akker relation (Eq. 11).

A distinction between two clay thickness groups is applied. One using all clay thicknesses (from 0 - 11 m) to show the relation for all data points and one using clay thickness from 0 - 0.6 m. This second group is made because most of the subsidence is expected to happen in the shallower parts of the soil above the water table. Within this shallower part there are three large data clusters at 0, 0.3 and 0.6 m clay which make up 93% of the data points within the shallower soil. Thus the 0,6m cut off holds sufficient points for an appropriate multiple regression relation.

Data presented

Relation land subsidence vs. surface water subsidence

The relation between land subsidence and SW subsidence is directly put in a geographical context using the average peilindexation between 1970 and 2010 for the polders as established for this master thesis, thus demonstrating the degree with which the SW levels have been adjusted to match the land subsidence rate for these polders. The polder average peilindexation is used because the policy decisions are made on a polder scale and not the scale of the individual points. No graph is plotted with land subsidence vs. surface water subsidence as this demonstrates no pattern and an r^2 of zero.

Multiple regression relation land subsidence vs. clay thickness, freeboard

By combining the 2nd order land subsidence rate, freeboard and clay thickness as variables using Matlab a 3D relation is established. The resulting formulas and correlation of the multiple regression relations are entered into tables. This includes the five moments in time for two different clay thickness categories. The actual plots corresponding to the formulas are added in Appendix E and F. This results in the following general formula:

$$\Delta L = a * FB + b * C + c \qquad \text{(Eq. 12)}$$

Year	r^2	'a'-variable	'b'-variable	'c'-variable

The correlation of the obtained multiple regression relation can be used to demonstrate the reliability of the formula. However a bad correlation (r^2) does not necessarily mean that the relation is unreliable, it could also mean that it is not uniform throughout the study area, i.e. regional differences are present. If one region has a faster subsidence rate under the same conditions (FB and C) compared to another region both these regions are compared and used to obtain an average land subsidence relation, and both affect the correlation. A correlation of r^2 =1 can only be obtained when all the input data are perfect (no errors) and there is no regional difference to be observed and thus everything can be explained using one formula.

In the tables a colour scheme is added to represent whether or not the obtained relation is comparable to the conjugation of the van den Akker formulas for ditch water (Eq.11).This is done in the following way:

Table 2: *Colour scheme to visualize the comparison of the obtained relation with the conjugated van den Akker formula for surface water (Eq. 11)*

'abc'-variable falls within the range of ... compared to (Eq.11)	±1	±2	±3	±4	±5	±6	±7>
r^2	<0.6	0.5	0.4	0.3	0.2	0.1	>0.1

So for example if the obtained 'a'-variable, 'b'-variable or 'c'-variable is 1 higher or lower compared to (Eq.11) the colour will be dark green, when this difference is 4 it will be yellow etc.. This allows for a quick visual whether or not the formula resembles the existing formula (Eq.11). The 3D graphs connected to the respective relations will be added as well in Appendix E and F.

3.1.5 [RQ1.4] Obtaining and implementing regional differences in Phoenix

Data used

The formulas obtained in RQ 1.3 together with the observed land subsidence connected to the DPs forms the basis of the data used in this RQ.

Data processed

Using the relations found in RQ1.3 as a general relation the difference between the expected value, being this relation, and the observed land subsidence rate it is possible to see whether or not the relation under or overestimates the land subsidence.

$$RD = \Delta L_{relation} - \Delta L_{observed} \quad \text{(Eq.13)}$$

Wherein:
RD :Regional differences [m y^{-1}]
$\Delta L_{relation}$:Land subsidence rate from obtained relation [m y^{-1}]
$\Delta L_{observed}$:Land subsidence rate as observed from elevation data [m y^{-1}]

Table 3: *Meaning of the RD value*

RD	Meaning
>> 0	Severe underestimation
>0	Underestimation
=0	Good approximation
<0	Overestimation
<< 0	Severe overestimation

The obtained regional differences would have been used to adjust Phoenix by changing the "a and b" variables of the general formula (Eq.7) per Phoenix data point. As will be shown in the results (chapter 4.1.4) the regional differences are explained by an error, hence the regional differences were not implemented in Phoenix. Therefore, the exact method for implementing is not explained in more detail.

Data presented

The value of RD are visualized in a geographical map using the DPs for each time period using quantiles for the different value categories. The legend used will be stated in text rather than numbers, for example predicted >> observed. This geographical map shows the patterns of locations where for some reason the land subsides faster or slower than expected. The RD patterns are compared to the elevation variation found in AHN1 (Appendix C).

3.2 [RQ2] Effect of increasing temperatures due to climate change on land subsidence

The impact of climate change (CC) on groundwater levels and evaporation during the summer and winter was included in Phoenix in prior studies (van Bokhoven, 2014b). However currently the model does not contain the temperature change due to CC, which influences the biological activity, as a separate parameter (van der Schans & Houhuessen, 2011). The implementation of the temperature impact is explained below.

3.2.1 [RQ2.1]Predicted temperature increase due to climate change

Data used

The climate scenario used is the W+ scenario of (Koninklijk Nederlands Meteorologisch Instituut, 2006), which is the worst case scenario for climate change in the Netherlands. Although other scenarios are available this climate change scenario is the same version used in previous climate change studies using Phoenix (van Bokhoven, 2014b).

Data processed

The temperature increase of the W+ scenario goes up to 2100. Since Phoenix calculates up to 2200 the W+ scenario has to be extrapolated to 2200. This is done by using the growth function of Excel which uses previous values being the temperature in 1990, 2050 and 2100 as predicted in (Koninklijk Nederlands Meteorologisch Instituut, 2006) and extrapolates this trend towards 2150 and 2200. This results in a near linear extrapolation. This is done for the summer average temperature as most oxidation takes place during the summer (van den Akker, 2007).

Data presented

The data is presented using a graph with average summer temperature increase vs. time.

3.2.2 [RQ2.2]Influence of temperature on land subsidence

Data processed

First a general relation between an increase in temperature and the biological activity is established. The most commonly used formula for this relation is the Q_{10} value found in laboratory research (discussed in Chapter 2.1: physical theory)

$$f_{t,Q_{10}} = Q_{10}^{\left(\frac{T-Tr}{10}\right)} \qquad \text{(Eq. 3)}$$

Where Q10 represents the impact 10˚C temperature change has on the biological activity. This relation is then multiplied by the fraction of land subsidence contributed to oxidation, which is the only process that changes. This fraction is an assumption based on literature (Chapter 2.1: physical theory). The reason for this is that the formula (Eq.7) is based on empirical black box formulas which does not go into detail about the exact fractions for each land subsidence process. The output of this sub question is a general formula for the increase in land subsidence per degree of temperature increase.

Data presented

The general formula is presented using a graph with activity in percent vs. temperature in ˚C. The impact climate change has on land subsidence is then is established by combining the temperature increase of RQ2.1 and the increase in land subsidence per ˚C from RQ2.2 and plotted in a similar graph.

3.2.3 [RQ2.3]Implementing the increase in land subsidence due to climate change in Phoenix

Data processed

The increase in oxidation rate due to climate change is implemented by using the following formula. The fraction named CC (T_{i+2000}), represents the impact of climate change for the period of T_{2000} until T_i. This can be reported in one formula seen below (Eq.14).

$$\mathrm{CC}(T_{i+2000} - T_{1990}) = \frac{\sum_i^n (F_{oxidation} * \left(\mathrm{Q}_{10}^{\left(\frac{T_{i+2000} - T_{1990}}{10}\right)} \right))}{n} \qquad \text{(Eq. 14)}$$

Wherein:

CC (T_{i+2000})	:Increase in ΔL due to CC [%]
$F_{oxidation}$	:Fraction of land subsidence contributed to oxidation [%]
Q_{10}	:Increase biological activity 10˚C [%]
T_{i+2000}	:Temperature in year i+2000 [y]
T_{1990}	:Temperature in 1990 [y]

What this formula does is essentially the same as what the graphs demonstrated in RQ2 show but allows for a quick calculation of one number rather than having to look in the figures for the average increase in oxidation due to climate change. The CC (T_{i+2000}) is incorporated in the general Phoenix formula (Eq.7) by multiplying the velocity term 'a' by the actual increase.

$$\Delta \mathrm{L} = (\mathrm{CC}(\mathrm{T}_{\mathrm{i+2000}}) * -0.023537) * \mathrm{D} + 0.01263 * \mathrm{C} + \ 0.00668 \qquad \text{(Eq.7.CC)}$$

Data presented

The new ‘a’ variables are given in a table for four time periods with a 50 year interval, and the value for a run from 2000-2200.

3.3 [RQ3] Aggregated effects on simulated land subsidence in Phoenix

Data processed

The final step is verifying how (where, and how much) the regional differences in land subsidence (RQ1) and temperature (RQ2) increase due to climate change give a different simulated land subsidence compared to the original model. This results in a total of four model runs. However because no useable regional patterns could be obtained only two runs are done. The base run without changes and the model implementing climate change. These runs are done for the Variant0 scenario, which can be considered a business as usual scenario (van Bokhoven, 2014b).

The comparison between the outputs will be done by examining the absolute difference as well as the percentage difference between the cumulative land subsidence.

Data presented

For both runs the cumulative land subsidence is displayed in a geographical map of the Western area of HDSR. The two graphs obtained from the comparison will be displayed next to one another, one including the absolute difference and one including the percentage difference.

4 Results

4.1 [RQ1] Effects of regional differences in soil type and in surface water subsidence on land subsidence

4.1.1 [RQ1.1] Determination of historical land subsidence

Linear function for land subsidence

The total land subsidence in the study area over the last 40 years, looks as follows (figure 8):

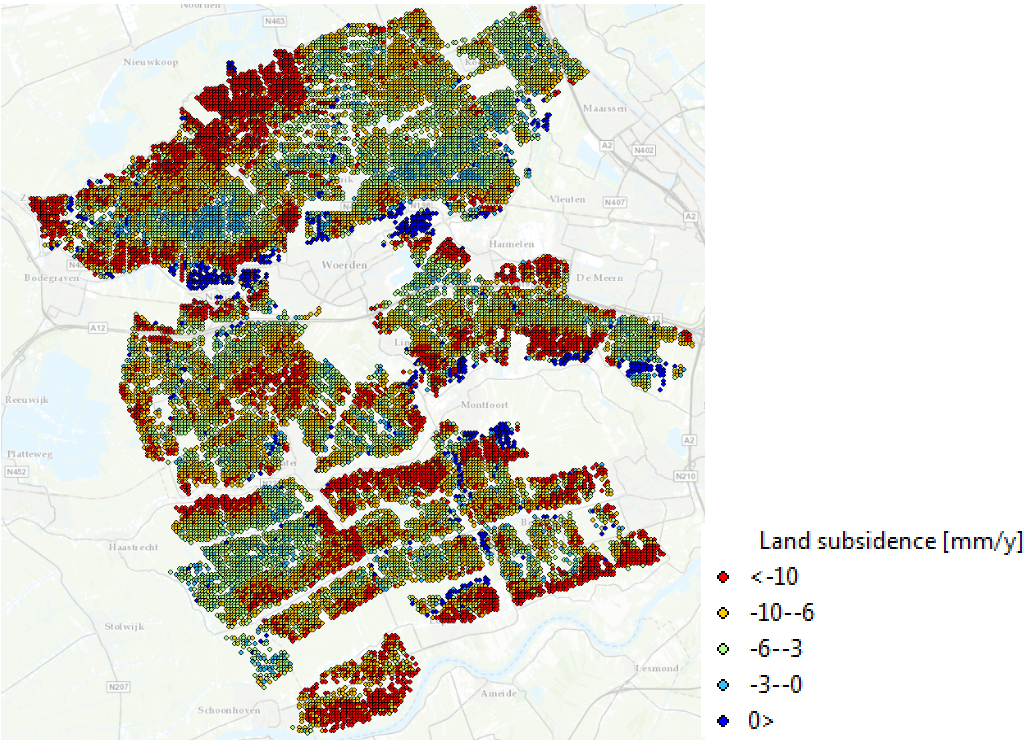

Figure 8: *Average(/linear) land subsidence in the study area between 1970 and 2010*

On average the land subsidence rate has been 7,7 mm/y. The top part of Zegveld, which is located in the north western part of the study area, has the fastest subsidence rates going up to 61 mm/y and is the only part where the subsidence exceeded 30 mm/y within the study area. The slowest subsiding soils trace the Oude Rijn which are just above the middle of the study area going from east to west past Woerden. Several of these points indicate land rise going up to 29 mm/y. There is no real explanation as to why these points appear to rise other than a possible measurement error in the data used.

Polynomial second order function for land subsidence.

In the methods the reasoning as to why a second order function is required when examining land subsidence in different moments in time is explained. Here the results of using a second order function are given starting with the average land elevation and average land subsidence rate vs. time (figure 9).

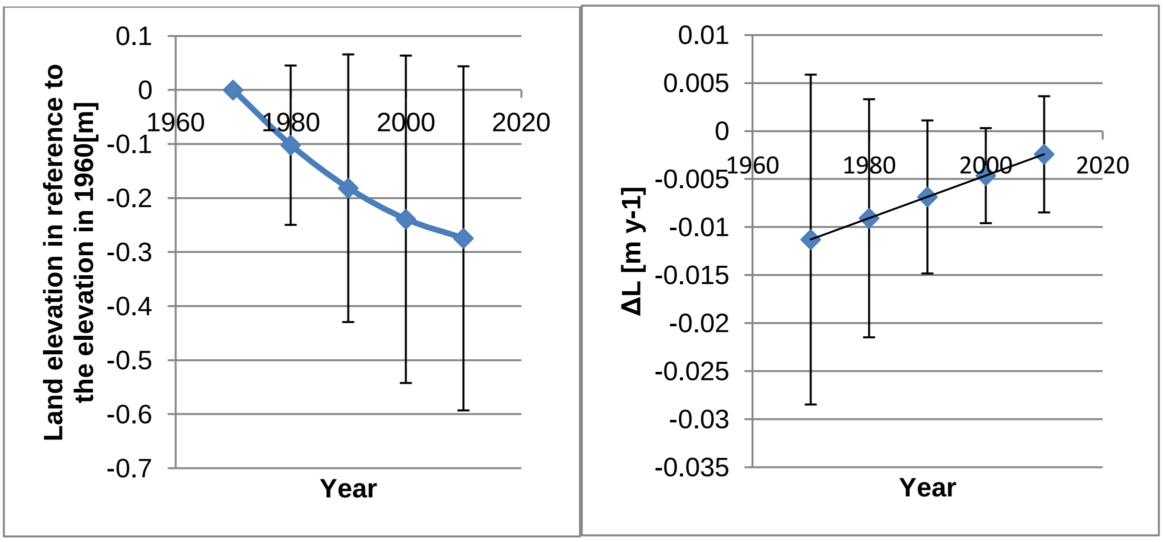

Figure 9: *Average land subsidence as second order function vs. time, including standard deviation(left), The derivative being the land subsidence rate vs. time, including the land standard deviation (right).*

Figure 9(left) shows that on average the shape indeed resembles a second order function where the land subsidence rate decreases over time figure 9(right). This thus proves that according to the data used a polynomial function is more suited to illustrate the land subsidence over time, since land subsidence rates have not been constant since 1970. This observed difference, combined with the reasoning provided in the methods, means that the linear land subsidence can't be used for the establishment of land subsidence relations (RQ1.3).

The geographical distribution of the land subsidence rates using this polynomial function in 1970 and 2010 look as follows (figure 10).

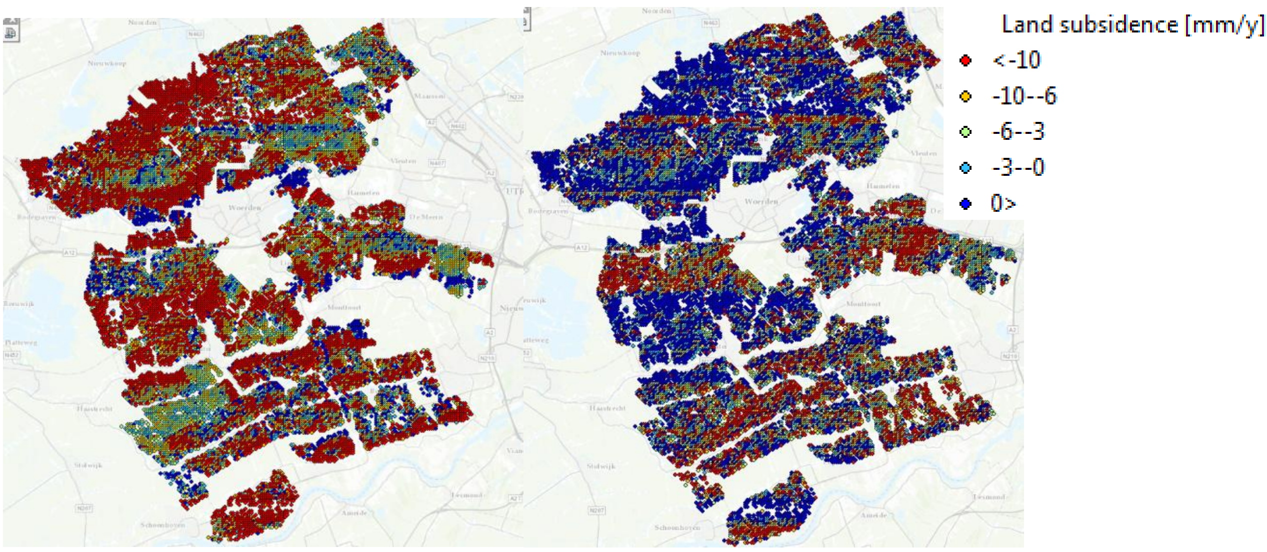

Figure 10: *Land subsidence rate as the derivative of the 2nd order function in 1970 (left) and 2010 (right) for the study area.*

The pattern of the 2nd order land subsidence rate in 1970 (figure 10(left)) is somewhat similar to the average(/linear) land subsidence (figure 8). Zegveld (north) still has the fastest subsiding soils, albeit much faster and the soils near the Oude Rijn still do not subside. It can clearly be observed that the land subsidence rates in 1970 are far higher than they were in 2010 (figure 10(right)) (the same scale is used for both). Areas that subsided fast in 1970 no longer do so in

2010 and in most cases show land rise, rather than subsidence. This is illogical and unexpected. Additionally within the figure horizontal lines can be detected, most notably in figure 10(right). Both the land rise and horizontal lines are likely due to measurement errors which play a major role when using a polynomial function. The measurement in 1999 (AHN1) appears to have an error that often causes the land elevation to be lower than expected. Much of this error can be traced back to specific laser altimetry flights. In Appendix C these errors in measurement of AHN1 are explored. The impact of this consistently lower land elevation of AHN1 is that the land subsidence rate for the first half of the selected time period (1970-1990) is higher than would be expected and the second half of the selected time period (1990-2010) the land subsidence rate is slower, i.e. the slope in figure 9 is too steep compared to the actual land subsidence rate.

4.1.2 [RQ1.2] Determination of historical surface water subsidence

As described in the methods there are three data sets. The first uses all available SW data (SW1850), the second data set represents data after the establishment of the NAP as a nationwide ordnance level (SW1910) which takes out possible errors in the interpolation of the AP-NAP relation and the final data set is the period after the increase in freeboard (SW1967) which makes the water management situation comparable to the current situation. The linear SW subsidence for the three temporal boundaries looks as follows (Figure 11).

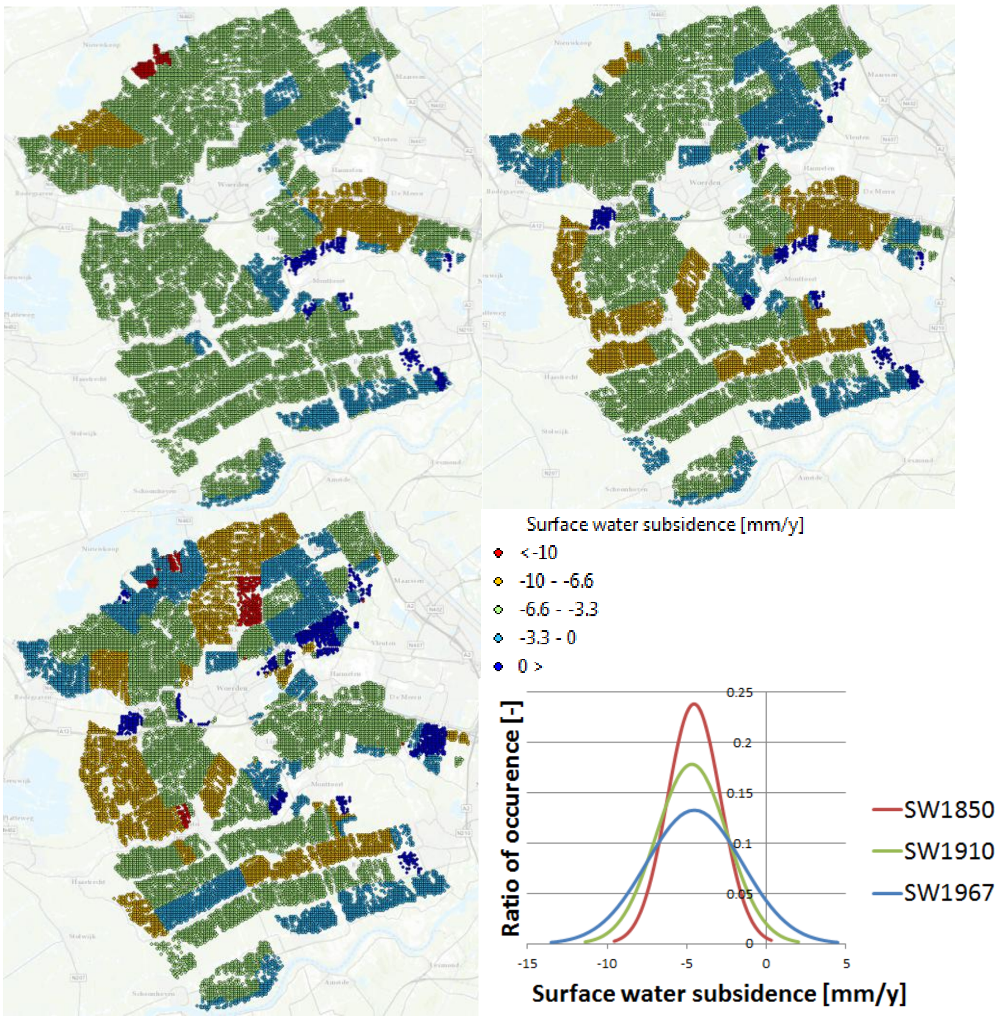

Figure 11: *The surface water subsidence for SW1850 (top left), SW1910 (top right), SW1967 (bottom left) and the normal distribution for all three datasets (bottom right).*

Overall the average subsidence rate for all polders regardless of the data set is around 5 mm a year (figure 11: bottom right). However it can be seen that the variation in subsidence rates increases the shorter the total time span of the data set becomes, both when looking at the standard distribution as well as the maps with subsidence rates. This means that SW1967 has more polders with fast subsiding SW levels and more polders where the SW levels are relatively stable as opposed to SW1850.

The freeboard was increased significantly in between the 1960s and 1970s for agricultural purposes (van den Akker et al, 2007). This "jump" has two effects namely that the freeboard results in faster land subsidence after 1967 (van den Akker et al, 2007). This then may result in faster SW subsidence in order to keep up with the faster land subsidence (Figure 12: bottom red line). Another effect is that a part of the SW subsidence rates of SW1850 and SW1910 are a direct consequence of a change in policy. This can be seen in the subsidence rate of SW1850 and SW1910, i.e. the slope of the coloured lines (blue and yellow). The influence of this increase in freeboard is larger on the trendline, and thus the subsidence rate, of SW1910 as ΔT is smaller. Especially in the slow subsiding soils this creates a significantly larger SW subsidence rate for SW1850 and SW1910 (Figure 12: top trendlines).

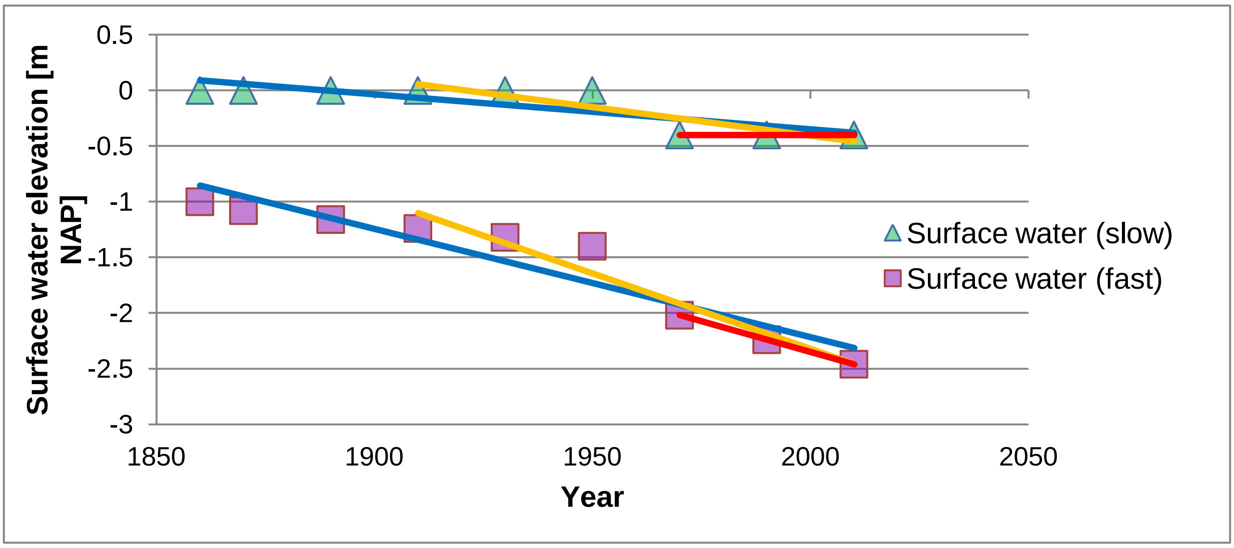

Figure 12: *Fictional graph for the purpose of demonstrating the impact of the increase in freeboard on the surface water subsidence rate. Two locations one with slow subsiding soil (green triangles), one with fast subsiding soil (purple). Linear relations SW1850 (blue line), SW1910 (yellow line) and SW1967 (red line)*

As of this point the choice is made to use the data of SW1967 as being the appropriate SW data. This was done for the following reasons:

- The elevation data used is available for this same time period (RQ 1.1). This elevation data of the same time period is required in order to establish any relation in RQ1.3.
- With a relatively large freeboard, the water management scheme is similar to that of the current situation
- The "jump" caused by the increase in freeboard is not part of the SW subsidence rate of SW1967 so the actual policy change is not part of the data, just the impact of this policy change.

4.1.3 [RQ1.3] Relations between land subsidence and surface water subsidence (as a function of soil characteristics)

4.1.3.1 Relation between land subsidence and surface water subsidence

The policy variable “peilindexation” describes the degree to which land subsidence dictates the maintained surface water levels. The area averaged peilindexation for each individual polder gives the following geographical distribution (figure 13).

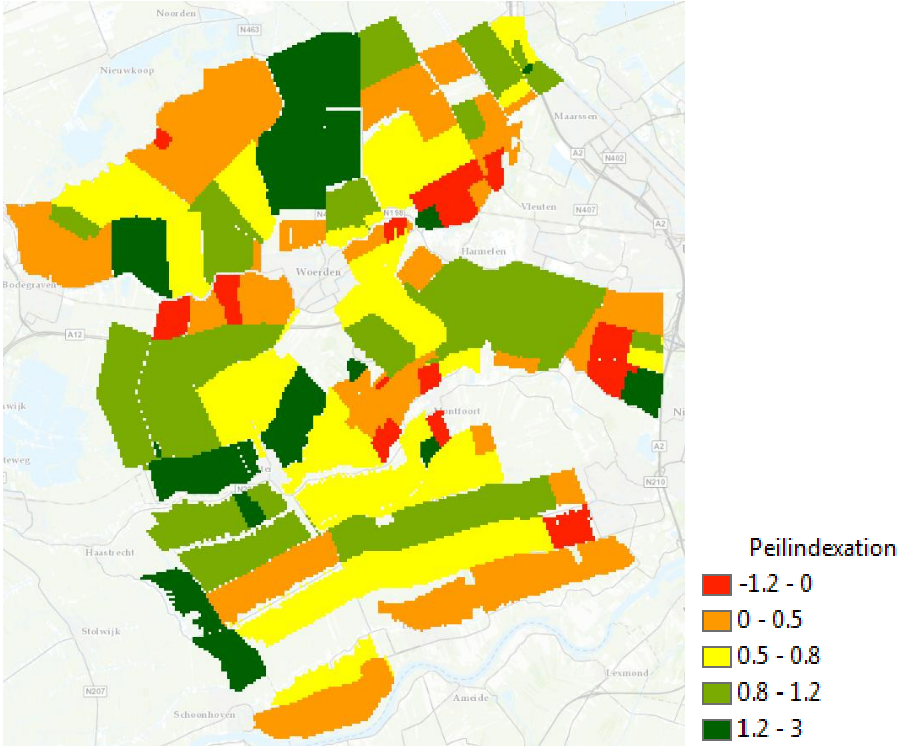

Figure 13: *Peilindexation colours represent the degree to which land subsidence dictates surface water subsidence, The meaning of the values can be observed in the table 1 (3.3: Methods).*

This figure shows that only for a small portion the land subsidence dictates the policy (light green). For most polders the policy on adjusting surface water subsidence is not dictated by land subsidence. A large part of this can be explained considering that the current guidelines for freeboard in peatland areas dictate a smaller freeboard compared to what the guidelines stated in 1980 (Nederlof, 2014). So overall the peilindexation is expected to be below one, which indeed is the case, moreso for some polders then others. One such polderareas is Lopikwaard, which are the southern most polders of the study area between Hollandse Ijssel and the Lek, here a land development plan was executed in 1978. In this development plan a relatively large freeboard was chosen. Thus when desciding the water levels in the current *peilbesluit* and considering the new guidelines the previous surface water levels were not adjusted (Nederlof, 2014). Another location where the peilindexation is very low is Zegveld. Here the same reasoning applies but with the addition of an increasing number of *onderbemaling* (locations where the maintained water level may deviate from the *peilbesluit* water levels), so here too the surface water levels were not adjusted compared to 1980 (Nederlof, 2014).

The average Peilindexation has been 0,71. This means that overall it appears that land subsidence is not dictating the maintained surface water levels and thus that there is a downward trend in thickness of the freeboard. Overall according to the general formula (Eq.7) the current day land subsidence ought to be less rapid then it was in the 70s. This is indeed the case (see 4.1.1).

Phoenix uses peilindexation as a future policy variable, which varies between 0 and 1. Figure 13 shows that serious thought has to be put in this value as this variable over the last 40 years (since 1970) has not been uniform, nor necesarily between 0 and 1. One of the current Phoenix scenario developed in (van Bokhoven, 2014b) and consequently also used in this thesis for the comparison of the input of regional differences and temperature changes due to climate change [RQ3] is called “Variant0”. This scenario uses either 0 or 1 as a value for peilindexation (figure 14). When looking at the past this does not seem to be an accurate descripition of the policy applied.

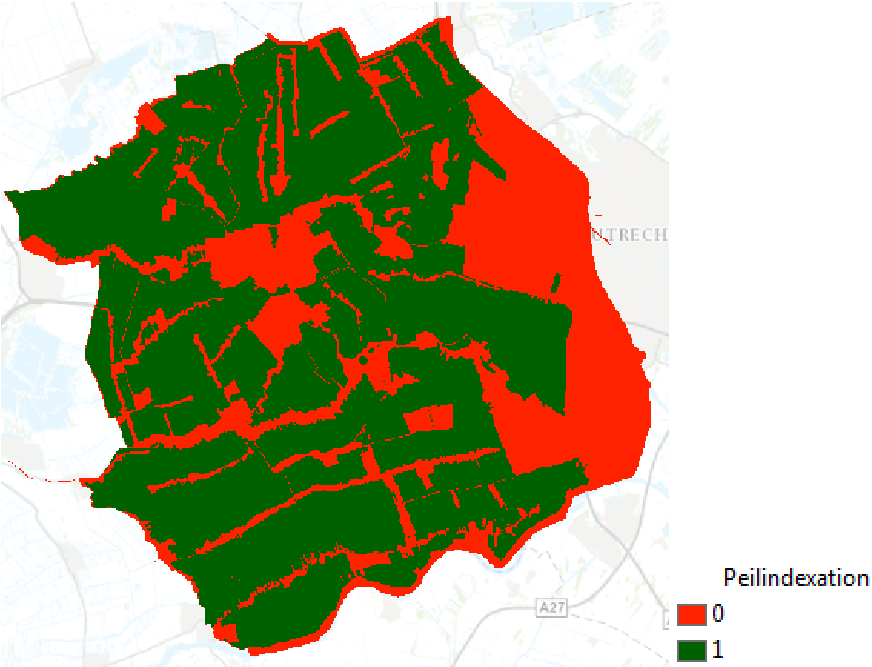

Figure 14: *Peilindexation used for variant0 scenario for Phoenix. For the polders within the study area this value is thus set at 1, being surface water adjustments in full accordance with land subsidence.*

4.1.3.2 Relation of freeboard, clay thickness and land subsidence

As described in the methods ten multiple regression relations are established. Five time intervals for each of the two categories wherein the first category includes all clay data (0 – 11 m) and the second uses clay data between 0 - 0.6 m. This thus looks as follows for the plots in 1970 (figure 15):

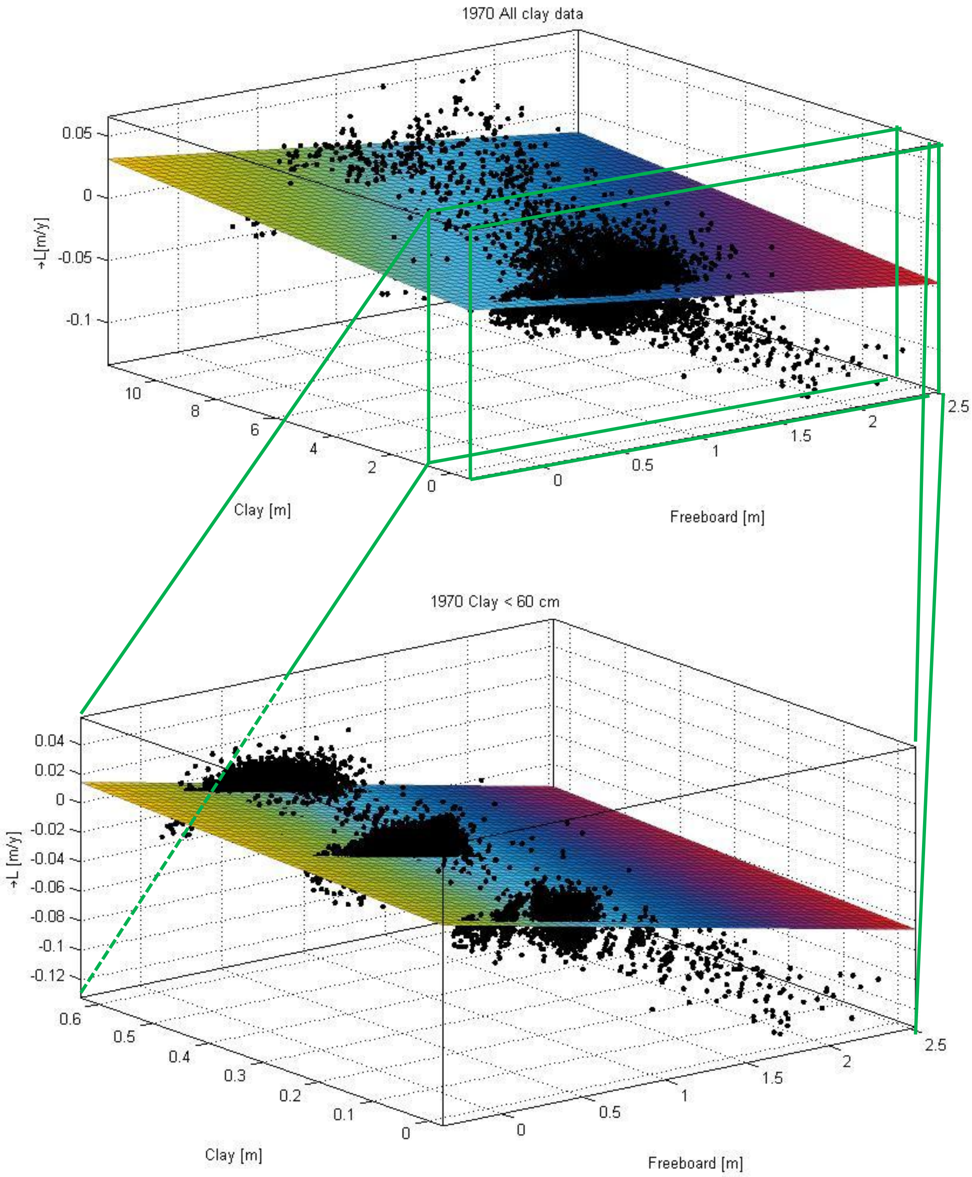

Figure 15: *Multiple regression relation land subsidence vs. freeboard and clay thickness in 1970.The inclusion of all clay data (top) and the exclusion of data over 60 cm clay cover (bottom).The formulas of the chart surface area can be found in Table 4 or Appendix E and F.*

All 10 different multiple regression relations can be found in the appendix. The relations with the inclusion of all clay data is located in Appendix F. The corresponding correlation and surface chart formula can be seen in the table below according to the visualisation as demonstrated in the methods (table 3).

***Table 4**: Relation al l clay data, r^2: correlation, a: land subsidence variable, b: clay constant, c: soil composition constant, actual plots can be found in Appendix F*

Year	r^2	'a'-variable	'b'-variable	'c'-variable
1970	0.16	-16.30	2.40	-4.00
1980	0.07	-1.20	1.20	-9.60
1990	0.07	-0.59	0.70	-7.20
2000	0.03	-4.60	0.10	-3.00
2010	0.01	4.50	-0.50	-4.20

It can be seen that the correlation is reasonably bad in 1970 and gets even worse towards 2010. So overall the function does not really accurately describe the overall land subsidence.

For every relation except 2010 the result shows that lands subside due to freeboards ('a'-variable is negative) and that clay has an inhibiting effect on this land subsidence ('b'-variable is positive). However the effect freeboard has is only comparable to the van den Akker relation for surface water (Eq. 11) in 1970 but after that point has a very small impact. The clay inhibition term is also 1 or 2 orders of magnitude smaller compared to (Eq.11). Both observations contribute to the conclusion that clay soils do not subside and that freeboard has little effect on land subsidence when including all data. This can be explained when assuming most land subsidence happens above the groundwater table (0-2m). The parts below the groundwater table, being the clay layers between 2-11 m however have a more significant impact on the multiple regression relation as they make up the largest part of the surface area of the chart (ΔC is large), and thus determine most of the function of the surface area.

The second observation is that the relation reverses in 2010, so rather than freeboard causing land subsidence it now results in land rise as the 'a'-variable is positive. When considering that a total of 5125 points have a higher elevation in 1998 compared to 2008 (Appendix C), thus have land rise but still have a positive freeboard these points demonstrate a land rise due to freeboard. These errors skew the result of the entire plot in favour of a reverse relation.

When taking less clay thicknesses into account by looking at soils with a maximum clay thickness of 60 cm still the vast majority of the data points within the study area can be used, 15490 DPs out of 18174 DPs. The actual multiple regression relations are located in Appendix E. The correlation and surface chart formula of these relations can be seen in the table below (table 5).

***Table 5:** Relation clay data up to 60 cm, r^2: correlation, a: land subsidence variable, b: clay constant, c: soil composition constant, actual plots can be found in Appendix E*

	r^2	'a'-variable	'b'-variable	'c'-variable
1970	0.23	-24.2	15.3	-4.9
1980	0.05	-7.0	6.9	-8.8
1990	0.06	-6.1	4.1	-6.0
2000	0.09	-11.7	3.3	-0.9
2010	0.02	8.4	-5.9	-3.8

For these relations the correlation still decreases after 1970, although on average it is slightly better compared to relations obtained for all clay data.

The multiple regression relations obtained for this category show the behaviour to be closer to what is expected. The impact of clay ('b'-variable) comes closer to the general formula for ditch water (Eq.11) and freeboard has a significant impact on land subsidence ('a'-variable) especially in 1970. This shows that indeed land subsidence happens in the shallower parts of the soil. The fact that land rises in 2010 is for the same reason as for the "all clay data" scenario. When looking at the actual data plots (Figure 15 (bottom) or Appendix E) three large DP clusters can be observed, this is because most DPs have an elevation of 0, 30 or 60 cm clay and the intermediate thicknesses are much less. As stated before this is related to the translation from soil type to the respective clay thickness.

Two remarks can be made for both obtained multiple regression relations. Firstly land subsidence in 2010 is the reverse from what is expected and can be reasoned back to the high amount of DPs that have a higher elevation in 1998 than in 2008 (Appendix C). Secondly the correlation gets worse towards 2010, but as stated in the methods (3.1.4) a bad r^2 could indicate that the land subsidence relation is non-uniform and thus regional differences are present. The obtained relations are put in a geographical context in 4.1.4 this will demonstrate the actual regional differences.

4.1.4 [RQ1.4] Obtaining and implementing regional differences in Phoenix

Data points located above the surface area in the charts of the various multiple regression relations obtained in RQ1.3 are points where the relation overestimates the land subsidence, DPs below the surface area are points where the relation underestimates the land subsidence. Figure 16 shows the regional patterns that result from this over and underestimation for the run excluding clay thickness over 60 cm in 1970.

As can be seen in figure 16 the patterns of the left and right map appear similar. Although the run shown in figure 16 is for one of the 10 relations the same pattern can be observed for every individual relation, albeit that the relation reverses towards 2010. This means that overestimations in 1970 becomes underestimation in 2010 and understimation in 1970 becomes overestimation in 2010. As discussed in Appendix D the difference between the elevation measurements of AHN1 and AHN2 can be traced back to individual laser altimetry flights. Patterns explained by an error should not be used as an implementation for new regional differences, hence no new “abc” values can be incorporated. This also means that the formula as it currently is (Eq. 7) should not be changed eventhough nothing new can be said about the robustness of this formula.

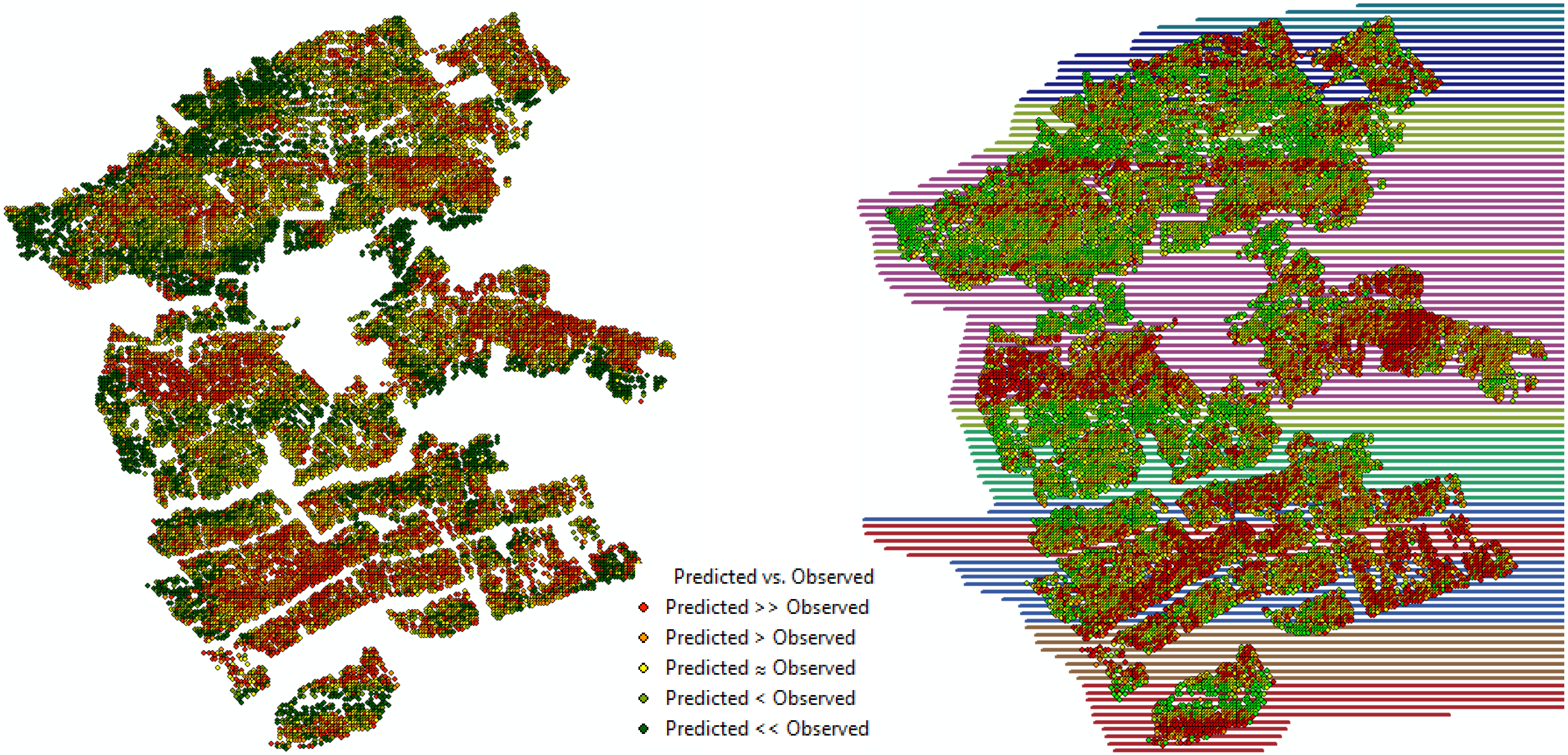

Figure16: *Comparison of the multiple regression relations and the observed land subsidence in 1970 (left). Elevation of 1999 vs. elevation in 2008 including the flight days in various colours (right), the map on the right represents the measurement error as examined in Appendix C.*

4.2 [RQ2] Impact of temperature increase due to CC on land subsidence

4.2.1 [RQ2.1] Predicted temperature increase due to climate change

There are several climate change studies that each have different scenarios, such as the climate scenarios of the International Panel for Climate Change and the Royal Dutch Meteorological Institute (KNMI) (Koninklijk Nederlands Meteorologisch Instituut, 2006). The KNMI has a G, G+, W and W+ scenario which each have an equal chance of occurring (Querner et al, 2012). For the previous climate studies using Phoenix the W+ scenario of the KNMI is used. The KNMI scenarios go up to 2100, since Phoenix models land subsidence up to 2200 all the values have to be extrapolated up to this year. This was done using a linear extrapolation.

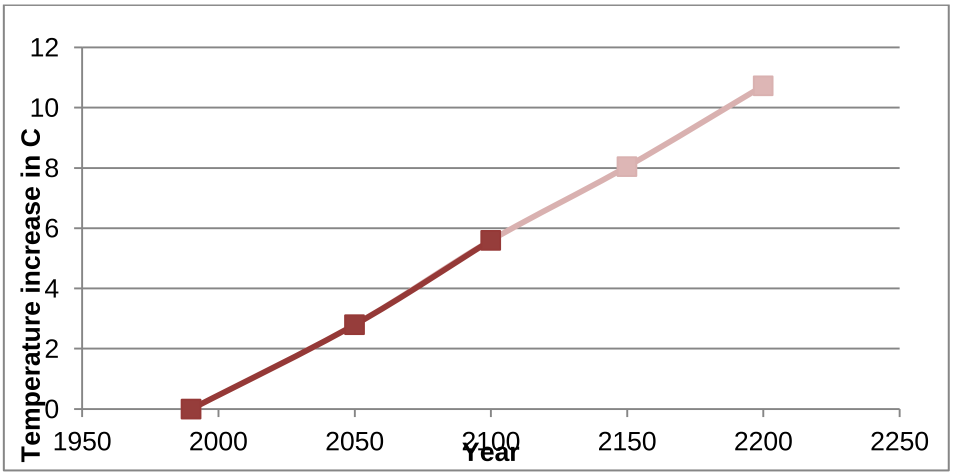

Figure 17: *Increase in summer average temperature due to Climate change according to (Koninklijk Nederlands Meteorologisch Instituut, 2006) up to 2100 (dark red), with an extrapolation to 2200 (transparent red).*

As can be seen in figure 17 the mean average summer temperature is expected to increase up to 10,7°C by 2200, which is a significant change compared to current day temperatures.

4.2.2 [RQ2.2] Influence of temperature on land subsidence

The process of oxidation and the chemical equations are explained in the theory (Eq.1 and Eq.2). Although the influence of temperature is addressed in the theory it is examined in more detail in this sub question.

Temperature plays an important role on the decomposition of organic matter. The process doesn't change due to temperature increase, the rate of oxidation however does change (Allison, 1973). With the exception of situations where the dominant microorganism gets replaced by another as a consequence of temperature change (Hendriks, 1991). This plays no significant role as long as the temperature does not exceed 40 °C after which actinomyceten and thermofile bacteria become dominant and change the end products. It is expected that this change in dominant species will be very limited as the increase due to climate change will still result in an average temperature well below 40 °C (Klimaatatlas, sine anno).

The range between which organic decomposition takes place is between 0-70°C . Some organisms die of at temperatures below 0 °C, but most are in a form of hibernation where they wait for a temperature increase so that they can become active again. Most microorganisms in the soil are mesophilic which become active starting at 0 °C (Allison, 1973; Hunt, 1978 in Hendriks, 1991), although according to Stephens and Speir 1969 in Hendriks, 1991 mainly fungi are active below 4 °C. At temperatures above 70 °C most microorganisms can't survive and die, this means that decomposition taking place above this temperature is likely to be chemical in nature (Hendriks, 1991). Mesophilic organisms have an optimum performance at a temperature of 35 °C. (Hendriks, 1991).

There are two ways to mathematically determine the effect of temperature on the decomposition of organic matter; either the Q_{10}-equation (Eq. 3) or the Arrhenius equation. The first is more adequate for determining the impact of temperature on the subsidence rate for a specific substrate, i.e. soil, and the latter is more adequate at determining the impact on the subsidence rate for a specific microbial specie (Bunnel et al, 1977 in Hendriks, 1991). For this master thesis the best approximation is the Q_{10}-equation as the substrates are known and not necessarily the microbial species.

The higher the Q_{10}-value is the more impact temperature has on oxidation (Hendriks, 1991). The Q_{10} value increases with depth (Otten, 1985). This is due to the variation in microorganism species. The species present near the surface are more resistant to temperature fluctuations due to seasonal temperature changes, therefore they react less to temperature changes then the species deeper into the soil (Bunnel, Tait, Flanagan, & van Cleve, 1977). Although there are differences in Q_{10} values for specific depths it is possible to use one Q_{10} value for an entire soil profile regardless of depth (Jansen, Hendriks, & Kwakernaak, 2009).

The Q_{10} value used is adopted from a model study using the land subsidence model SIMGRO made by Alterra. In this study different scenarios for water management schemes in Zegveld are analysed. The Q_{10} value used in this model is three which is established for Zegveld (Jansen et al,, 2007). Because Zegveld is inside the study area of this master thesis this value is expected to be appropriate. The resulting increase in activity thus looks as follows (figure 18):

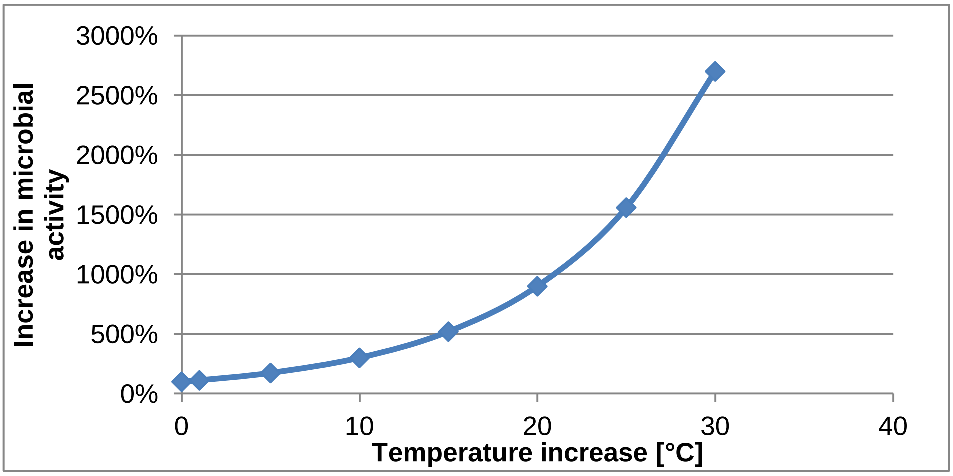

Figure 18: *Impact of temperature on the increase in microbial activity for peat soils*

The impact of temperature on the rate of oxidation in figure 18 shows that microorganisms have a large variation in decomposition rate of the organic matter, and that this is highly dependent on the temperature. This will have a significant impact on the land subsidence. For this relation it is assumed that oxygen availability is sufficient regardless of the decomposition rate, in reality the availability of oxygen in the deeper layers within a soil may hinder the aerobic decomposition (see Discussion).

Oxidation is not the only process that results in land subsidence. It however is the largest one making up 60% of the total land subsidence (Stouthamer et al, 2008) (figure 2 in 2.1.4). The increase in temperature only has an impact on the rate at which oxidation takes place. Therefore the impact of temperature on oxidation has to be multiplied by the fraction of oxidation within the total subsidence process, being 60%, so that the total increase in subsidence contributed to the increase in temperature can be determined.

By combining the land subsidence per 1 °C and the increase in temperature due to global climate change according to the KNMI the following increase land subsidence can be found. This increase is compared to the land subsidence with the average annual temperature in 1990.

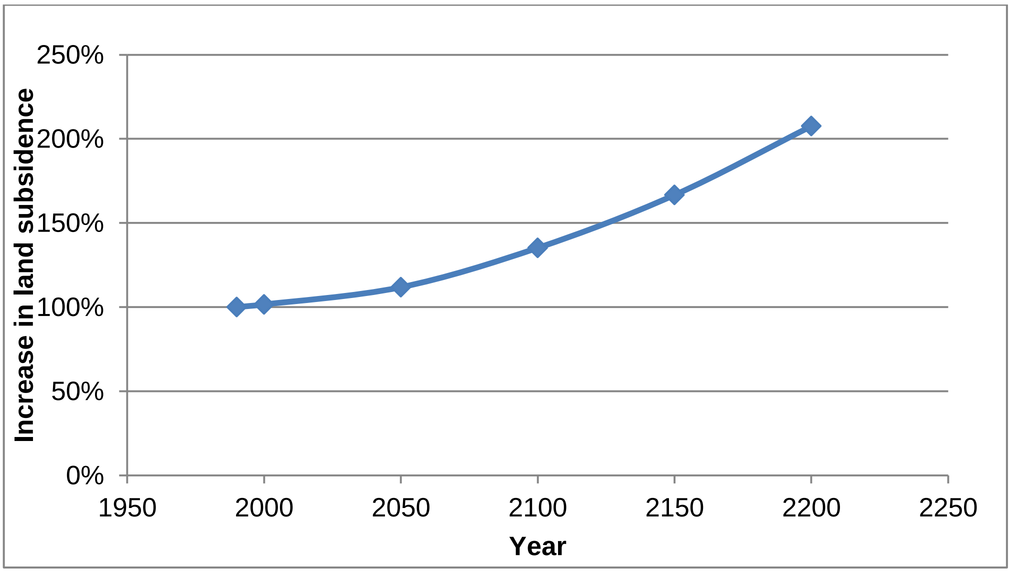

Figure 19: *Increase in land subsidence due to global climate change for various soil types using the W+ scenario of the KNMI*

4.2.3 [RQ2.3] Implementing the increase in land subsidence due to climate change in Phoenix

The impact on land subsidence is implemented on the "a" variable of the general formula (Eq.7). This different "a"- variable depends on the time period. It is calculated and implemented as described in the methods. The new 'a' -variables are as follows:

Table 6*: New "a"-variables to be used in Phoenix.*

Time period	"a" -variable
2000-2050	0.026313
2050-2100	0.031817
2100-2150	0.039224
2150-2200	0.048862
2000-2200	**0.036554**

4.3 [RQ3] Aggregated effects on simulated land subsidence in Phoenix

The conclusion of RQ1 is that no regional patterns can be obtained due to errors in elevation data (Appendix C). This means that only the base run and the climate change run have been performed. The runs are done using the scenario named Variant0. This scenario describes what the effects would be if current land uses remain facilitated. No new build locations and nature areas are added or taken out. The land subsidence is calculated every 10 years.

Base run

The base run was conducted using the formula as stated in (Eq.7). This run was repeated because the previous runs which are reported in (van der Schans & Houhuessen, 2012) were conducted using a formula which is slightly different (Appendix A). The result is the following (figure 20).

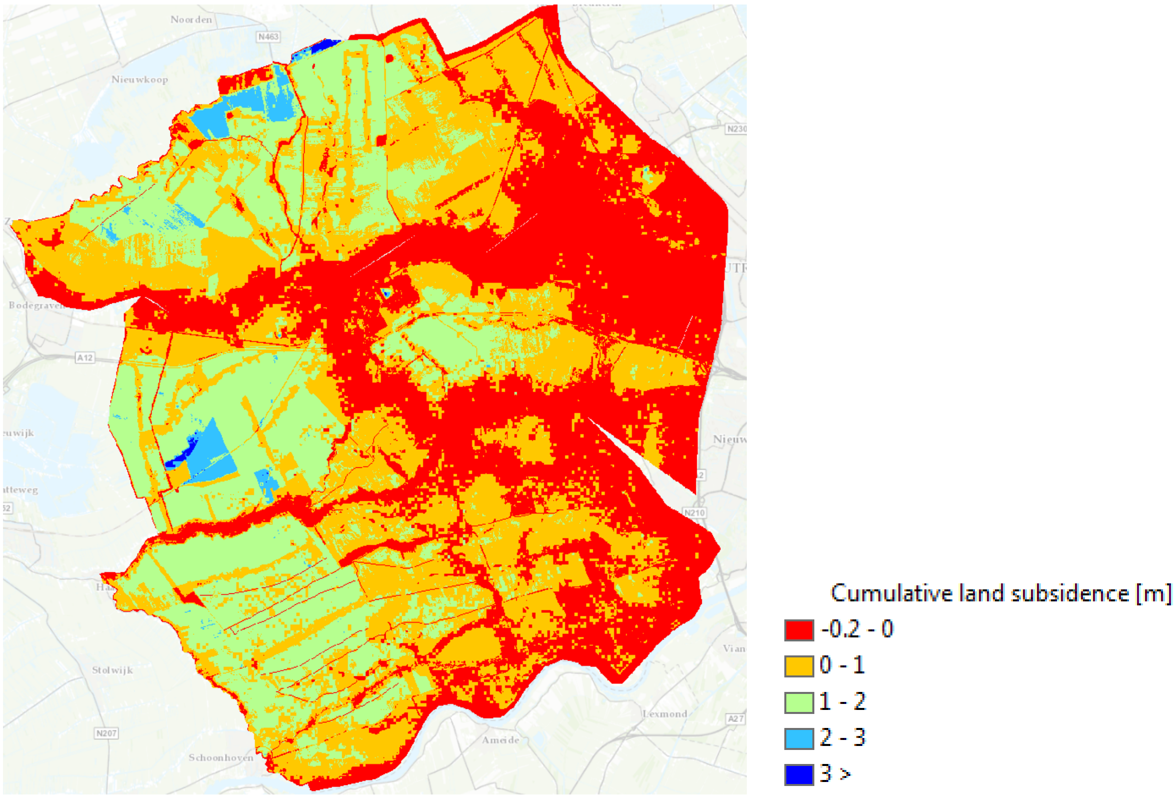

Figure 20: *Cumulative land subsidence in 2200 using Phoenix without any additional adjustments other than the change in the base formula as described in Appendix A.*

In this figure it is possible to clearly see the impact of clay on land subsidence, which is logical because clay thickness is the subsidence inhibitor of the used formula (Eq.7). The most rapidly subsiding areas can be traced back directly to the regions without any clay cover (figure 6, preprocessing) and make up most of the 2-3 meter (light blue) subsidence areas, the regions where 30 cm clay is present make up most of the 1-2 meter category (light green) and finally the regions 60 cm clay make up most of the 0-1 meter category (orange). The soils fully consisting out of mineral soils show almost no subsidence and create thick red bands that trace the river beds in the western part and gradually consume the entire region towards the east as the dominant soil type changes from a peaty soil to a mineral soil. The largest simulated (realistic) cumulative land subsidence is around 3.3 meter and is located in the dark blue region in the mid-west. The largest simulated (unrealistic) cumulative land subsidence can be found in the north. Here there is one small polder which subsides with 10.5 meter, and is related to a (garbage) dump present in the elevation map, but not in the soil map resulting in an anomaly in land subsidence (van Hardeveld, 2014). The average cumulative land subsidence was roughly 0.6m

Climate change run including effects of temperature increase

The run is conducted from 2000-2200 using the new selected “a”-variable is 0.036554 as can be seen in table 6 (RQ2.3).When implementing this new “a”-varaible the new land subsidence including climate change looks as follows (figure 21).

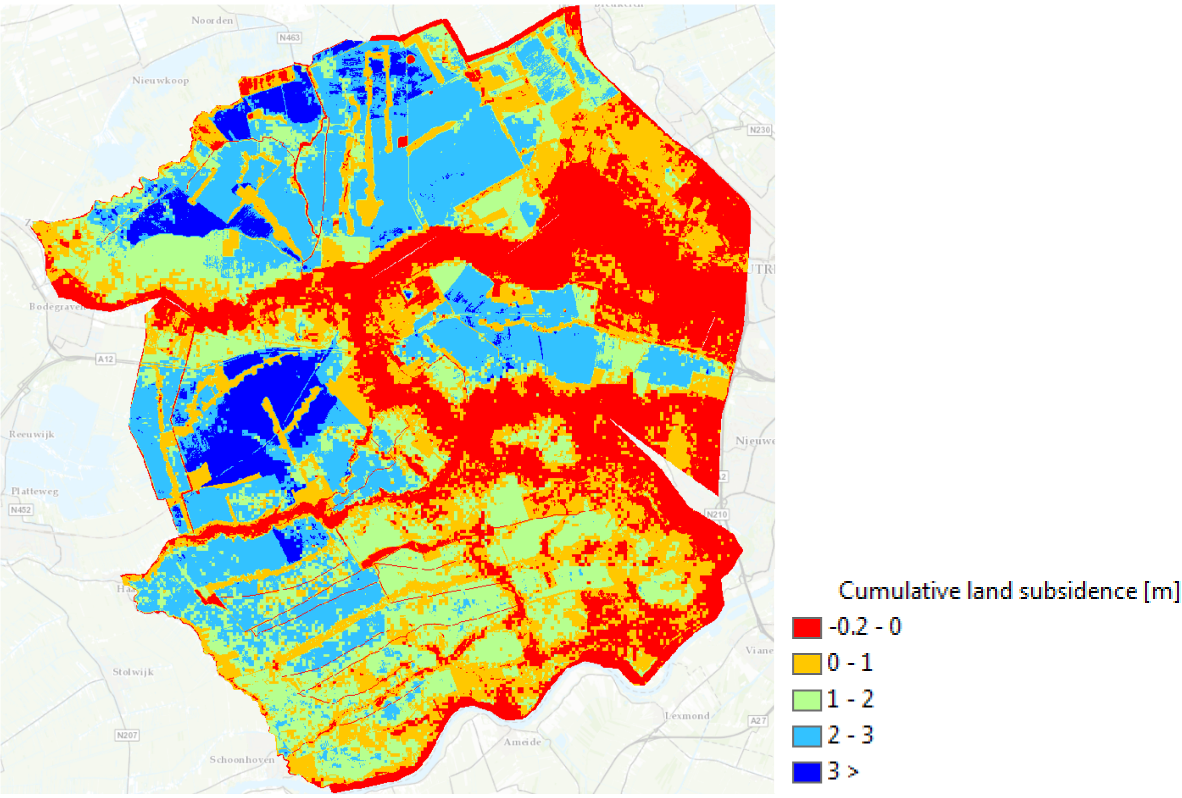

Figure 21: *Cumulative land subsidence in 2200 using Phoenix with the impact of temperature due to climate change on land subsidence*

When observing the land subsidence for the climate change scenarios it is possible to still see the different clay soils. This time however the difference is more distinct. The 0 cm clay soils are most notably visible as the dark blue soils with a subsidence over 3 m. The 30 cm clay soils now subside mostly between 2-3 meter and the 60 cm clay soils mostly subside between 1-2 meter (light green). The maximum observed (realistic) cumulative land subsidence is 4.8 m and is found in the dark blue area in the Midwest. On average the total cumulative land subsidence was 1.2 m.

Comparison between base run and climate change run

When comparing the land subsidence for the base run with the land subsidence of the climate change run the following increased land subsidence becomes apparent (figure 22).

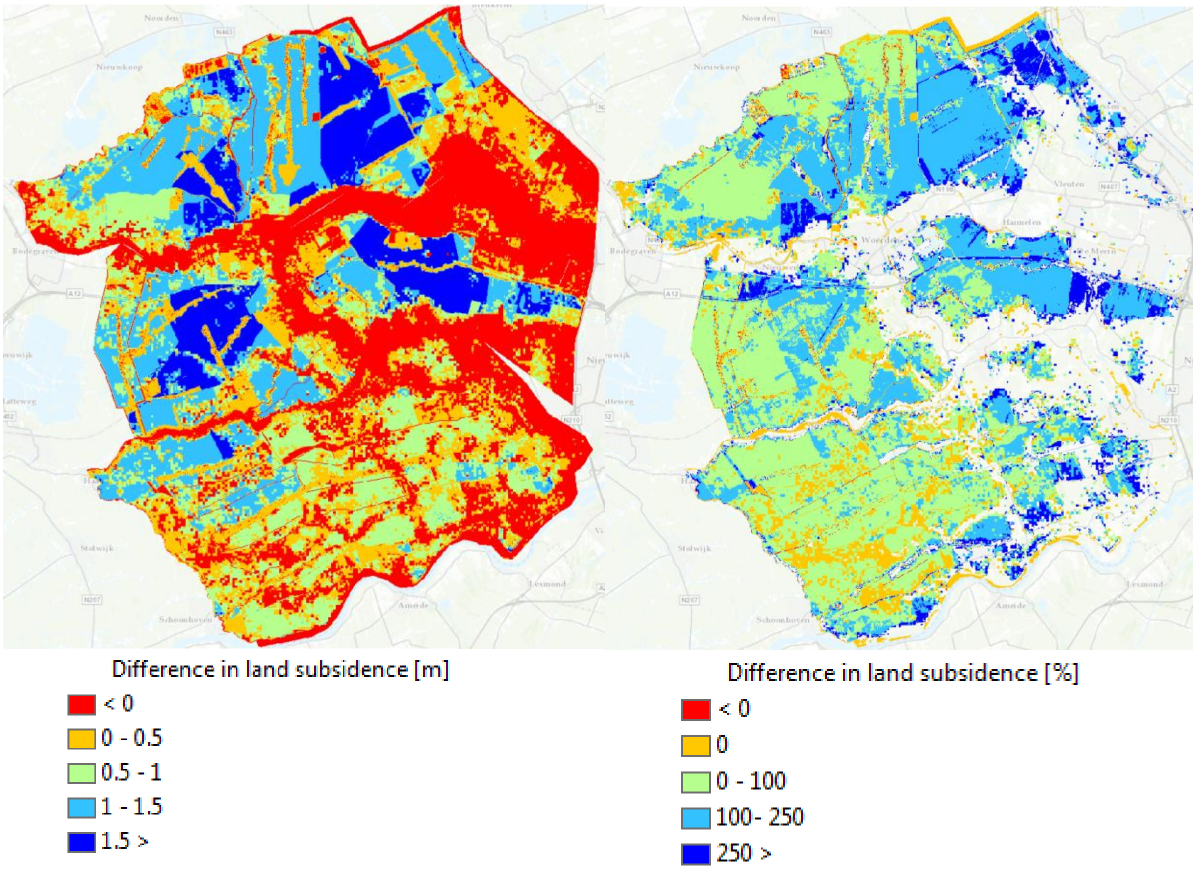

Figure 22: *Difference in absolute cumulative land subsidence (left) and difference in percentage cumulative land subsidence (right) between the base run and the climate change run. The right shows several regions without data, these regions have no subsidence in at least one of the two runs being the base run and the climate change run. The reason that this gives no data is because dividing by zero is impossible thus no value can be calculated.*

In figure 22(right) it is possible to see several orange spots in the southern areas, these orange spots mean that there is no difference between land subsidence in the base run compared to the climate run. These areas represent areas where somewhere between 2000 and 2200 the peat layers have been burned up resulting in no further land subsidence. Therefore the difference due to climate change is less in the southern regions compared to the northern regions.

In total the regions without a clay cover have the largest subsidence (figure 20 and figure 21). However the biggest absolute difference in land subsidence can be observed in the locations with 30 cm clay and the largest percentage increase can be observed in the 60 cm clay regions. The absolute difference can be as large as 2,4 m and the percentage difference as high as 270%. The reason that the largest absolute difference can be observed in the 30 cm clay soils is because the clay inhibition term (‘b’-variable*clay thickness) often exceeds the velocity term (‘a’-variable*drainage) in the base run resulting in no land subsidence, whereas the velocity term is larger in the climate change run because the ‘a’-variable is larger this results in land subsidence for the same boundary conditions. This principle is explained visually in figure 23.

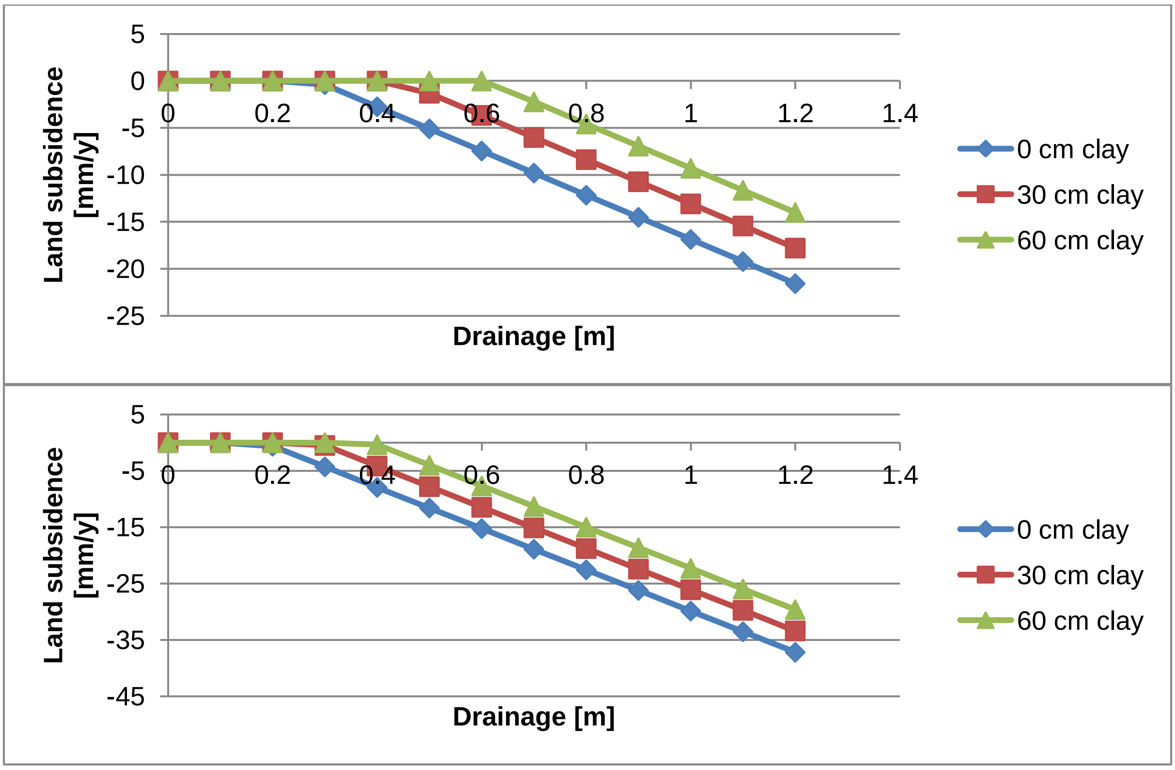

Figure 23: *Land subsidence function used to demonstrate the occurrence of land subsidence with various clay thicknesses. The function used in the base run (top) and the function used for the climate change run (bottom).*

This figure shows that the moment subsidence occurs is different for each of the two runs. In the climate change run subsidence in the 60 cm clay soils occurs starting at 0.4m drainage whereas in the base run under the same conditions this happens starting at 0.6 m drainage. So regions with a drainage between 0.4 and 0.6 m will show subsidence in the climate change scenario but no subsidence in the base run scenario, which allows for a percentage difference larger than the actual increase due to temperature (figure 19). This also means that the frequency with which the land does not subside in one scenario and does in the other is larger in case of 60 cm clay then it is for the 30 cm clay soils. Since soils with 0.3m drainage cause subsidence in both 30 and 60 cm clay soils but soils with 0.3-0.6m drainage only cause subsidence in the 60 cm clay soils. When subsidence in the 30 cm clay soils occurs, the difference between the base run and climate change run is larger compared to the 60 cm clay soils. This explains the largest percentage difference for the 60 cm clay soils and the largest absolute difference for the 30 cm clay soils.

Comparing the impact on land subsidence of the temperature increase due to climate change with the previous Phoenix study where the additional land subsidence due to the increase in evaporation which results in an increase in drainage as a consequence of climate change it is found that the temperature impact is far larger. In the climate run conducted in this thesis it was found that the difference may be up to 270%, or roughly 100% on average, whereas the additional land subsidence found in the previous climate change study was an additional 8% land subsidence (van Bokhoven, 2014b) for the same scenario (Variant0) and the same climate change scenario (W+ scenario).

5 Discussion:

Several remarks can be made about the reliability of the elevation, soil and surface water data, about the assumptions that the thickness of the clay cover has been constant over time and that temperature increase due to CC is linear past 2100. Finally the lack of the oxygen availability is addressed. For RQ1, a short reflection is given on another land subsidence study that used similar geographical data.

Regional differences

Elevation data

There is a limited amount of reliable elevation data available. For the sources that were available the allowed errors are large considering a process which is measured in mm's a year. The allowed errors for AHN1 and AHN2 can be found in Appendix C (van der Zon, 2013). The measurement error of TOPhoogteMD (Meetkundige Dienst van Rijkswaterstaat, 1992) is possibly larger, although no exact error could be found. For this research the errors in measurement, which can be reasoned back to individual flight days (Appendix C), result in the inability to observe useable patterns (RQ1.4). Having more measurements in time will reduce the impact of these errors.

A starting point would be the addition of AHN3 which will be introduced in November 2014 (Het Waterschapshuis, 2014) extending the elevation measurements. Four measurements will likely be better but still not sufficient. A different approach, which will likely give a significantly better result, is to look at a completely different way of obtaining elevation maps. A relatively new technique named aerial photogrammetry can be used to create digital elevation maps (DEM) out of two overlapping aerial photographs (Photogrammetry, sine anno) using models. This technique has been proven to work in urbanized areas where relief differences are large. This might possibly work for polder areas as well. The availability of aerial photos is much larger and are available for a longer time period. Overall, these measurements will likely shift the land subsidence 2nd order function more back to reality and less towards the error of AHN1 (Appendix C). All the relations obtained following from these additional land elevations are likely to be more realistic compared to the relations obtained in this thesis.

A second discussion point is related to the moment the laser altimetry flights of AHN1 and AHN2 (Actueel Hoogtebestand Nederland, sine anno; Actueel Hoogtebestand Nederland, sine anno) are taken. These are flown in during the winter because of the lower vegetation cover (van der Zon, 2013). However for TOPhoogteMD the season of measurement is not known. Since there is a difference between the elevation in the winter and the summer (van den Akker et al, 2007) this might influence the results in favour of higher surface elevations for the AHN measurements compared to the TOPhoogteMD measurements and thus result in a slower overall land subsidence.

Onderbemalingen

Onderbemalingen are locations where the maintained water level may deviate from the *peilbesluit* water levels. No exact surface water data on the maintained water levels exist for these *onderbemalingen* (van Hardeveld, 2014; Nederlof, 2014). For the results this means that for the locations where *onderbemalingen* are present incorrect SW levels are used, and thus falsely demonstrating a relation for land subsidence with a smaller freeboard than what in reality is the case. Overall these *onderbemalingen* change the results towards more rapid land subsidence with only a small reported freeboard, thus the “a” variable will be too large in the areas of *onderbemalingen.*

Peilbesluit surface water levels

The water data used is based on SW levels. Land subsidence however is dependent on the unsaturated zone. This does not necessarily have to be a problem if the groundwater table was fully dependent on the surface water levels, the relation would then simply have a slightly higher base (“c”-variable). The problem is that the groundwater levels are also influenced by other factors such as evaporation, precipitation, distance between ditches, (downward) seepage and permeability. These cannot be accounted for when using the SW levels (van den Akker et al, 2007). Additionally, the surface water levels fluctuate around the *peilbesluitpeil*. This fluctuation however is not present within all the data. The SW levels are for a large part directly or indirectly (in historical maps) based on *peilbesluitpeilen* and only partly based on the measured SW levels in (WIS-HDSR, 2013). Relations with respect to GLG do take into account these fluctuations as they are based on the three lowest groundwater levels every year over eight years.

From the start of this research it was clear that the relations obtained using *peilbesluitpeilen* would be less reliable than the ones obtained using measured groundwater levels for the two abovementioned reasons. But as there is almost no historical data on groundwater levels compared to the historical surface water data no relations would have been established at all if groundwater data was pursued.

Soil data

The clay thickness map used is a direct translation from the soil map (Stouthamer et al, 2008), by for example defining a soil type which has a top clay layer of between 15-50 cm as 30 cm clay. The variation in clay thickness is larger in reality than what is used for this thesis. Additionally the assumption made that the current top clay layer had the same thickness now as it did in 1970 may be false. If a thin peat cover existed on top of a clay cover between 1970 and 2010 but burned off due to oxidation somewhere in between the cover layer would be clay in 2010. The data falsely reflects this clay cover presence for the entire period. These two observations add to the uncertainty in the obtained ΔL vs. C and FB relations where values are falsely reported of having a certain clay cover. This mainly influences the correlation and "b" variable of the obtained multiple regression relations.

Reflection on another study

The research method used in a study by Hoogland et al. (2012) is comparable to the one applied in RQ1 of this thesis. The study, conducted in Groot-Mijdrecht, also bases a large part of the output on geographical maps such as TOPhoogteMD, AHN1, various soil maps and several maps displaying maintained surface water levels. There are various differences between this thesis and Hoogland et al., one being, the approximation of land subsidence. In Hoogland et al, land subsidence is treated as a linear function. In this thesis it was reasoned and observed that land subsidence cannot be treated as a linear function. Some other large differences are that:

- two different soil maps are used, resulting in an approximation of actual oxidized peat in Hoogland et al., 2012;
- Groot-Mijdrecht has no clay cover meaning that there is no clay variable, it however does have different peat types;

- the land subsidence equation is separated in land subsidence due to oxidation and land subsidence due to other causes such as the tectonic subsidence. This tectonic subsidence was explored for this thesis but deemed negligible as it contributes roughly 0.15-0.4 mm y^{-1} land subsidence for the study area depending on the location (Kwaad, sine anno).

These are but a few differences for more information Hoogland et al., 2012 can be consulted. Unfortunately no solutions for obstacles encountered in this thesis could be obtained from Hoogland et al., 2012, although they were likely to encounter similar obstacles such as the measurement errors in AHN1.

Climate change

Climate change scenario used

The assumption made in prior-Phoenix studies concerning the linear extrapolation of climate change after 2100 was adopted in this thesis. This assumption is likely incorrect. Cubasch, et al illustrate a strong temperature increase from 2000-2100, but a far less rapid increase from 2100-2200 (Figure 24).

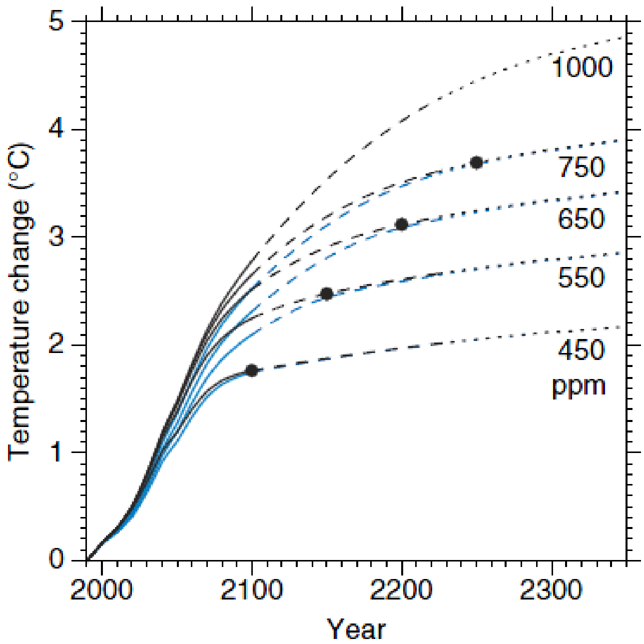

Figure 24: *Projected global mean temperature changes for the IPCC baseline scenario A1B up to 2100 and all emissions of gases other than CO_2 are assumed to remain constant at their A1B 2100 values. The broken lines after 2100 indicate increased uncertainty in the simple climate model used. The black dots represent the time of CO_2 stabilisation (Cubasch, et al., 2004).*

The scenarios used in Cubash et al, is not the same scenario used in this thesis. The focus should not be on the exact numbers but rather on the direction of the line. It can be seen that the behaviour towards 2100 is close to linear but after this point the temperature increase levels out. If the top line (1000 ppm) of figure 24 is an indication the temperature increase in 2200 will be in the order of 8.3 °C[5] rather than the linear 10.7 °C obtained in this thesis. The

[5] $\Delta C_{2000\text{-}2100}$ = 2.8 °C $\Delta C_{2100\text{-}2200}$ = 4 °C. 2.8/4 = 0.7. So 70% of total increase is in the first 100 years, applying this to W+ scenario. 5.8/0.7=8.3 °C.

difference in land subsidence between the non-linear and linear approximation using Eq.3 would be an 18,3% slower subsidence rate for the non-linear approximation in 2200. This raw approximation of the difference in temperature increase should not be used as fact. The calculation was done to illustrate what the impact could be if the temperature changed non-linearly after 2100.

A non-linear approximation of the temperature increase between 2100 and 2200 is likely a better approximation of reality. Regardless of the climate change model, the uncertainties increase rapidly the further in the future one models. So unless modelling up to 2200 in Phoenix is necessary it is recommended to model up to the 2100 where actual climate change scenario data is available, or a climate change scenario modelled up to 2200 has to be consulted.

Oxygen availability

In this thesis it is assumed that the availability of oxygen does not change due to CC. However considering that the oxidation rate goes up significantly in the future the oxygen demand is likely to go up as well. Over time, this demand may exceed supply. The lack of oxygen then inhibits the organisms to work up to their full potential, thus becoming a limiting factor. For the results this would mean that the impact of CC on land subsidence as provided in this thesis might be an overestimation of what in reality will happen. This could be corrected in a future addition to Phoenix by determining the aerated pores, diffusion coefficient of oxygen and oxygen demand per soil layer and increasing this demand by the respective increase in activity due to CC. When oxygen demand in the soil layer exceeds supply the increase in activity will no longer have an effect on the land subsidence. A possible starting point to implement this in Phoenix could be the ANIMO model of Alterra, which is able to calculate this supply and demand (Hendriks, 1991).

6 Conclusion

Regional differences in land subsidence as a function of freeboard and clay thicknesses were observed using the historical land subsidence, historical surface water subsidence and soil characteristics. However, these regional differences were explained by a measurement error of the elevation data obtained in 1999. This error was traced back to the laser altimetry flights for this measurement. Because the observed regional differences are explained by an error in measurement these cannot be added responsibly to Phoenix.

The temperature increase due to climate change will have a significant impacts on the land subsidence rate. Using the W+ scenario of the KNMI and a linear extrapolation after 2100 the expected land subsidence rate increases just over 200% in 2200. When adding this impact to Phoenix and comparing the result with a base run without any adaptations to the model, the average cumulative land subsidence increases from 0.6m in the base run to 1.2m for the climate change run within the study area. The lowest observed cumulative land subsidence is -0.2m (i.e. land rise) which is directly related to the assumption that peat growth occurs when land is under water. The maximum cumulative land subsidence can be observed in the mid-west of the study area and is 3.3m and 4.9m for the base run and climate run respectively. The largest absolute difference of up to 2,4m additional subsidence can be observed in the soils with 30 cm clay on top of the peat and the largest percentage difference, up to 270% additional land subsidence, in the soils with a 60 cm clay cover. These differences can be explained by looking at the land subsidence inhibition due to clay.

7 Recommendations

Hereunder a short enumeration of recommendations. For more detail the discussion (Ch.5) should be consulted.

Regional differences

It is recommended not to pursue the search for regional differences, unless significantly more historical elevation data is found. The addition of AHN3, which is to be released at the end of 2014, and possible digital elevation maps created using aerial photogrammetry to the current data set might create more accurate relations and show regional differences not explained by errors.

Climate change

It is recommended to search for a non-linear extrapolation for CC post 2100, as climate change is likely not linear past this point or model up to 2100 and not 2200. The resulting temperature changes could then be computed in the same way as it was done in this thesis. This different non-linear climate change scenario should also be used for the already conducted study of the impact of evaporation on land subsidence.

Regarding the oxidation process, the addition of oxygen availability will likely result in more accurate land subsidence increase due to climate change as it may hinder the actual oxidation rate. A good starting point would be the Alterra model ANIMO (Hendriks, 1991).

Phoenix model runs

Make sure the 'abc'-variables of the formula conjugated in Appendix A (Eq.7) are used for future Phoenix studies and not the originally reported variables of the formula in the Phoenix documentation. Additionally, if past policy is an indication of future policy the peilindexation values of the Phoenix model scenarios have to be revised.

Additional recommendation outside of the research questions

The current implementation of increase in drainage due to increased evaporation following climate change as was done in the previous climate change study using Phoenix might require revisiting (Ad van Bokhoven, 2014). It is important to note that the extremes will increase due to climate change, so extremely dry summers will become more frequent (IPCC,2006). In one such a summer the groundwater levels may drop up to an additional 20 cm and result in large additional land subsidence (van den Akker, 2014). For Phoenix it is recommended to look into the effect of these extreme events, which in the end may have a larger impact on the land subsidence then just the average deepening of 1-1,5 cm per 25 years.

8 Bibliography

Actueel Hoogtebestand Nederland. (sine anno). *Vluchten AHN1*. Retrieved march 25, 2014, from Retrieved from Database HDSR

Actueel Hoogtebestand Nederland. (sine anno). *Vluchten AHN2*. Retrieved march 25, 2014, from Retrieved from HDSR Database

Allison, F. E. (1973). Soil organic matter and its role in crop production: developments in soil science no. 3. *Elsevier* , 3-637.

Amstelland. (1898). Kaart van het Hoogheemraadschap Amstelland.

Brouwer groep. (1994). *Toelichting op het ontwerp-peilbesluit Meijepolder(hoog).* Leerdam: Brouwer groep.

Bunnel, F. L., Tait, D. E., Flanagan, P. W., & van Cleve, K. (1977). Microbial respiration and substrate weight loss I. A general model of the influences of abiotic variables. *Soil Biology and Biochemistry* , 9: 33-40.

Cubasch, U., Meehl, G. A., Boer, G. J., Stouffer, R. J., Dix, M., Noda, A., et al. (2004). *Projections of Future Climate Change.*

Das, B., & Sobhan, K. (2012). *Principles of geotechnical engineering, eighth edition.* Perth, Australia: Edith Cowan University.

den Haan, E. J. (2003). Het a,b,c-ISOTACHENMODEL: Hoeksteen van een nieuwe aanpak van zettingsberekeningen. *Geotechniek* , 28-35.

Dinesh, S. (sine anno). *Consolidation of Soils*. Retrieved Februari 10, 2014, from elearning: elearning.vtu.ac.in/11/enotes/geotechengg/Unit6-SVD.pdf

Groot-Waterschap van Woerden. (1994i). *Peilbesluit: Polder Weijland en de Bree.* Woerden: Groot-Waterschap van Woerden.

Groot-Waterschap van Woerden. (1994h). *Samenvatting Toelichting Peilbesluit: Noordzijderpolder, Meije (hoog), Groot-Houtdijk (hoog), Gerverscop, Breudijk en Klein-Houtdijk, Oudeland en Indijk, Noord-Linschoten, Snelrewaard, Rapijnen, Wulverhorst.* Woerden: Groot-Waterschap van Woerden.

Groot-Waterschap van Woerden. (1994j). *Toelichting op het ontwerp-peilbesluit Noordzijderpolder.* Leerdam: Groot-Waterschap van Woerden.

Groot-Waterschap van Woerden. (1994d). *Toelichting Peilbesluit: Oudeland en Indijk.* Leerdam: Groot-Waterschap van Woerden.

Groot-Waterschap van Woerden. (1994f). *Toelichting Peilbesluit: Polder Gerverscop, polder Breudijk, polder Klein-Houtdijk.* Leerdam: Groot-Waterschap van Woerden.

Groot-Waterschap van Woerden. (1994g). *Toelichting Peilbesluit: polder Groot-Houtdijk (hoog).* Leerdam: Groot-Waterschap van Woerden.

Groot-Waterschap van Woerden. (1994a). *Toelichting Peilbesluit: Polder Noord-Linschoten.* Woerden: Groot-Waterschap van Woerden.

Groot-Waterschap van Woerden. (1994c). *Toelichting Peilbesluit: Polder Snelrewaard.* Woerden: Groot-Waterschap van Woerden.

Groot-Waterschap van Woerden. (1994b). *Toelichting Peilbesluit: Polder Wulverhorst.* Woerden: Groot-Waterschap van Woerden.

Groot-Waterschap van Woerden. (1994e). *Toelichting Peilbesluit: Rapijnen.* Woerden: Groot-Waterschap van Woerden.

Hazue, G. W., Schuiling, G. J., Dorland, J., Oldengarm, & Gijsbertse, H. A. (2012). *Landelijk Grondgebruiksbestand Nederland versie 6 (LGN 6).* Wageningen: Alterra.

Hendriks, R. F. (1991). *Afbraak en mineralisatie van veen; literatuuronderzoek.* Wageningen: DLO Staring Centrum rapport 199.

Het Waterschapshuis. (1998). *Actueel Hoogtebestand Nederland 1.* Retrieved Februari 20, 2014, from University Utrecht Database: AHN 5x5m

Het Waterschapshuis. (2008). *Actueel Hoogtebestand Nederland 2.* Retrieved Februari 20, 2014, from University Utrecht Database: AHN2

Het Waterschapshuis. (2014, March 3). *Inwinning AHN2014 op de helft*. Retrieved Juli 10, 2014, from Algemeen Hoogtenbestand Nederland: http://www.ahn.nl/nieuws/2014/inwinning_ahn2014

Hoekwater, W. (1901). Polderkaart van de landen tusschen Maas en IJ. Amsterdam, North Holland, The Netherlands: Bebrs. Braakensiek.

Hoogheemraadschap De Stichtse Rijnlanden. (sine anno). *O BR Peilgebieden*. Retrieved Februari 25, 2014, from ArcGIS file: Retrieved from HDSR Database

Hoogheemraadschap De Stichtse Rijnlanden. (1997). *Toelichting Peilbesluit Meijepolder (Laag).* Leerdam: Hoogheemraadschap De Stichtse.

Hoogheemraadschap De Stichtse Rijnlanden. (2002). *Toelichting Peilbesluit: Oud-Kamerik.* Leerdam: Hoogheemraadschap De Stichtse Rijnlanden.

Hoogheemraadschap De Stichtse Rijnlanden. (1997). *Toelichting Peilbesluit: Polder Kockengen, Teckop-Noord, Teckop-Zuid en Spengen.* Leerdam: Hoogheemraadschap De Stichtse Rijnlanden.

Hoogheemraadschap De Stichtse Rijnlanden. (1996). *Toelichting Peilbesluit: 'S Gravesloot.* Leerdam: Hoogheemraadschap De Stichtse Rijnlanden.

Hoogland, T., van den Akker, J. J., & Brus, D. J. (2012). Modeling the subsidence of peat soils in the Dutch coastal area. *Geoderma* , (171-172), 92-97.

Hunt, H. W. (1978). A simulation model for decomposition in grasslands. *Innis* .

Ingenieurs bureau BCC. (2003). *Toelichting op het peilbesluit Rietveld.* Leerdam: Hoogheemraadschap De Stichtse Rijnlanden.

International Panel for Climate Change. (sine anno). *Working Group I: The scientific Basis*. Retrieved Juli 10, 2014, from IPCC: http://www.ipcc.ch/ipccreports/tar/wg1/029.htm

Jansen, P. C., Hendriks, R. F., & Kwakernaak, C. (2009). *Behoud van veenbodems door ander peilbeheer.* Wageningen: Alterra.

Kadaster. (2009). *TOP10NL*. Retrieved March 21, 2014, from Gedetailleerd topografisch bestand van het Kadaster: Database of University Utrecht

Klimaatatlas. (sine anno). *De Bilt, langjarige gemiddelden, tijdvak 1981-2010*. Retrieved 07 01, 2014, from Klimaatatlas: http://www.klimaatatlas.nl/tabel/stationsdata/klimtab_8110_260.pdf

Koninklijk Nederlands Meteorologisch Instituut. (2006). *Klimaat in de 21e eeuw: vier scenario's voor Nederland.* De Bilt: KNMI.

Kwaad, F. J. (sine anno). *Het Normaal Amsterdams Peil (NAP) - Achtergronden en geschiedenis*. Retrieved June 25, 2014, from Tiscali: http://home.tiscali.nl/~wr2777/NAP-niveau.htm#CorrectievanNAPhoogten20januari2005

Landelijk Samenwerkingsverband GBKN. (2005). *GBKN*. Retrieved March 21, 2014, from Database from University Utrecht

Meetkundige Dienst van Rijkswaterstaat. (1992). *TOPhoogteMD.* Retrieved March 2, 2014, from University of Utrecht Database: TophoogteMD

Ministerie van Oorlog. (1910). *Topographische en militaire kaart van het Koningrijk der Nederlanden: Blad 31.* 'S Gravenhage: Ministerie van Oorlog.

Ministerie van Oorlog. (1910a). *Topographische en militaire kaart van het Koningrijk der Nederlanden: Blad 31.* 'S Gravenhage: Ministerie van Oorlog.

Ministerie van Oorlog. (1910). *Topographische en militaire kaart van het Koningrijk der Nederlanden: Blad 38.* 'S Gravenhage: Ministerie van Oorlog.

Ministerie van Oorlog. (1910b). *Topographische en militaire kaart van het Koningrijk der Nederlanden: Blad 38.* 'S Gravenhage: Ministerie van Oorlog.

Nederlandsche Rijkscommissie voor Graadmetingen Waterpassing. (1888). *Gemiddelden voor eenige gemeenten in de provincie's van de aldaar aangetroffen verschillen tussen A.P.hoogte en N.A.P. hoogte.* location unknown: Rijkswaterstaat afdeling NAP.

Nederlof, L. (2014, June 25). Personal contact. (L. Geisler, Interviewer)

Otten, W. (1985). *Nader onderzoek naar oxydatie van veengronden, literatuuroverzicht en metingen aan veenmosters.* Wageningen: ICW.

Photogrammetry. (sine anno). *What is Photogrammetry?* Retrieved July 29, 2014, from Photogrammetry: http://www.photogrammetry.com/

Provinciale Waterstaat. (1883). *Waterschappen in de Provincie Utrecht: Grootte, zomerpeilen en bemalingen.* Utrecht: Provinciale Waterstaat.

Querner, E., J. P., v. d., & K. C. (2012). Analysing water level strategies to reduce soil subsidence in Dutch peat meadows. *Journal of Hydrology* , (446-447), 59-69.

Rijksoverheid. (2014, may 29). *TophoogteMD*. Retrieved June 3, 2014, from Data Overheid: https://data.overheid.nl/data/dataset/tophoogtemd

Rijksoverheid. (sine anno). *Water verdelen*. Retrieved June 28, 2014, from Watertekort en zoetwatervoozieningen: http://www.rijksoverheid.nl/onderwerpen/watertekort-en-zoetwatervoorziening/ingrijpen-bij-watertekort/water-verdelen

Rijkswaterstaat. (1870a). De Waterstaatskaart van Nederland, Gorinchem 1. Blad 38-1. Retrieved from Database of University Utrecht.

Rijkswaterstaat. (1870b). De Waterstaatskaart van Nederland, Gorinchem 1. Blad 38-2. Retrieved from Database of University Utrecht.

Rijkswaterstaat. (1870c). De Waterstaatskaart van Nederland, Gorinchem 1. Blad 38-3. Retrieved from Database of University Utrecht.

Rijkswaterstaat. (1870d). De Waterstaatskaart van Nederland, Gorinchem 1. Blad 38-4. Retrieved from Database of University Utrecht.

Rijkswaterstaat. (1882a). De Waterstaatskaart van Nederland, Gorinchem 2. Blad 38-1. Retrieved from Database of University Utrecht.

Rijkswaterstaat. (1920a). De Waterstaatskaart van Nederland, Gorinchem 2. Blad 38-2. Retrieved from Database of University Utrecht.

Rijkswaterstaat. (1882b). De Waterstaatskaart van Nederland, Gorinchem 2. Blad 38-3. Retrieved from Database of University Utrecht.

Rijkswaterstaat. (1921). De Waterstaatskaart van Nederland, Gorinchem 2. Blad 38-4. Retrieved from Database of University Utrecht.

Rijkswaterstaat. (1950b). De Waterstaatskaart van Nederland, Gorinchem Oost 3. Blad 38. Retrieved from database of University Utrecht.

Rijkswaterstaat. (1941). De Waterstaatskaart van Nederland, Gorinchem West 3. Blad 38. Retrieved from database of University Utrecht.

Rijkswaterstaat. (1869a). De Waterstaatskaart van Nederland, Utrecht 1. Blad 31-1. Retrieved from database of University Utrecht.

Rijkswaterstaat. (1869b). De Waterstaatskaart van Nederland, Utrecht 1. Blad 31-2. Retrieved from Database of University Utrecht.

Rijkswaterstaat. (1869c). De Waterstaatskaart van Nederland, Utrecht 1. Blad 31-3. Retrieved from Database of University Utrecht.

Rijkswaterstaat. (1869d). De Waterstaatskaart van Nederland, Utrecht 1. Blad 31-4. Retrieved from Database of University Utrecht.

Rijkswaterstaat. (1920b). De Waterstaatskaart van Nederland, Utrecht 2. Blad 31-4. Retrieved from Database of University Utrecht.

Rijkswaterstaat. (1940). De Waterstaatskaart van Nederland, Utrecht 2. Blad 31-West. Retrieved from Database of University Utrecht.

Rijkswaterstaat. (1919). De Waterstaatskaart van Nederland, Utrecht 2. Blad 31-2. Retrieved from Database of University Utrecht.

Rijkswaterstaat. (1950a). De Waterstaatskaart van Nederland, Utrecht Oost 3. Blad 31. Retrieved from Database of University Utrecht.

Rijkswaterstaat. (1959). De Waterstaatskaart van Nederland, Utrecht West 3. Blad 31. Retrieved from database of University Utrecht.

Rijkswaterstaat Directie Algemene Dienst. (1967). De Waterstaatskaart van Nederland, Gorinchem-Oost 4. Blad 38. Retrieved from University Utrech Database.

Rijkswaterstaat Directie Algemene Dienst. (1960). De Waterstaatskaart van Nederland, Gorinchem-West 4. Blad 38. Retrieved from University Utrecht Database.

Rijkswaterstaat Directie Algemene Dienst. (1972). De Waterstaatskaart van Nederland, Utrecht-Oost 4. Blad 31. Retrieved from database of University Utrecht.

Rijkswaterstaat Directie Algemene Dienst. (1969). De Waterstaatskaart van Nederland, Utrecht-West 4. Blad 31. Retrieved from University Utrecht Database.

Rijkswaterstaat. (1981a). Waterstaatskaart van Nederland, Gorinchem-Oost vijfde editie, Blad 38. Topografische Dienst, Delft, Retrieved from database of University Utrecht.

Rijkswaterstaat. (1981d). Waterstaatskaart van Nederland, Utrecht-West vijfde editie, Blad 31.

Roscience Inc. (2001-2009). *Settle3D: Settlement and consolidation analysis.* Roscience Inc.

Schothorst, C. (1977). Subsidence of low moor peat soils in the western Netherlands. *Geodarma* , (17), 265-291.

Stephens, J. C., Allen, L. H., & Chen, E. (1984). Organic soil subsidence. *Geological Society of America* , (VI), 107-114.

Stichting Normaal Amsterdams Peil. (sine anno). *What does NAP mean?* Retrieved March 20, 2014, from normaalamsterdamspeil: http://www.normaalamsterdamspeil.nl/?lang=en

Stouthamer, E., Berendsen, H., Peeters, J., & Boumand, M. (2008). *Toelichting Bodemkaart Veengebieden provincie Utrecht, schaal 1:25000.* Utrecht: Departement Fysische Geografie: Provincie Utrecht, afdeling Groen.

University Utrecht. (sine anno). *nl_1885*. Retrieved June 3, 2014, from Municipality map of the Netherlands in 1885: Retrieved from University Utrecht Database

van Bokhoven, A. (2014b). *De laagste hoogte: Bodemdaling op de lange termijn in het beheersgebied van HDSR.* De Bilt: VEMDA, commisioned by province of Utrecht, HDSR and province of Zuid Holland.

van Bokhoven, A. (2014). Personal contact. (L. Geisler, Interviewer)

van de Kasteele, L. (1850). Statistieke kaart van de provincie Utrecht. Utrecht, Utrecht, The Netherlands: W.C.J.Bollaan.

van den Akker, J. J. (2014). personal contact. (L. Geisler, Interviewer)

van den Akker, J., Beuving, J., Hendriks, R., & Wolleswinkel, R. (2007). Maaivelddaling, afbraak en CO2-emissie van Nederlandse veenweidegebieden. *Leidraad Bodembescherming* , (83), 1:5510-30:5510.

van der Schans, M. (2014, May 7). Questions about derivation of Phoenix formula. (L. Geisler, Interviewer)

van der Schans, M., & Houhuessen, Y. (2011). *Phoenix 1.0: Deelrapport 1: Onderbouwing rekenregels regionale bodemdalingsapplicatie.* Houten: Grontmij Nederland B.V.

van der Schans, M., & Houhuessen, Y. (2012). *Phoenix 1.0: Deelrapport 3: Vervaardiging en evaluatie regionale bodemdalingsapplicatie westelijk deel Provincie Utrecht/HDSR.* De Bilt: Grontmij Nederland B.V.

van der Schans, M., & Houhuessen, Y. (2013). *Phoenix 1.1: Deelrapport 2: ArcGIS-gebruikershandleiding voor regionale bodemdalingsapplicatie.* De Bilt: Grontmij Nederland B.V.

van der Zon, N. (2013). *Kwaliteitsdocument AHN2.* Amersfoort: Rijkswaterstaat Data-ICT-Dienst.

van Hardeveld, H. (2014). personal contact. (L. Geisler, Interviewer)

van Hardeveld, H., de Jong, H., van der Werf, E., de Boer - Riebel, A., Bronkhorst, J. W., & van de Haterd, R. (2013). *Nut en noodzaak hoogwatervoorzieningen HDSR: aanbevelingen voor beheervisie.* Houten: Hoogheemraadschap De Stichtse Rijnlanden.

Waterstaatskartografie. (1981c). Waterstaatskaart van Nederland, Gorinchem-West vijfde editie, Blad 38. Topografische Dienst, Delft, Retrieved from database of University Utrecht.

Waterstaatskartografie. (1981b). Waterstaatskaart van Nederland, Utrecht-Oost vijfde editie, Blad 31. Topografische Dienst, Delft, Retrieved from database of University Utrecht.

Waterstaatskartografie. (1981). Waterstaatskaart van Nederland, Utrecht-West vijfde editie, Blad 31.

Waterwet. (2014, Februari 18). *Wet- en regelgeving: Waterwet.* Retrieved Februari 19, 2014, from overheid.nl: http://wetten.overheid.nl/BWBR0025458/Hoofdstuk3/1/Artikel31/geldigheidsdatum_18-02-2014

WIS-HDSR. (2013). *Waterkwantiteits Informatie Systeem 2.* Retrieved April 5, 2014, from HDSR software programm: WIS2.0

Wolters, A., Hoekstra, J., & Boerefij, M. (2011). *Kockengen Waterproof: Inventarisatie bodemdaling en invulling zorgplicht Grondwater.* Utrecht: Tauw.

9 Appendix A: Conjugation van den Akker formulas for Phoenix

There appears to be some conflict in the manner of the conjugation of the van den Akker et al, 2007 formulas (Eq. 4) and (Eq. 5) to the clay independent formula used in Phoenix (7). Therefore in this Appendix a step by step reconstruction is done explaining how this conjugation process (likely) went, resulting in the basis why a new basic Phoenix formula is better suited.

Step 1:

The clay thickness varies throughout the study area. The Phoenix formula requires a form that allows for a variation in clay thickness resulting in different subsidence rates. Therefore the clay dependant term “b” was introduced. The general form is thus:

$$\Delta L = a * GLG - b * K - c \quad \text{(Eq.A.1)}$$

In the model the GLG being as described in *the function terms* is changed to O, being the depth of the groundwater table in a 1:1 ratio. Also the land subsidence is changed so that it is always negative, i.e. multiplied by -1. The actual formula used in Phoenix thus looks as follows:

$$\Delta L = -a * O + b * C + c \quad \text{(Eq.A.2)}$$

Here the units are also changed to [m] instead of [mm], hence dividing all values by 1000.

Step 2:

The values for ‘a’, ‘b’ and ‘c’ were obtained using (Eq. 4) and (Eq. 5). Since formula (Eq. 5) is written for a layer with clay < 0,4 m no exact clay thickness is known. According to phoenix documentation (van der Schans & Houhuessen, 2011; van der Schans & Houhuessen, 2012) the clay is assumed to have an average thickness of 0,205 m. The exact basis of this assumption is not documented but after personal contact with (van der Schans M. , 2014) it is assumed that this comes from the median between 0,01 m < K < and 0,4 m clay, being 0,205 m. This would result in the following ‘abc’-values:

$$-23.537 * GLG + 10.47 + 0 * b = -23.537 * GLG + 6.68 + 0.205 * b$$

$$10.47 - 6.68 = 0.205 * b$$

$$\frac{10.47-6.68}{0.205} = b = 18.49 \quad \text{(Eq.A.3)}$$

However the value reported in (van der Schans & Houhuessen, 2011; van der Schans & Houhuessen, 2012) is 18,34 and not 18,49.

Step 3:

Only after finding an internal excel document it becomes apparent where this value came from. In this document an assumed average clay thickness of 0,325 m is used as opposed to the 0,205 m as documented. Where this assumption came from is not documented however it is assumed that this value likely came from determining the clay thickness at Zegveld using (Stouthamer et al., 2008) where (Eq. 4) and (Eq. 5) for the most part were established (de

Jong, personal contact 2014). The conjugation in this document however was done differently, being as follows:

$$6.68 + \frac{10.47-6.68}{0.325} = 18.34 \quad \text{(Eq.A.4)}$$

Here the ‘b’ of (Eq. 4) is used double, why this is done is unknown.

Step 4:

The answer found in step 3 was added as the answer to the approach documented in step 2. Adding up to the following formula:

$$\frac{10.47-6.68}{0.205} = 18.34 \quad \text{(Eq.A.5)}$$

Which is incorrect.

Suggested new basic formula:

Due to the uncertainty revolving around the method of conjugation previously done in Phoenix a new general Phoenix formula is suggested. The assumption of an average clay thickness of 0,3 is used as it is supported by (Stouthamer et al, 2008) at the Zegveld location and confirmed to be a reasonable assumption by (van den Akker J. J., 2014). This would thus result in the following conjugation of the ABC-values:

$$-23.537 * GLG + 10.47 + 0 * b = -23.537 * GLG + 6.68 + 0.3 * b$$

$$10.47 - 6.68 = 0.3 * b$$

$$\frac{10.47-6.68}{0.3} = b = 12.63 \quad \text{(Eq.A.6)}$$

Filling in the general form of (B.2) the new general formula of Phoenix in [m] is obtained:

$$\Delta L = -0.023537 * O + 0.01263 * C + 0.00668 \quad \text{(Eq.7)}$$

10 Appendix B: Pre-processing of RQ1 data set

This appendix is divided in three major parts. First a base data set is selected, followed by the addition of base information to this data set, this base information is then adjusted when needed and in the end data points are deleted based on various criteria.

Step 1: Selection of the data set

Using the elevation data a land subsidence over time is established. The elevation sources are divided into two data bases. The first data base includes All Available Elevation Data (AAED) which includes the *waterstaatskaarten*, *peilbesluiten*, TOPhoogteMD, AHN1 and AHN2, consisting of 453 DP. The second data base includes only the Digital Elevation Maps (DEM) which include TOPhoogteMD, AHN1 and AHN2 consisting of 28174 DP.

Both the AHN1 and AHN2 maps were aggregated from 5x5 m to 25x25 m. This makes sure surface elevation irregularities, such as ditches which are not discernible in TOPhoogteMD, are averaged over a similar sized cell. Using these two elevation data sets a linear historical land subsidence relations is established for each (Figure A.1.a and figure A.1.f). The derivative of this linear line is the land subsidence rate. In figure A.1 the data points and the Inverse Distance Weighting interpolation of the land subsidence rates are visualized for both data sets.

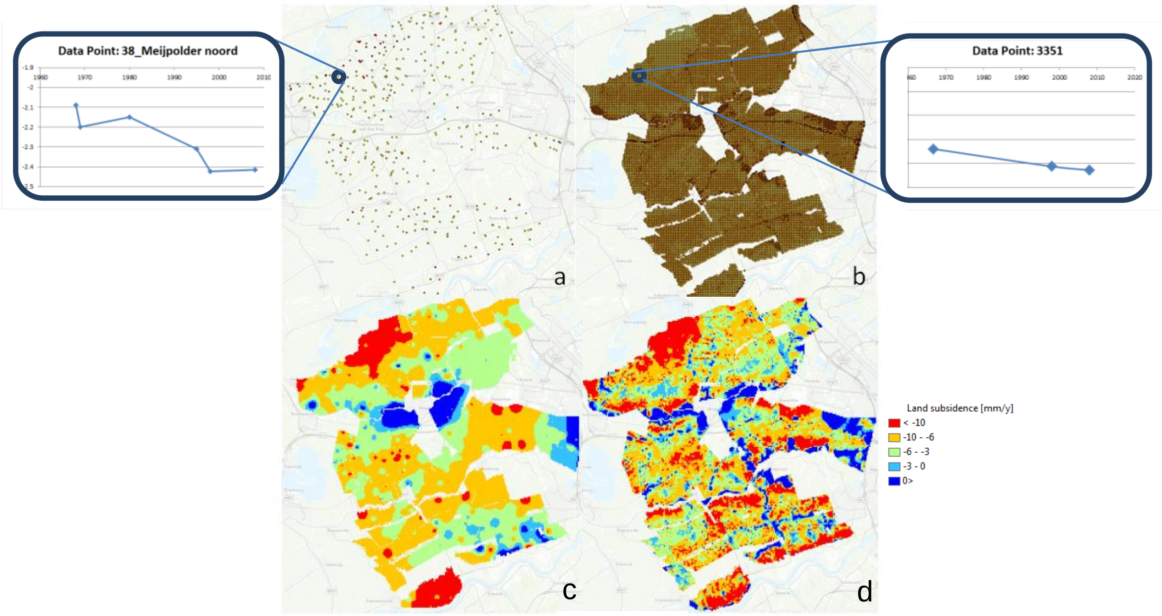

Figure A.1: *Data points of AAED (a), Data points of DEM (b), Land subsidence in [m/y] for AAED (c), Land subsidence in m/y for DEM (d), land subsidence of data point: 38_Meijpolder noord (e) and land subsidence of data point 3351 (f)*

The patterns of both datasets appear similar, albeit more crude for AAED as there are less data points to interpolate with. The difference between DEM vs AAED depends on location. The geographical distribution of the percentile difference for the DEM and AAED data looks as follows (figure A.2). As the data points are too small to visually see a pattern this data was interpolated so that a raster with indications of locations where an overestimation and where underestimation occurs. This Inverse Distance Weighting interpolation was only done in order to show the pattern and should not be taken as fact.

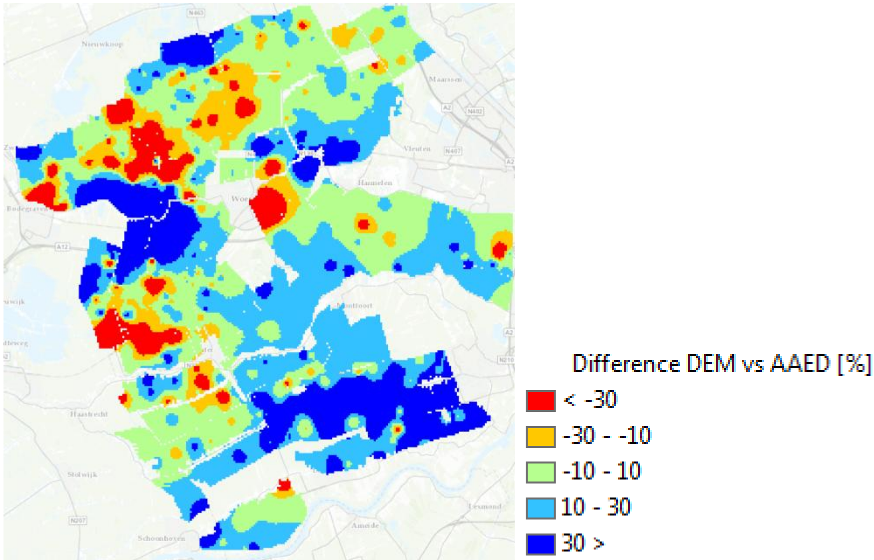

Figure A.2: *The differences between DEM and AD were interpolated using the difference for each of the points above.*

Although it is possible to use AAED resulting in more measurements over time the choice was made to use DEM as of this point. This choice was made for the following reasons:

1. The distribution and amount of data points of the DEM dataset allows for better pattern recognition.
2. Each polder has multiple data points, whereas some polders have 0 data points when using AED.
3. The reliability of the three Digital Elevation Maps appears better since it was made in one consistent manner by the Dutch topographic institute or using laser altimetry. By whom and the manner in which the soil elevation of other sources such as the *Waterstaatskaarten* or *peilbesluiten* was done is less known.
4. The elevation measurements of the *Waterstaatskaarten* is in decimals only.

Step 2: Applying basic information

Surface water data

The historical maps are added to ArcGIS and given correct geographical coordinates. The SW levels are read from these maps and added to 138 different polder polygons. These polders have one and the same SW level at some point in time. Polders tend to split up over time (observed in historical maps), this means that polders as they existed in 1890 might currently exist as 5 smaller polders. For this reason polder shapes in ArcGIS are established reasoning backwards from current (small) polders to historic (large) polders. In case of the above mentioned example this would mean that the polder exists out of five different polygons with all the same summer water level in 1890 and five different summer water levels in 2014. The SW data is added to the selected data set (using spatial join in ArcGIS).

Clay data

In order to find out what the relation for land subsidence with relation to freeboard and clay thickness is first the clay thickness has to be applied to the data points. The data used is the same as used in Phoenix. Here the clay thickness is given for 10 cm intervals. Although the clay thickness is reported as being every 10 cm there appear to be three major groups, most of the DP have either 0, 30 or 60 cm clay. This is due to the translation from soil type in (Stouthamer et al., 2008) to clay thickness (van der Schans & Houhuessen, 2012).

Soil type data

For the soil types the soil map 1:25000 of the province of Utrecht is used (Stouthamer et al, 2012). This map was obtained from the Phoenix database where the entire study area has specified soil types, whereas the same 1:25000 map present on the database of the University of Utrecht only has data within the province of Utrecht itself and thus missing a small part to the west of the province of Utrecht but still within the jurisdictional area of HDSR.

Step 3: Adjustment of data points

Correction AP to NAP

In (Nederlandsche Rijkscommissie voor Graadmetingen Waterpassing, 1888) the difference between NAP and AP for several municipalities in the Netherlands was published. By combining this with a municipality map for the moment the last measurements were taken, being 1885 (University Utrecht, sine anno) the NAP-AP relation can be distributed geographically. For the study area there are a total of six known AP and NAP relations out of forty existing municipalities (figure A.3.c). For the total of the Netherlands there are 178 known AP-NAP relations (figure A.3.d). By using an interpolation named spherical areal interpolation in ArcGIS these relations become available on a nationwide scale it is possible to get values for the missing municipalities (Figure A.3). This does however assumes that there is a relation between the distance from Amsterdam, where the NAP was established, and NAP-AP relation. In figure A.3.a and figure A.3.c. the known NAP-AP relations for the municipalities are given and in figure A.3.b and figure A.3.d the interpolated values for all the municipalities are visible.

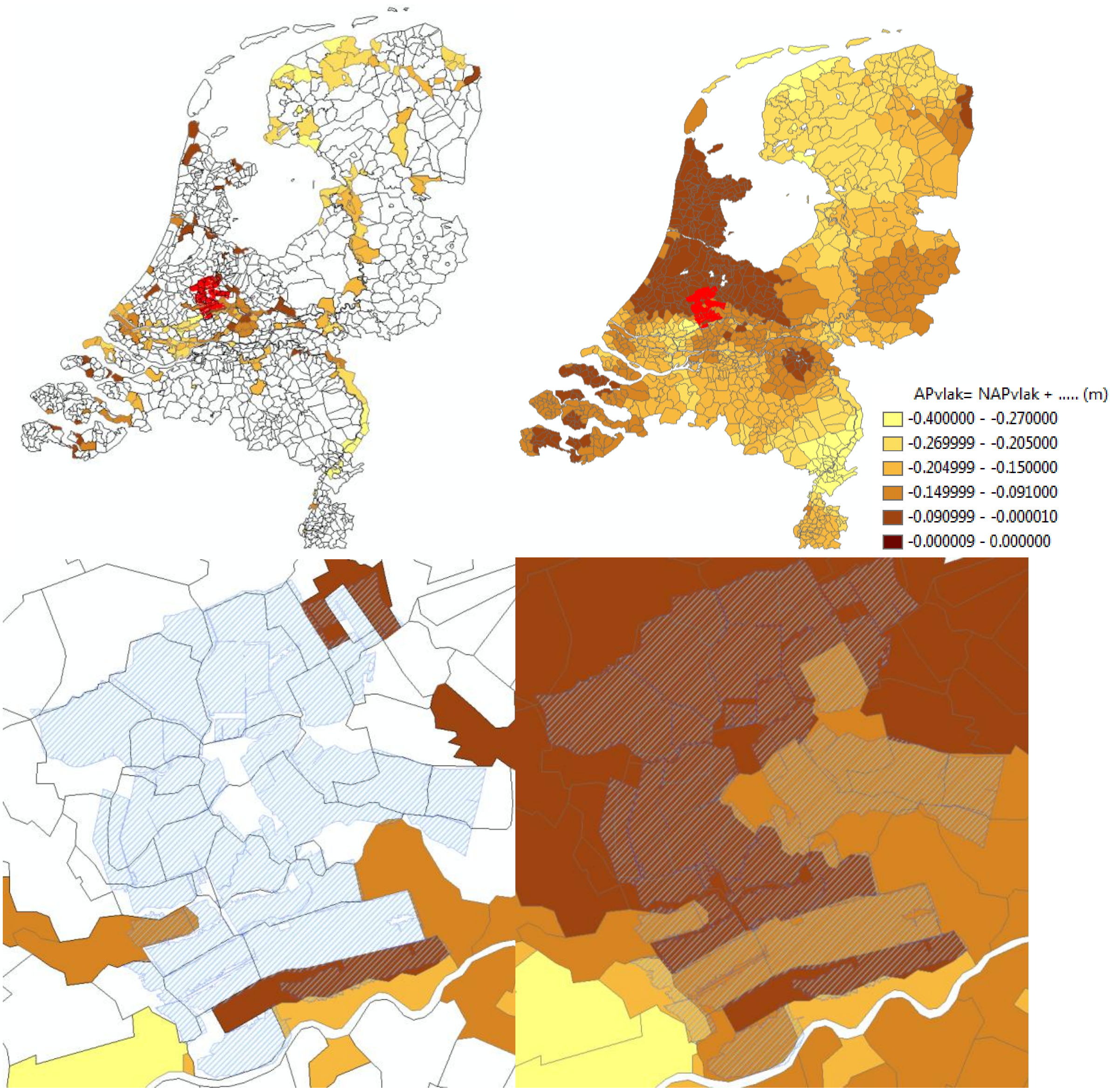

Figure A.3: *Known AP-NAP relations for the municipalities in the Netherlands, (the study area (red)) (a), Interpolated AP-NAP relations for all the municipalities in the Netherlands, (the study area (red)) (b), Known AP-NAP relations for the study area, (the study area (shaded)) (c), Interpolated AP-NAP relations for the study area, (the study area (shaded)) (d). (University Utrecht, sine anno; Nederlandsche Rijkscommissie voor Graadmetingen Waterpassing, 1888)*

The AP-NAP relation is added to the measurements prior to 1910 so that all AP values can now be considered NAP values and are thus comparable.

Step 4: Exclusion of data points

Impact of land use

When looking at the land subsidence in the study area there are several areas that appear to be significantly different from the surrounding subsidence rates. After overlaying the data points with a topographic map a pattern becomes visible showing that urbanized areas, roads and water bodies have a significantly different land subsidence rate or a large surface elevation increase over time. The difference in land subsidence between four land use types looks as follows (figure A.3).

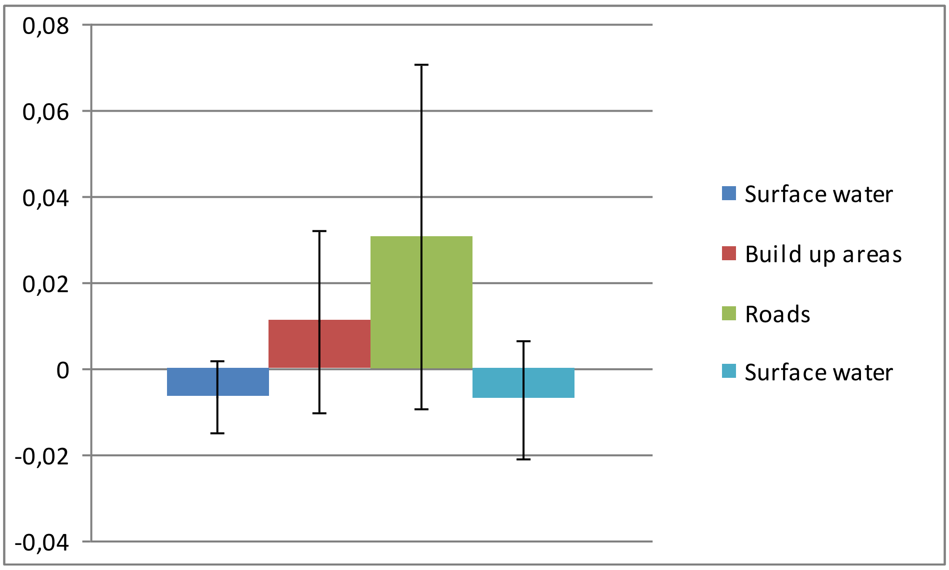

Figure A.3: *Difference in land subsidence rates [m/y] based on different land use.*

This relation was established using LGN6 (Hazue et al, 2012) as a basis of land use, other sources such as (Kadaster, 2009) or (Landelijk Samenwerkingsverband GBKN, 2005) represent similar data but LGN6 is the most up to date (Hazue et al, 2012) and easiest to combine with the data points. Surface waters are a special case as for the AHN1 and AHN2 the surface of the water body is measure and for TOPhoogteMD the surface of the bottom of the pool or lake is interpolated between various land measurements. Often the water body did not exist during the TOPhoogteMD measurements. The relation to be established is based on variations in soil type, clay thickness, or freeboard the land use has to be uniform so that it does not affect the subsidence relation found. Therefore only agricultural grasslands are taken into account, all other land uses are excluded. This leaves a total of 21894 data points.

Exclusion based in low correlation

Many of the linear historical elevations vs. time relations have a reasonably low correlation (r^2). The variation in height over time is large, especially if changes took place between 1998 and 2008 (AHN1 vs. AHN2). Therefore all the data points with an r^2<0,75 are excluded.

Exclusion of visual outliers

Some points are classified as being agricultural grass but in fact show patterns that are not representative of an agricultural field. DP in-between or just outside of roads and urbanized areas, on dikes or close to rivers display significantly different elevations compared to its surroundings these points are visually deleted (Figure A.4).

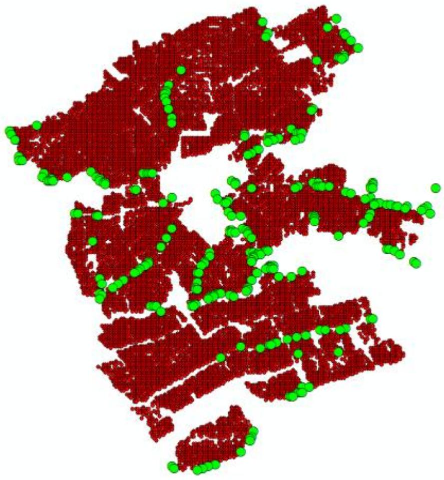

Figure A.4: *Deleted visual outliers (Green).*

Exclusion based on surface water levels

Throughout the study area there are several points that are located within ditches. This means that the surface level is below the surface water level, i.e. these points are under water. For a large part this error has already been corrected by excluding water bodies using (Hazue et al, 2012). However not all ditches, especially the tertiary waterways, were represented as “water” in LGN6. In order to correct this the points that have a SW level that exceeds the surface elevation in 2008 are excluded.

Exclusion based on missing soil data

Some DP lay outside of the soil maps used in Phoenix, which results in them having no clay thickness data. These points are deleted.

11 Appendix C: Laser altimetry measurement errors of AHN1

As with all elevation maps there are uncertainties with the measurements. Although both AHN1 and AHN2 are maps with great detail and accuracy these too have inaccuracies. In table A.1 the allowed inaccuracies are shown

Tabel A.1: *Allowed error for AHN1 and AHN2 (AHN2, Kwaliteitsdocument)*

	AHN1	**AHN2**
Systematic error	5 cm	5 cm
Stochastic error	15 cm	5 cm
At least 68.2% of the points are accurate up to:	5+1*15=20 cm	5+1*5=10 cm
At least 68.2% of the points are accurate up to:	5+2*15=35 cm	5+2*5=15 cm
At least 68.2% of the points are accurate up to:	5+3*15=50 cm	5+3*5=20 cm

When considering that the land subsidence process within the 10 year period between the two measurement could be in the order of 10 cm it appears that the error is large. Although one might expect the error to be random, a pattern does emerge when correlating to individual altimetry flights.

Within the study area laser altimetry flights for AHN1 were done on eight different days starting on 1-29-1999 till 11-3-2000 (Actueel Hoogtebestand Nederland, sine anno). In figure A.5 these flights are represented in different colours.

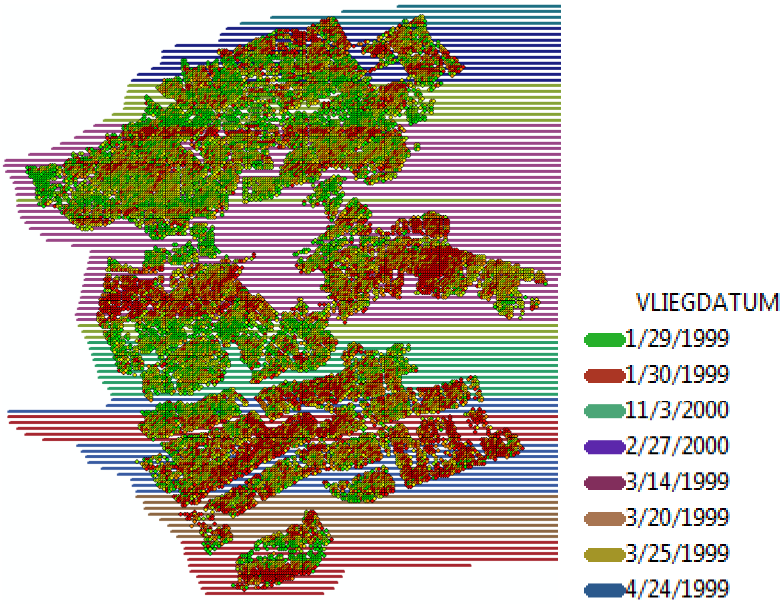

Figure A.5: *DP where elevation in 2008> elevation in 1998 (Light blue dots), Horizontal lines (individual flights). Red regions represent fast subsiding areas, green regions represent areas with slow subsidence often even land rise.*

In figure A.5 it is possible to see differences related to the different flight days, or individual flight runs, rather than clay thickness, freeboard or seepage in the form of straight horizontal lines.

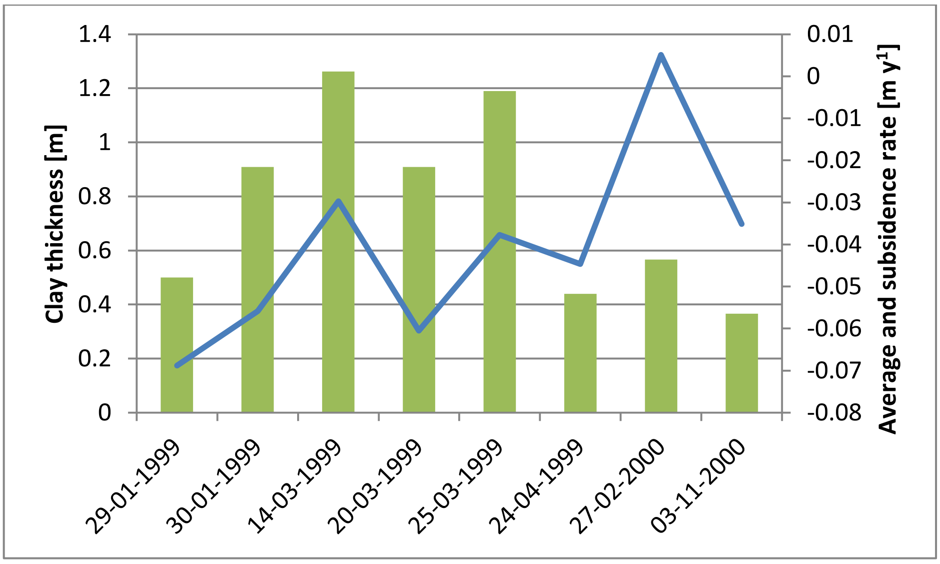

Figure A.6: *Difference between various flight days of the AHN1 laser altimetry measurements. Clay thickness (green bars), Land subsidence rate (blue line).*

In figure A.6 it can clearly be seen that each flight has a different average land subsidence rate which appears to be independent on clay thickness. For example the flights on 27-02-2000 have an average land rise, rather than subsidence eventhough the average clay thickness is 0,56 cm which is fairly low compared to the other flights.

It is also possible to see differences within a single flight day. Flights are registered with block numbers. Within the flight of 25-03-1999, block 4, has significantly different subsidence rates compared to the other two blocks as shown in figure A.7.

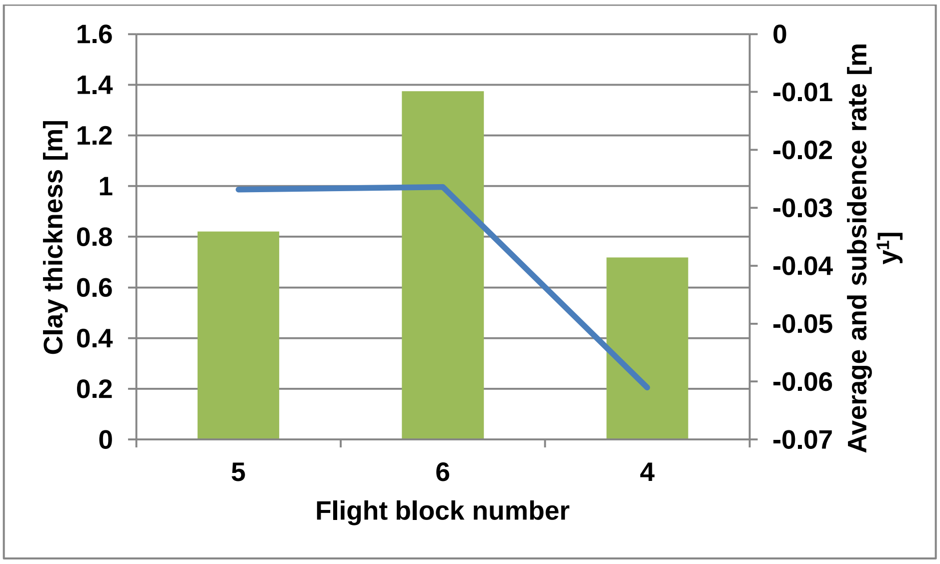

Figure A.7: *Difference between the elevations of the blocks within flight day 25-03-1999.Clay thickness (green bars), Land subsidence per flight (blue line).*

For the land subsidence again the average land subsidence appears to be independent on clay thickness. Flight block 4 indeed has the lowest amount of average clay but the difference between block 5 and 4 is 0.1 m but the average subsidence rate is far lower for block 4 then it is for block 5.

12 Appendix D: Conjugation van den Akker formulas for ditch water

This conjugation is the same as it was in Appendix A, but instead of using GLG now the ditch water formula is used. Formulas for no clay and <40 cm clay respectively as reported in van den Akker et al, 2007;

$$\Delta L = 15.455 * DW + 2.75 \quad \text{(Eq. A.8)}$$

$$\Delta L = 15.455 * DW - 3.53 \quad \text{(Eq. A.9)}$$

General form with respect to ditch water:

$$\Delta L = a * DW + b * C + c \quad \text{(Eq. A.10)}$$

wherein:
a, b and c are constants
ΔL = land subsidence over time [m y^{-1}]
DW = ditch water level [m]
C = clay thickness [m]

The conjugation yields:

$$-15.455 * DW + 3.53 + 0 * b = -15.455 * DW + 0.3 * b - 2.75$$

$$3.53 + 2.75 = 0.3 * b$$

$$\frac{3.53+2.75}{0.3} = b = 20.9333 \quad \text{(Eq.A.11)}$$

Filling in the general form of (Eq.A.10) the general formula obtained. Ditch water levels are considered the same as the surface water levels, thus DW is changed to SW:

$$\Delta L = -15.455 * SW + 20.9 * C + 2.75 \quad \text{(Eq.11)}$$

It is noteworthy that the impact clay has on the rate of land subsidence is far larger in this conjugation as it is for the version with respect to clay. This is also a notation made in van den Akker et al, 2007 remarking that the correction of the clay impact is 6,28 mm for surface water data and 3.8 mm for GLG.

13 Appendix E Multiple regression clay < 60 cm

This appendix includes the relation for land subsidence with respect to clay thickness and free-board using a polynomial second order function for land subsidence. Function of surface area.

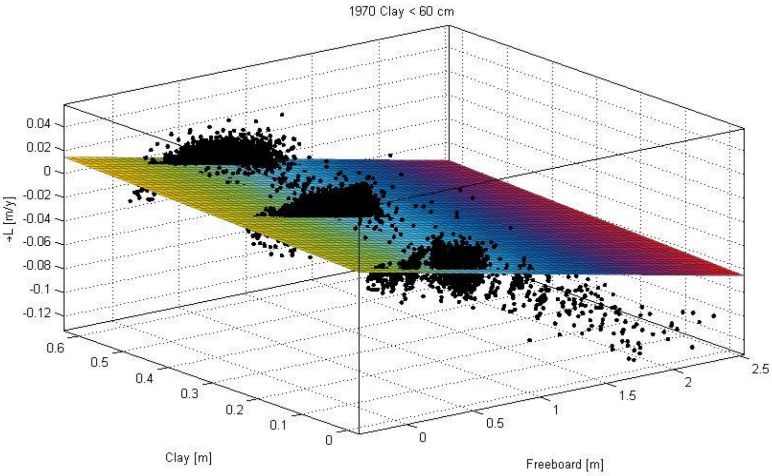

Figure A.8: *Relation in 1970: correlation of r^2: 0.2261 and a function of the surface area of -0.02415SW*0.01527C-0.0049*

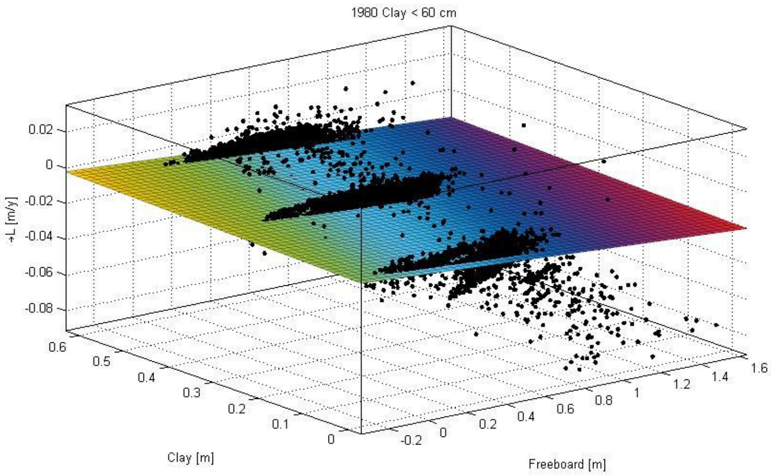

Figure A.9: *Relation in 1980: correlation of r^2: 0.0458 and a function of the surface area of -0.007SW*0.0069C-0.0088*

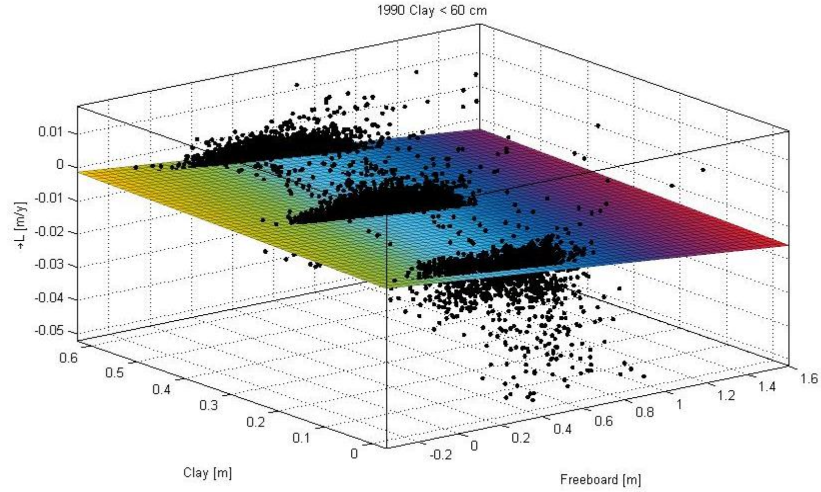

Figure A.10: *Relation in 1990: correlation of r^2: 0.064 and a function of the surface area of -0.0061SW*0.0041C-0.006*

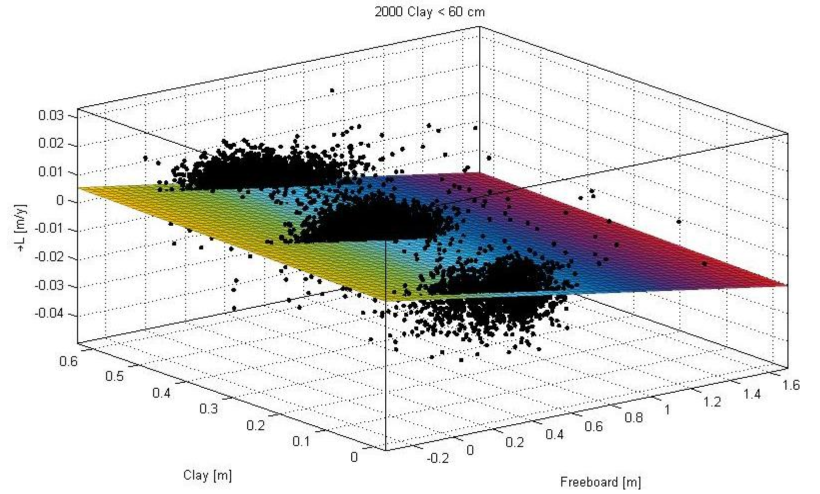

Figure A.11: *Relation in 2000: correlation of r^2: 0.093 and a function of the surface area of -0.0117SW*0.0033C-0.0009*

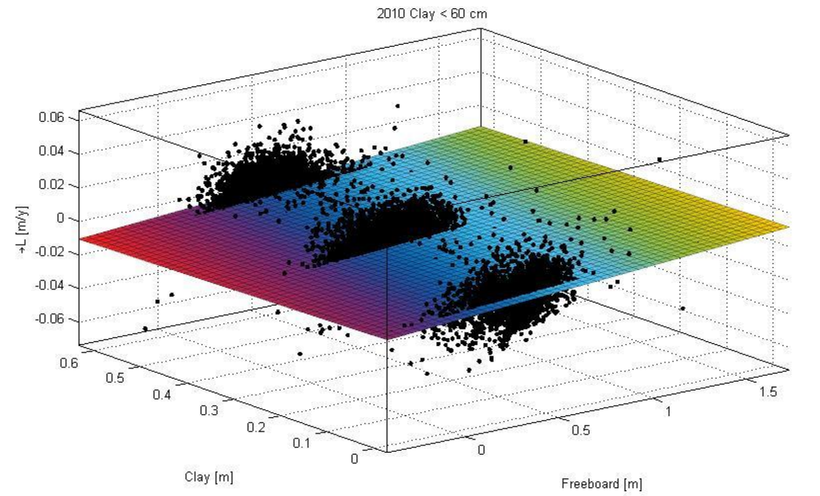

Figure A.12: *Relation in 2010: correlation of r^2: 0.0208 and a function of the surface area of 0.0084SW*-0.0059C-0.0038*

14 Appendix F Multiple regression clay all data

This appendix includes the relation for land subsidence with respect to clay thickness and freeboard using a polynomial second order function for land subsidence.

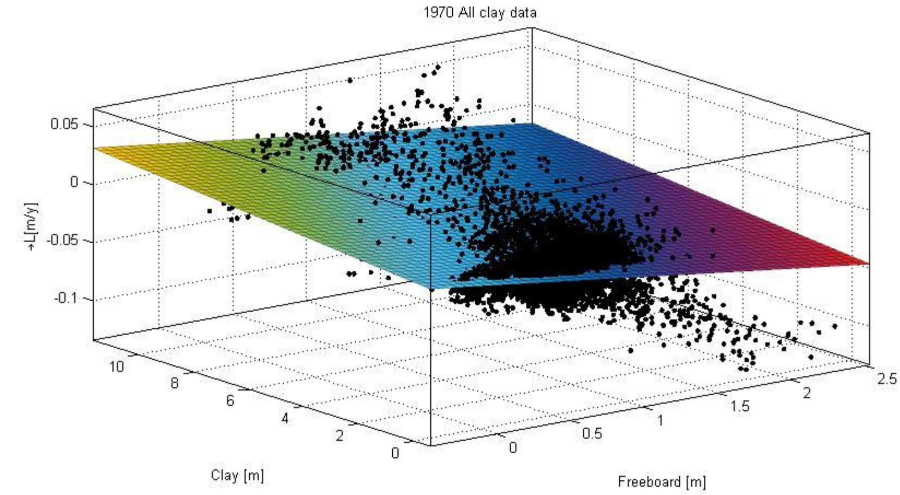

Figure A.12: *Relation in 1970: correlation of r^2: 0.163 and a function of the surface area of -0.0163SW*+0.0024C-0.004*

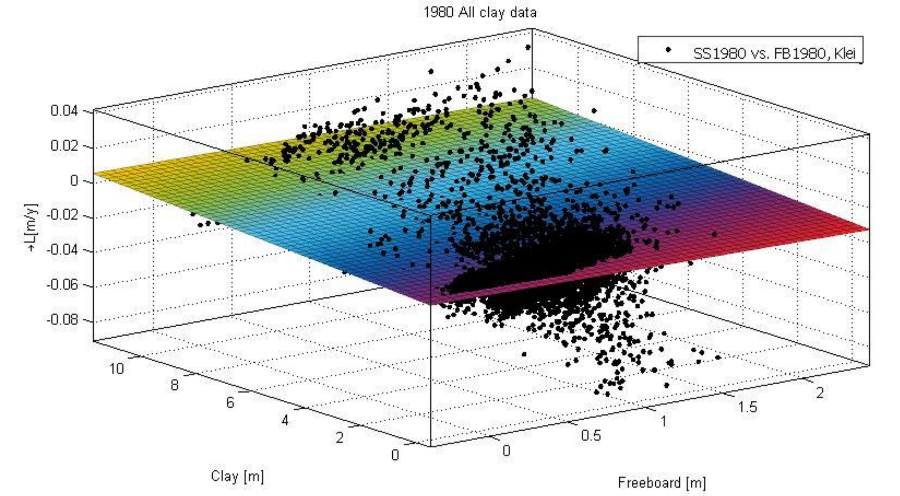

Figure A.13: *Relation in 1980: correlation of r^2: 0.093 and a function of the surface area of -0.0012SW*+0.0012C-0.0096*

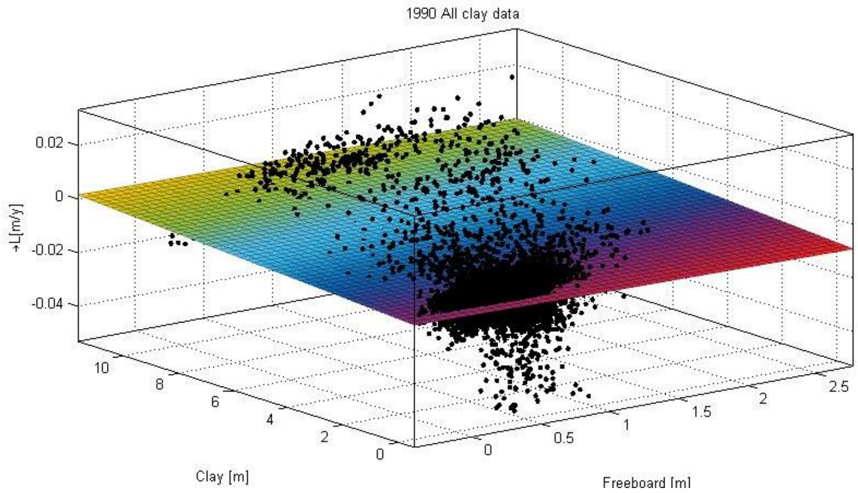

Figure A.14: *Relation in 1990: correlation of r^2: 0.065 and a function of the surface area of -0.0006SW*+0.0007C-0.0072*

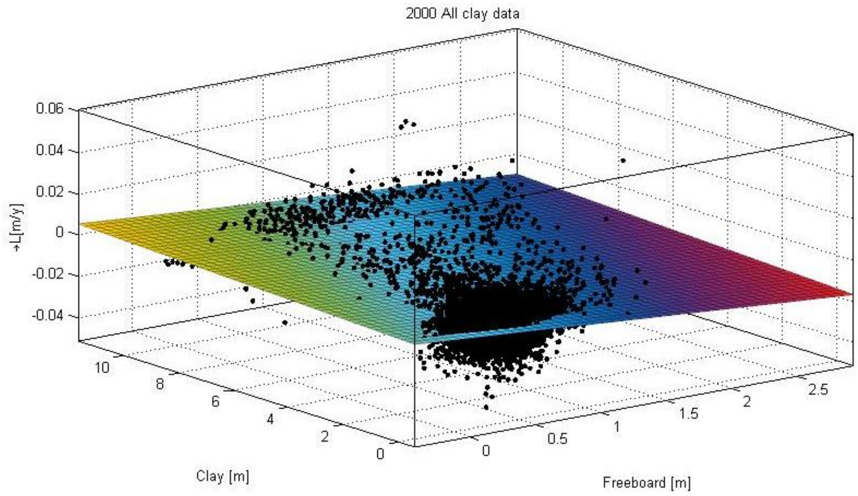

Figure A.15: *Relation in 2000: correlation of r^2: 0.0299 and a function of the surface area of -0.0046SW*+0.0001C-0.003*

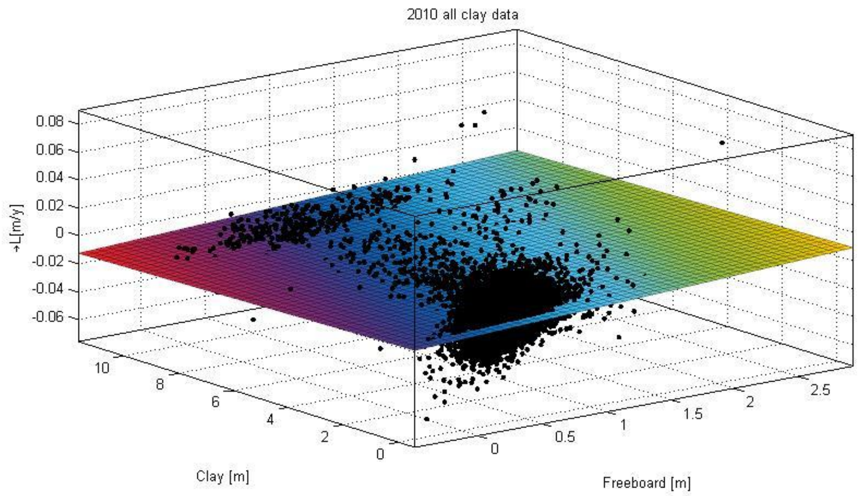

Figure A.16: *Relation in 2010: correlation of r^2: 0.01 and a function of the surface area of 0.00457SW*-0.0005C-0.0042*